The Cooperative Institute for Meteorological Satellite Studies (CIMSS)
Cooperative Agreement Award # NA07EC0676

Semi-Annual Report to NOAA/NESDIS/ORA
for the period
1 April 2003 to 31 October 2003

Submitted by Thomas H. Achtor
Executive Director – Science
tom.achtor@ssec.wisc.edu

on behalf of the
Cooperative Institute for Meteorological Satellite Studies (CIMSS)
Space Science Center (SSEC)
University of Wisconsin-Madison
1225 West Dayton Street
Madison, Wisconsin 53706
608-262-0544

December 2003

Table of Contents
CIMSS
Semi-Annual Report to NOAA/NESDIS/ORA

I. GOES Improved Measurements and Product Assurance Plan (GIMPAP)

1. Retrieval Science

1.1 Model Independent First Guess

Preliminary work has been performed towards development of a regression-based, numerical model-independent first guess for GOES Sounder retrievals of temperature and moisture. This research has shown that a numerical model-independent first guess for GOES Sounder retrievals does not improve the retrieved temperatures compared to retrieved temperatures derived from an NWP (Numerical Weather Prediction) first guess based on short-term forecasts (6-18 hr). Yet, mid/upper-level moisture derived from model-independent retrievals does show an improvement over moisture derived from retrievals that use an NWP first guess as their initial state profiles (see Figure 1). Unfortunately, the quality of the model-independent first guess GOES Sounder retrievals have been deemed unacceptable, to this point in time.

Discussions have begun to improve the model-independent retrieval algorithm via a hybrid first guess, with the temperature profile from NWP and a regression-based profile for moisture. This method will use the advantage of the numerical model (temperature profile) and use the satellite radiances where they have the most effect (to change the moisture), giving forecasters. the best hybrid product to evaluate. To fully evaluate this product, GOES Sounder Derived Product Imagery (DPI such as TPW, layers of WV, Skin temperature, CAPE, etc.) will be generated and displayed from retrievals that utilize the hybrid first guess. These DPI will then be compared to DPI generated from retrievals generated by using just NWP for the first guess. If interest warrants, these data will be made available in formats other than McIDAS areafiles.

Publications

T. J. Schmit, W. P. Menzel, J. Daniels, Y. Plokhenko, J. P. Nelson III, J. Jung, T. Schreiner, and E. Borbas, 2003: 2002 / 2003 Report on NOAA/NESDIS GOES Soundings. CGMS XXXI. Ascona, Switzerland, 3-7 November 2003. EUMETSAT publication.

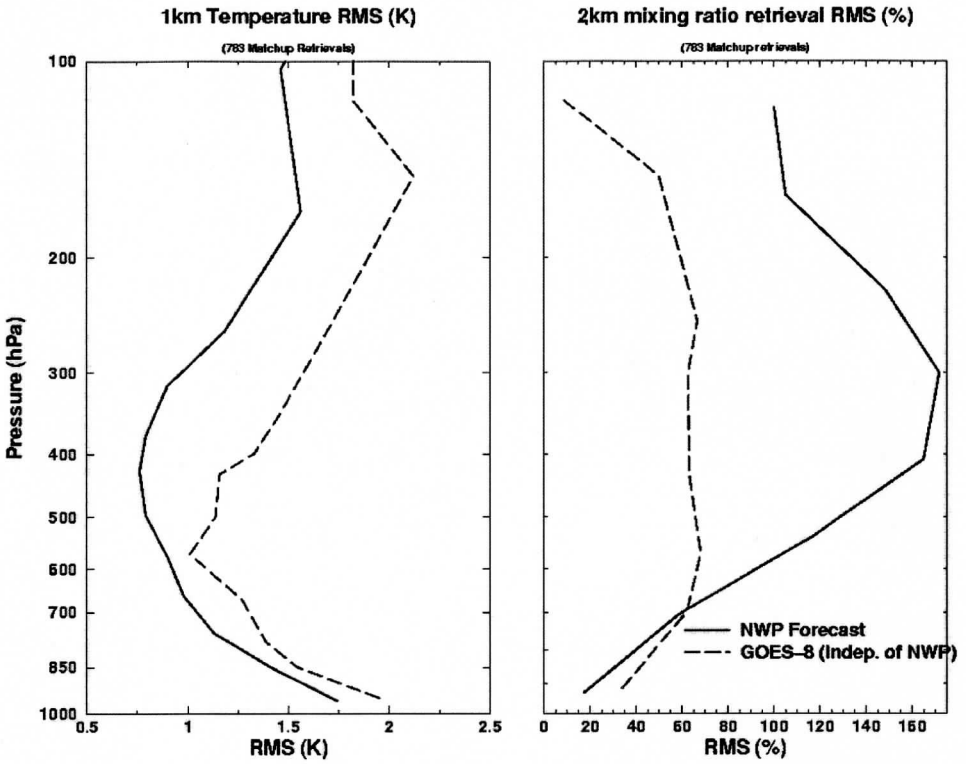

Figure 1. There are 783 match-ups between retrievals and co-located radiosondes. The black solid line is using the NWP forecast as the first guess. The dashed (blue) line is using a regression, based on the brightness temperatures as the first guess. In general, with respect to temperature, the regression-based first guess retrievals are worse than those made with a model first guess; however, with respect to moisture, the regression-based first guess retrievals are better for all but the lowest levels.

1.2 Surface Emissivity and 3 GOES

The goal of this project is to conduct research on improving GOES Sounder retrievals by using an improved estimate of surface emissivity.

A primary objective of meteorological remote sensing is to assess the temperature-humidity distribution of the "surface + atmosphere" system. The quantitative estimation of these parameters is based upon the numerical solution of the radiative transfer equation (RTE), wherein contributions to the measured radiances from the observed system are modeled. Since the numerical solution of the RTE is an ill-posed inverse problem, there is no one-to-one physical relationship between the measurement and the solution. Thus, the solution is sensitive to small variations in the measurement and the modeling parameters.

Insufficient modeling of the surface emissivity over land has been a severe limitation to meteorological remote sensing for a number of years. To this end, a model accounting

for surface emissivity has been developed at CIMSS. Improving the incorporation of the surface emissivity into the solution parameters introduces non-linear relations into the measurement model, and also between its solution components, which include surface emissivity, surface temperature, and atmospheric temperature and moisture profiles.

Retrievals have been generated with a version of the codes that account for surface emissivity. A summary of this work has been published.

Currently, three GOES satellites are in operation around the globe, allowing researchers unique opportunities for research. GOES-12 became operational in April 2003 when it replaced the GOES-8 satellite at approximately 75 degrees West longitude. GOES-9 has been moved to 155 degrees East longitude, replacing the Japanese GMS satellite. Experimental Sounder data from GOES-9 has been available since approximately May 2003. Finally, GOES-10 has continued to serve the western U.S. and eastern Pacific Ocean, providing coverage from its subpoint longitude of 135 degrees West.

CIMSS continued to create products from the GOES-12 Sounder data stream and compare them to those produced from the GOES-10 Sounder. These products included temperature and moisture retrievals and Total Precipitable Water (TPW), Lifted Index (LI), and Cloud-Top Pressure (CTP) DPI.

This suite of three GOES Sounders gives coverage from near Japan to the mid-Atlantic. Geographic coverage of this extent has never before been available from GOES. Data from these satellites together will allow for some unique studies: namely, the longitudinal and temporal variations of ozone, cloudiness, and total precipitable water over this large region (see Figure 2 for an example).

Publications

Hillger, D. W., T. J. Schmit, and J. M. Daniels, 2003: Imager and sounder radiance and product validations for the GOES-12 science test, NOAA Technical Report 115, U.S. Department of Commerce, Washington, DC.

Nelson, J. P. III, G. S. Wade, A. J. Schreiner, T. J. Schmit, W. F. Feltz, and C. C. Schmidt, 2004: A Study Of Data And Products From The GOES-9 Imager And Sounder Over The Western Pacific Ocean. Preprints, *20th Intl. Conf. on Interactive Information and Processing Systems (IIPS) for Meteorology, Oceanography and Hydrology*, Seattle, WA, 11-15 January 2004, Amer. Meteor. Soc.

Plokhenko, Y., and W. P. Menzel, 2003: Mathematical aspects of the meteorological processing of infrared spectral measurements from the GOES sounder. III. Emissivity estimation in solving the inverse problem of atmospheric remote sensing. Accepted by *J. Appl. Meteor*.

Schmit, T. J., W. P. Menzel, J. Daniels, Y. Plokhenko, J. P. Nelson III, J. Jung, T. Schreiner and E. Borbas, 2003: 2002 / 2003 Report on NOAA/NESDIS GOES Soundings. CGMS XXXI. Ascona, Switzerland, 3-7 November 2003. EUMETSAT publication.

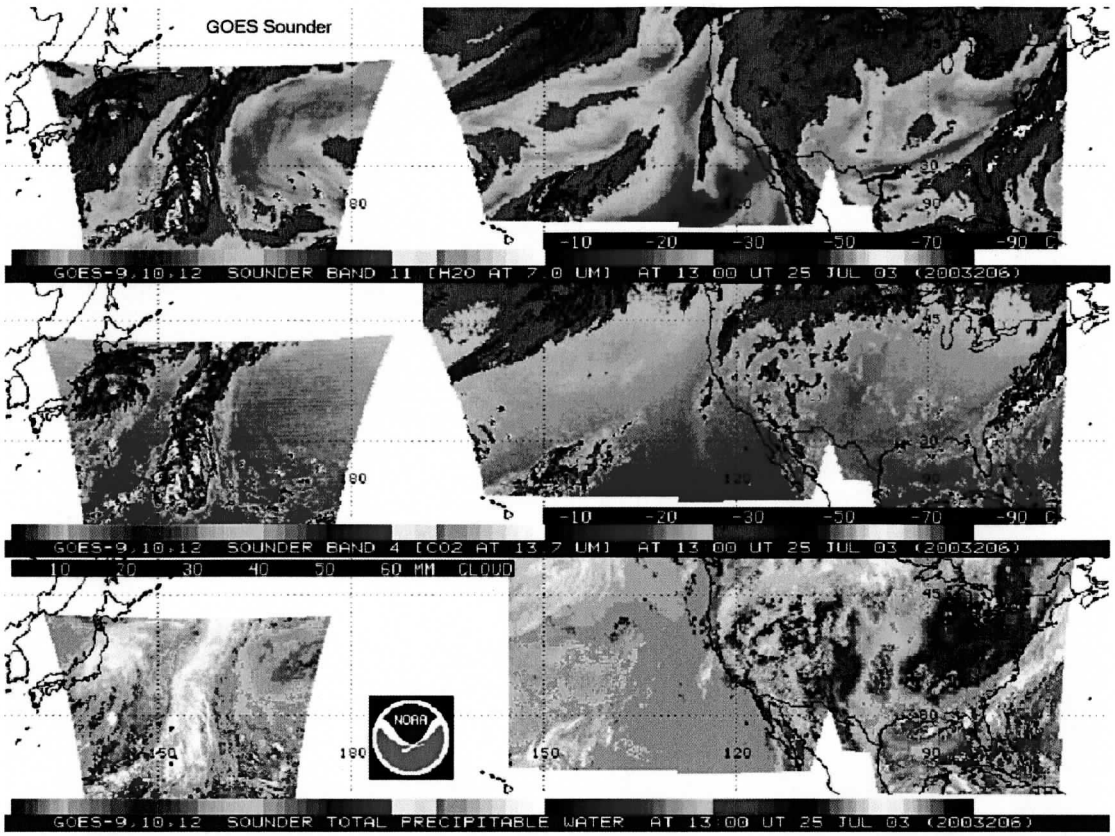

Figure 2. GOES-9/10/12 Sounder Data and Products. In addition to the TPW DPI (bottom panel), two representative Sounder radiance images are also shown, with matching color enhancements, illustrating the difference between a water vapor (H2O) sensitive band and a carbon dioxide (CO2) sensitive band. Band 11 (top) at 7.0 um shows the moisture patterns (quite structured), while band 4 (middle) at 13.7 um shows the thermal pattern, both for the mid troposphere (in clear air).

1.3 Multi-sensor studies

Generally, studies using multiple sensors from different platforms for better remote sensing the atmospheric parameters study the combination of GPS and IR/MW sounders such as ATOVS (LEO) and GOES sounder for better atmospheric sounding retrievals. Our proposed work was to perform more GPS+ATOVS analysis, to extend the study for data from sensors on EOS satellites; and to continue collecting GOES, GPS and RAOB data over the CART Site in Oklahoma.

Accomplishments and findings

GPS + ATOVS (NOAA16)

Combined CHAMP (GPS) and ATOVS soundings continue to be collected and compared with radiosonde soundings from four months: Oct 2001, Jan, Apr and July 2002. Results for clear and cloudy skies are shown in Figure 3. We found that the GPS/RO (CHAMP)

data improves the radiometric (ATOVS) temperature retrievals around and below the tropopause by 0.5 K (with larger impacts over the cloudy skies).

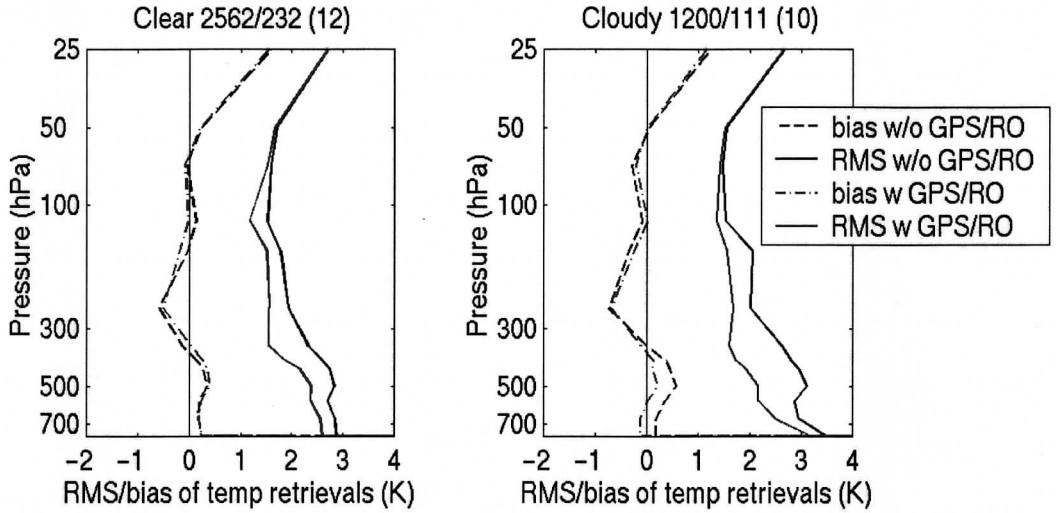

Figure 3. RMS and bias of temperature profile retrievals from ATOVS alone (blue) and ATOVS plus CHAMP (red) with respect to radiosonde measurements in clear and cloudy conditions for the months of October 2001, January 2002, April 2002, and July 2002.

GPS + AIRS (Aqua)

Three clear sky collocations of AIRS observations, GPS (both CHAMP and SAC-C) occultations, and RAOB measurements were found for 6 September 2002. Time and location interpolated NCEP reanalysis profiles for the GPS occultations were also accessed. The calculated AIRS brightness temperatures for 337 optimal channels and GPS refractivity profiles between 6 and 28 km (1km vertical resolution) were regressed against the temperature and humidity training profiles. Figure 4 shows a comparison of temperature profiles from the AIRS retrieval, RAOB observations, GPS CHAMP measurements, and the NCEP reanalysis for 6 September 2002 at 06 UTC under clear sky conditions. The current version of the AIRS retrieval exhibits problems in the tropopause region while the GPS temperature measurements fit nicely to the RAOB observation. This result suggests that the AIRS retrievals can be improved in this region when supplemented by GPS information. Work is progressing on the combined CHAMP/SAC-C + AIRS retrievals.

GPS+GOES

A total of 29 (27 with RAOB measurements) clear sky GOES collocated occultations over the SGP CART site were found between May 2001 and November 2002 for both CHAMP and SAC-C GPS satellites. The collocation time and distance criteria were 3 hours and 300 km. Figure 5 shows the validation of GOES temperature retrievals with GPS temperature profiles over the CART site, Lamont. The rms differences between GOES temperature retrievals and GPS temperature profiles are around 2 K. A large bias was found at 150 hPa which needs further investigation.

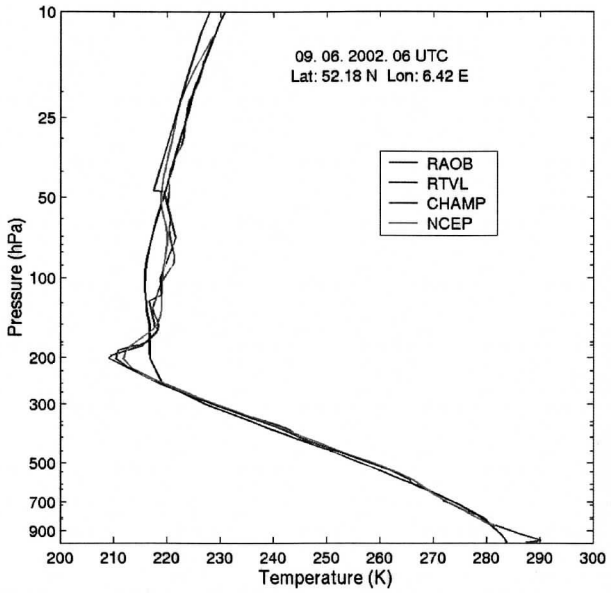

Figure 4. Comparison of temperature profiles from the AIRS retrieval (blue), nearest RAOB observation (red), GPS CHAMP measurements (green), and collocated NCEP reanalysis (cyan) for 06 UTC on 6 September 2002 under clear sky conditions.

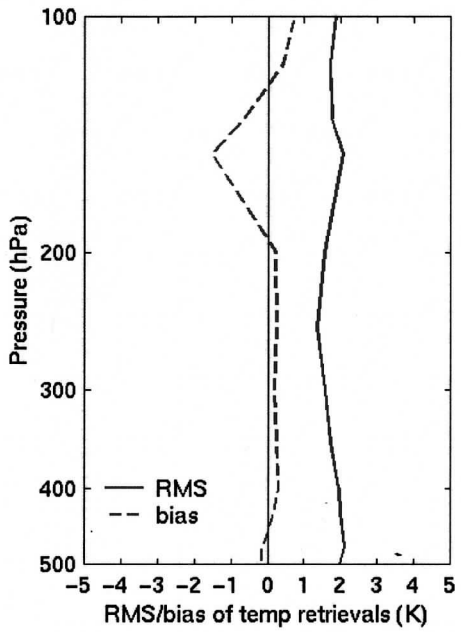

Figure 5. Validation of GOES temperature retrievals with GPS Radio Occultation temperature profiles over the SGP CART site between May 2001 and November 2002 for both CHAMP and SAC-C GPS satellites.

2. Derived Cloud Information

2.1 GOES-12 Imager Cloud Top Pressure and Volcanic Dust Cloud

With the launch of the GOES-12 in July 2001 (which became operational on April 1, 2003) and the introduction of a CO2 band (13.3 μm) as part of the suite of Infrared bands for the Imager, it is now possible to derive cloud top pressures and effective clouds for semi-transparent clouds using the CO2 Absorption Technique.

This is a newly proposed project within the Ground Systems program. Previous work, funded through the GIMPAP program, saw this project first come to fruition. In September 2001 (Schreiner et al. 2001) the cloud product was first demonstrated experimentally. By April 2003, routine production of the GOES-12 Imager Cloud Product began at CIMSS. Initially this hemispheric product was generated every three hours due to hardware limitations. During the summer of 2003 the algorithm was streamlined to allow for hourly production.

In addition science improvements have also been implemented. They include: (1) a technique to interpolate the cloud top pressure between fixed forward model levels, (2) an improved method for determining calculated radiances, (3) incorporation of an surface emissivity adjustment relative to local zenith angle, and (4) determination of a bias correction for the Long Wave Window and CO2 bands. In order to validate these data, comparisons of coincident GOES-12 Imager "cloud retrievals" to the DOE ARM CART site in Lamont, OK are being made.

This GOES-12 Imager Cloud Product Algorithm has been used to estimate the height of volcanic ash clouds for one or two examples over Mexico and the eastern Caribbean. For these examples the Cloud Product Algorithm calculated realistic heights of the dust clouds.

Publications

Ellrod, G., A. J. Schreiner, 2004: A First Look at Volcanic Ash Detection From GOES-12: Coping Without the 12um IR Band. AGU, December 2004, San Francisco, CA.

Hillger, D. W., T. J. Schmit, and J. M. Daniels, 2003: Imager and Sounder Radiance and Product Validations for the GOES-12 Science Test, NOAA Technical Report 115, U.S. Department of Commerce, Washington, DC.

Schreiner, A. J. and T. J. Schmit, 2001: Derived Cloud Products from the GOES-M Imager. American Meteorological Society. Preprints, 11th Conference on Satellite Meteorology, Madison, WI, 420-423.

Schreiner, A. J. and W. P. Menzel, 2002: Comparison of Cloud Motion Vector Height Assignment Techniques Using the GOES-12 Imager. EUMETSAT, 6th International Winds Workshop, Madison, WI, 301-305.

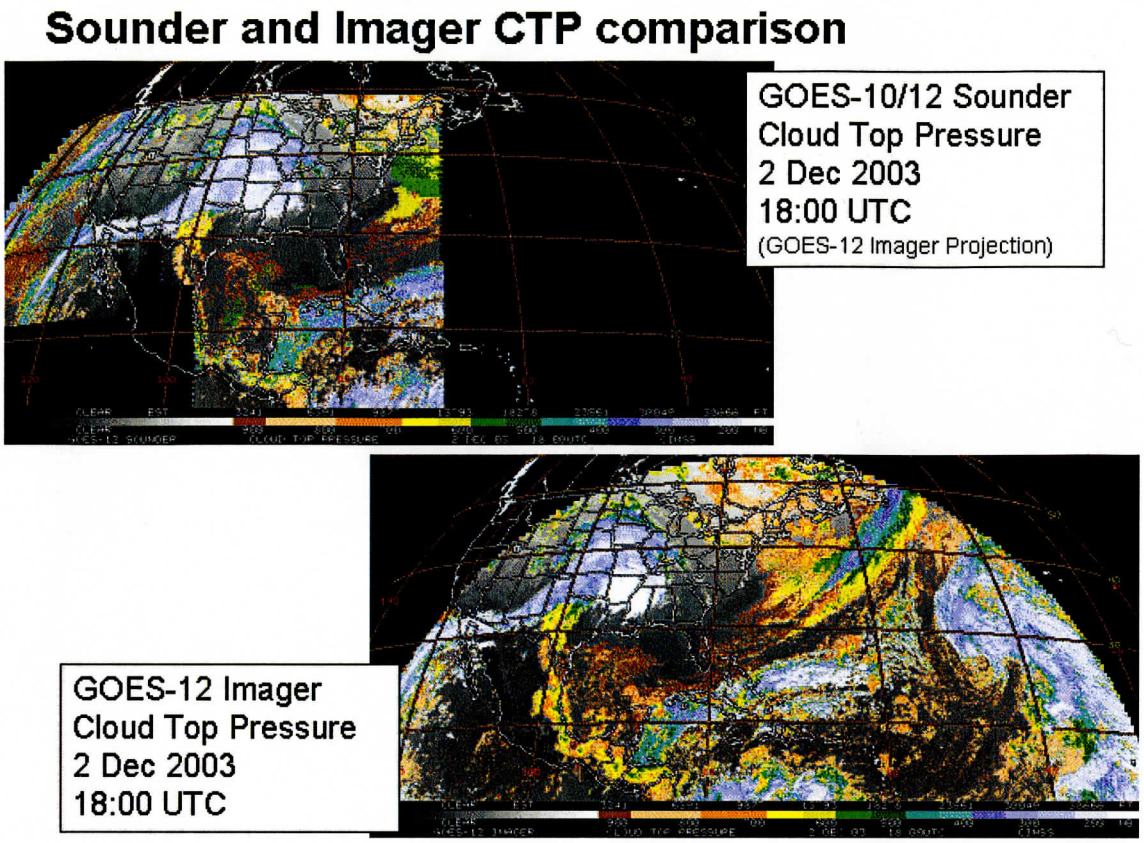

Figure 6. Comparison of areal coverage of the GOES – 10 & –12 Sounder Cloud Product System (upper left) and the GOES-12 Imager Cloud Product System.

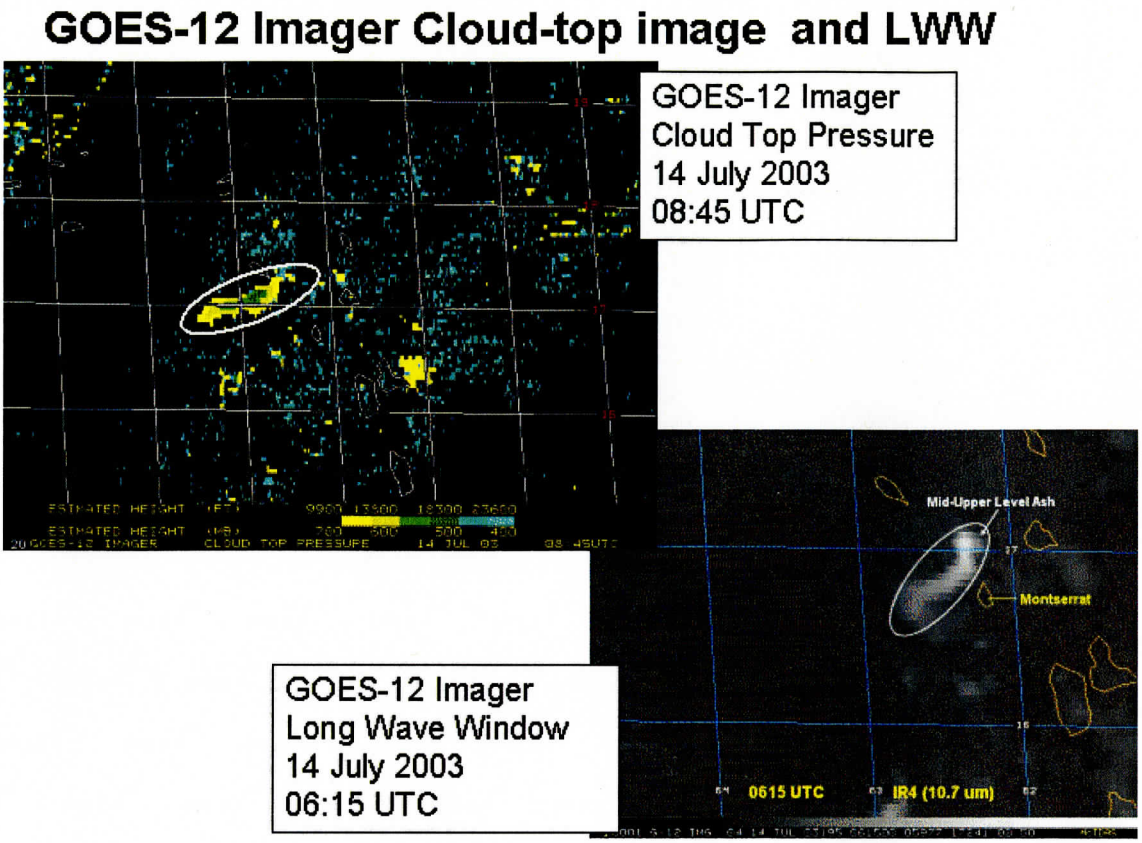

Figure 7. GOES-12 Imager Cloud Top Pressure with a special color enhancement compared to the GOES-12 Imager Long Wave Window including the Volcanic Ash Advisory Center (VAAC) location of the Mid-Upper Level Ash cloud.

2.2 GOES-12 Clear Sky Brightness Temperature

Since November 2001 the CIMSS has been determining Clear Sky Brightness Temperature (CSBT) information from the GOES –8 & -10 Imagers every hour. These observed data are provided through a research collaboration with the National Centers for Environmental Prediction (NCEP) and the European Centre for Medium-range Weather Forecasts (ECMWF) for assimilation into global weather prediction models. Processing frequency is hourly and hemispheric with respect to temporal and spatial coverage (Schreiner et al. 2003).

GOES-8 data were replaced with data from GOES-12 on April 1, 2003. This transition was accomplished after slight modifications were made to account for the loss of the 12.0 μm channel and its replacement with the 13.3 μm. Included in these modifications were changes to the cloud masking algorithm and the output files.

Since late May 2003, the GOES-9 platform has been providing radiance information over the western Pacific Ocean. The satellite is centered over the equator at 155 degrees east

longitude. Each hour, radiances from both the Imager and Sounder instruments are received and utilized to produce meteorologically useful products. From the Imager (visible band plus four infrared bands ranging from 3.9μm to 12.0 μm), hourly CSBT data and corresponding imagery are generated. The GOES-9 Imager CSBT data are being offered to numerical modelers at NCEP, and as of 7 Oct 2003 the CSBT data derived from the GOES-9 water vapor channel (6.75μm) are being assimilated operationally at ECMWF.

In addition to the GOES-9 Imager CSBT data, the GOES-10 & -12 CSBT hourly data from the "water vapor" band are being assimilated operationally at ECMWF (Szyndel et al. 2003). These data are available from CIMSS in Binary Universal Form for the Representation of meteorological data (BUFR) format via anonymous ftp. NCEP is evaluating the data at a six-hour interval.

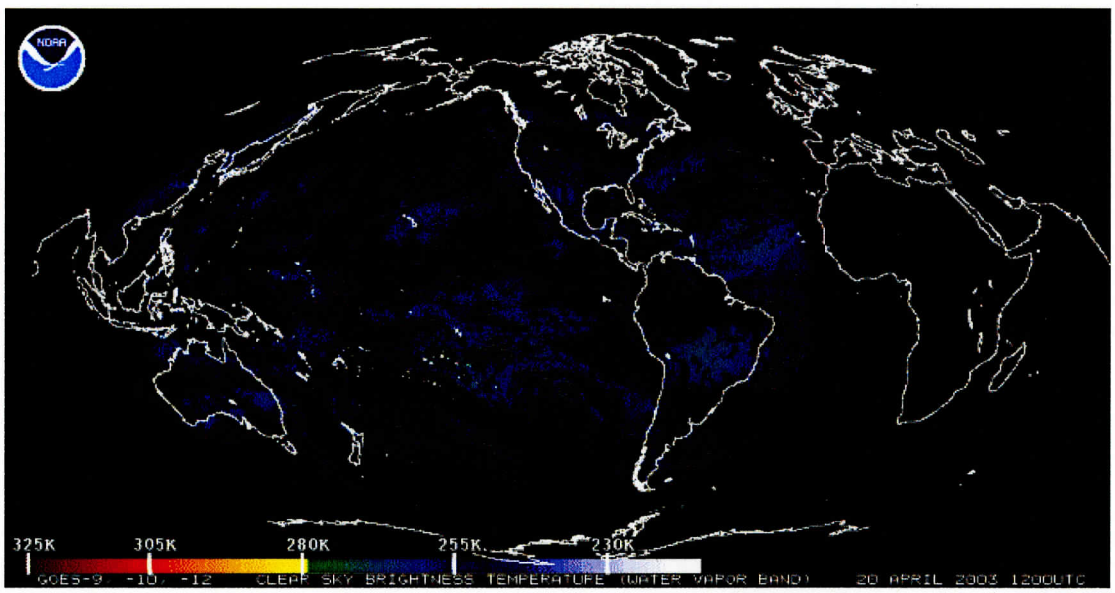

Combined GOES-9/10/12 Imager Coverage for CSBT

Figure 8. Combined GOES – 9,– 10, & – 12 Imager coverage for Clear Sky Brightness Temperature (CSBT) in the Water Vapor Band region (~6.7 μm) for 20 April 2003 at 12 UTC. The color bar represents a range in brightness temperature range for 220K to 325K.

Publications

Schreiner, A. J., T. J. Schmit, C. Kopken, X. Su, C. Holland, and J. A. Jung, 2003: Introducing the GOES Imager clear-sky brightness temperature (CSBT) product. Preprints, *12th Conf. On Satellite Meteorology and Oceanography*, Long Beach, CA, Amer. Meteor. Soc.

Szyndel, M., J.-N. Thepaut, and G. Kelly, 2003: Developments in the assimilation of geostationary radiances at ECMWF. EUMETSAT/ECMWF Fellowship Programme, 1st Year Report, 25 pp.

2.3 Unification of CLAVR

Brief Description of Work
This project aims at unifying and optimizing the different cloud algorithms run within NESDIS on the GOES and POES imager data.

During this period, very little work was done owing to the small amount of hours allotted to this particular task. The main accomplishment was the unification and improvement of the cloud-typing algorithm run on the GOES sounder. We were able to modify the AVHRR cloud type algorithm to run on the GOES sounder. Figure 9 shows an RGB image taken from the GOES sounder and Figure 10 shows the corresponding cloud type image. The cloud types derived from the sounder are now consistent with cloud types produced from AVHRR. This consistency helps NOAA's customers use products from different sensors.

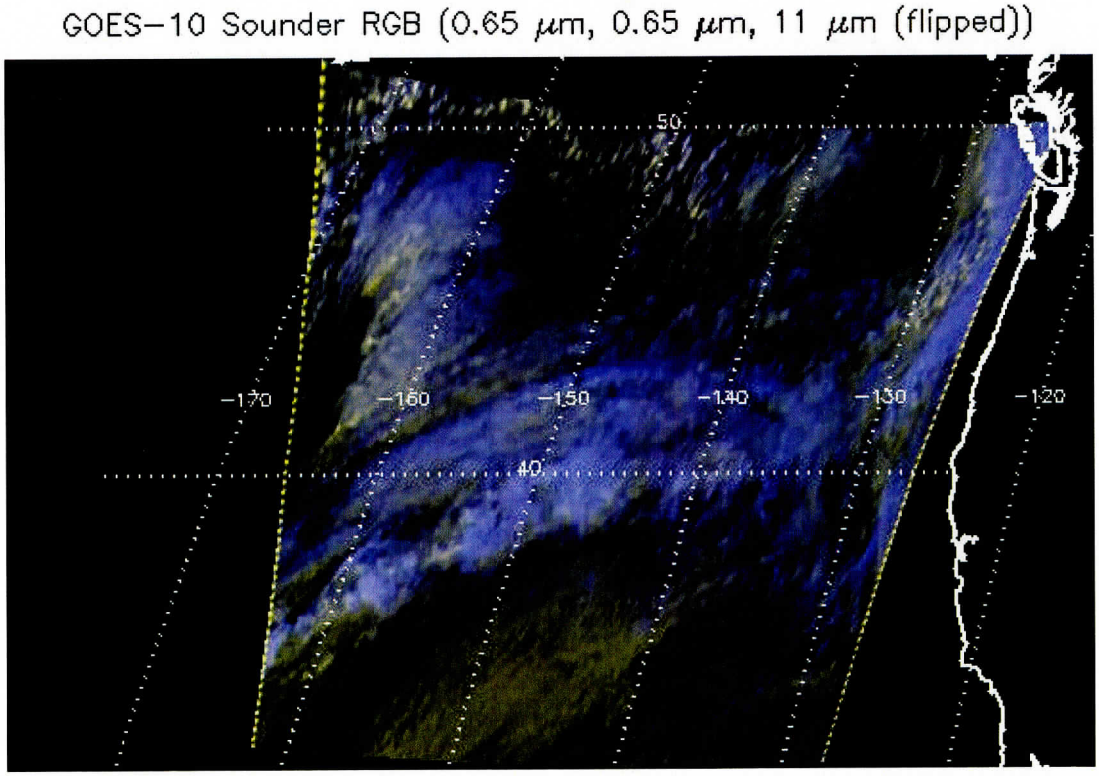

Figure 9. RGB image derived from GOES sounder data.

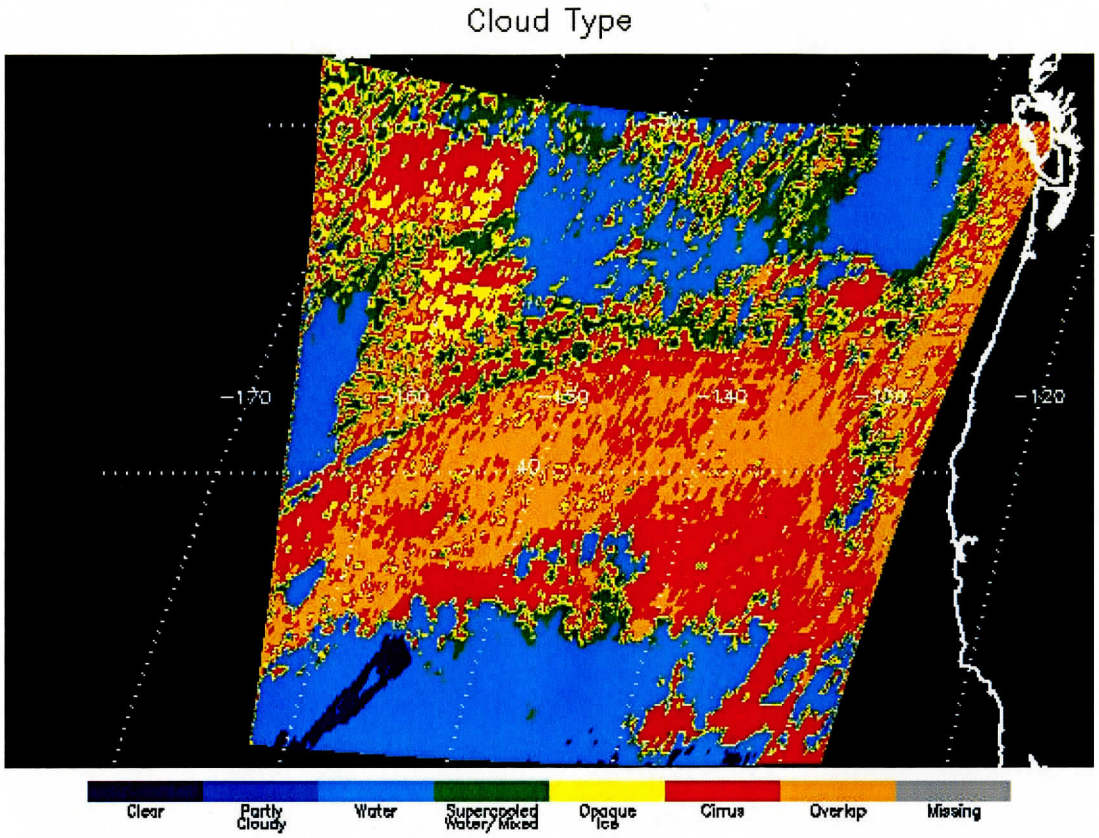

Figure 10. Cloud type results using GOES sounder data.

2.4 GOES Validation Studies using the DOE ARM Site

Background

The Department of Energy Atmospheric Radiation Measurement (DOE ARM) program has been collecting high temporal resolution in situ and remote sensed atmospheric state measurements since 1992. In FY 2003 CIMSS continued to use ground-based in situ and remote sensor meteorological data to validate GOES sounder temperature and moisture profiles as well as sounder derived parameters such as total precipitable water (TPW), stability indices, and cloud top pressure estimates. These measurements can be used to determine the quality of GOES satellite derived atmospheric state products over annual periods of time and provides diurnal rather than conventional synoptic (00 and 12 UTC radiosonde) satellite validation. DOE ARM data will continue to be used to validate current and future GOES sounder derived products.

Accomplishments

GOES-8 sounder 3x3 field of view SFOV TPW data were validated by comparing DOE ARM microwave radiometer (MWR) and radiosonde measurements during the International H_2O Program (IHOP) conducted from 13 May – 25 June 2002. Results indicate that careful decisions must be made when choosing validation sites. Figure 11 shows the dramatic impact GOES physically retrieved water vapor has upon the Eta analysis as compared to a microwave radiometer near Vici, Oklahoma (western OK) while the right plot in Figure 11 shows no improvement to the Eta model near Morris, Oklahoma (eastern OK). This result indicates that

GOES can significantly improve the background water vapor field in data sparse regions where upstream radiosondes and surface information become poor. GOES-12 boundary layer equivalent potential temperature validation against DOE ARM Lamont radiosonde launches from April – May 2003 was also conducted. Results shown in Figure 12 indicate good comparison to DOE ARM radiosondes. Validation of this parameter is crucial for indicating true skill in stability retrieval since lifted index, convective available potential energy, and convective inhibition all fundamentally rely on this measurement. Improvement of SFOV retrievals is ongoing. A two year study inter-comparing DOE ARM consensus cloud boundary products, called the Active Remote Sensing Cloud (ARSCL) data set, and GOES-8 sounder derived cloud top pressure was also completed (Figure 13). A paper has been submitted for peer review and a Master's thesis is available describing the validation project.

Accomplishment summary:

- Provided initial evaluation of GOES-12 sounder derived TPW and stability indices using DOE ARM microwave radiometer and radiosonde data
- Completed an evaluation of GOES sounder derived cloud top pressure using DOE ARM consensus cloud boundary measurements consisting of ground-based lidar, millimeter radar, and ceilometer data for the year 1999-2000
- New automated monitoring of GOES products is in progress

Publications

Feltz, W. F., D. J. Posselt, J. R. Mecikalski, G. S. Wade, and T. J. Schmit, 2003: Rapid Water Vapor Transitions During the IHOP Field Experiment. *Bull. Amer. Meteor. Soc.*, **84**, 29-30

Hawkinson, J. A., W. F. Feltz, and S. A. Ackerman, 2004: A Comparison Study Using the GOES Sounder Cloud Top Pressure Product and Cloud Lidar and Radar. In preparation. To be submitted to the Journal of Applied Meteorology.

Hawkinson, James A. A comparison study using the GOES sounder cloud top pressure products and cloud lidar and radar. Madison, WI, University of Wisconsin-Madison, Department of Atmospheric and Oceanic Sciences, 2003. M.S. thesis. UW MET Publication No.03.00.H1.

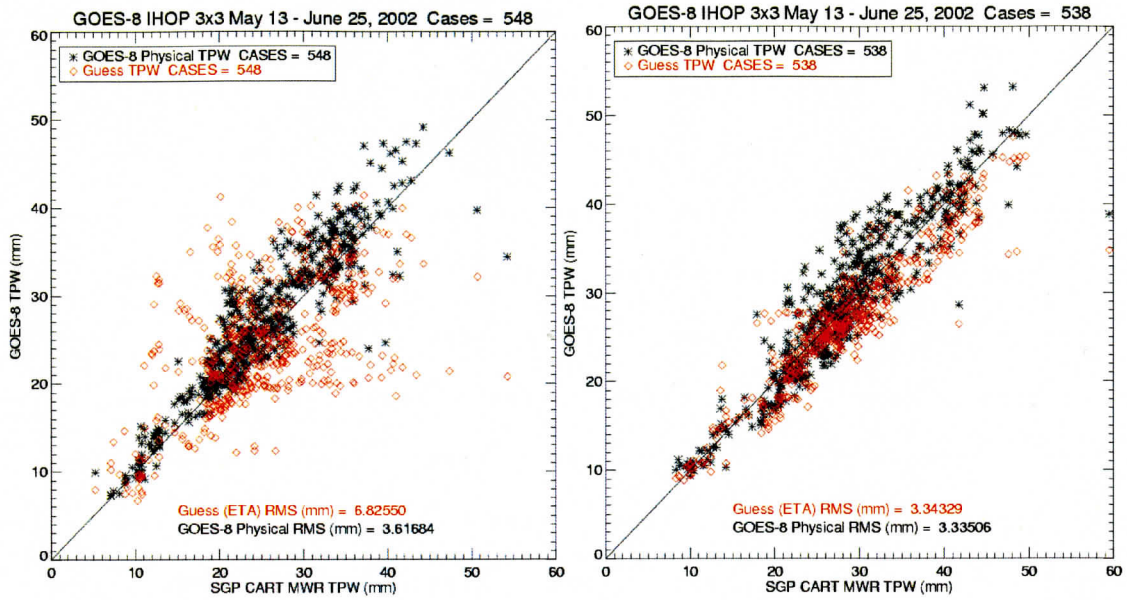

Figure 11. GOES-8 3x3 physically retrieved total precipitable water (TPW; black stars) and the ETA model first guess (red diamonds) compared to microwave radiometer TPW located at Vici (western Oklahoma) and Morris (eastern Oklahoma). Notice the vast improvements the GOES-8 radiances make to the NWP model background from 6.82 mm to 3.61 mm during the IHOP campaign from 13 May – 25 June 2003 near Vici however very little difference is seen between the first guess Eta and GOES-8 derived TPW near Morris with respect to root mean square differences.

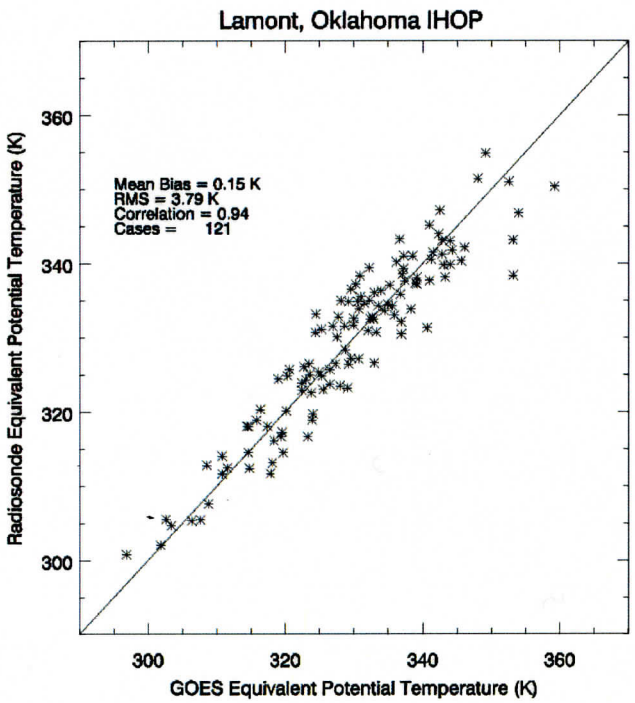

Figure 12. Inter-comparison of GOES-12 derived equivalent potential temperature to radiosondes launched during April, May, and June 2003 at the DOE ARM site. This measurement is fundamental to correctly calculating lifted index, cape, cin, and other stability indices.

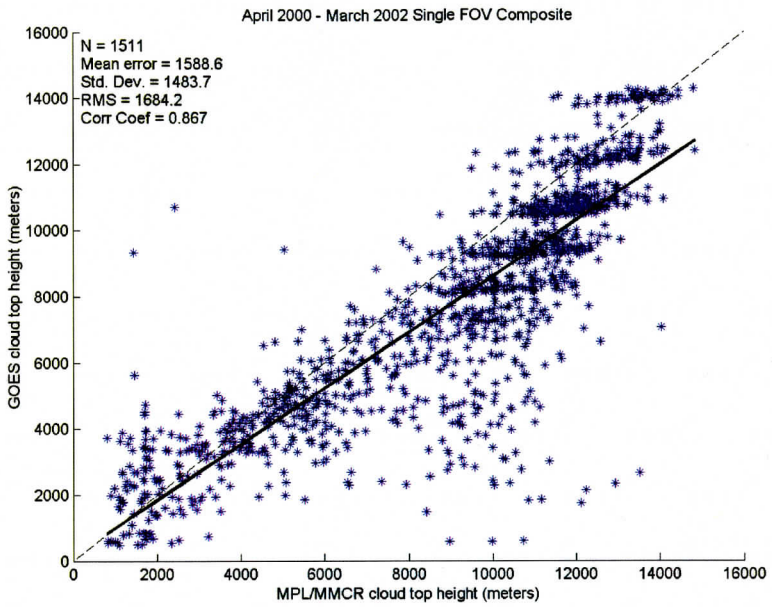

Figure 13. A two year (April 2000 - March 2002) comparison of GOES-8 derived cloud top pressure with a consensus lidar-radar cloud boundary product produced by DOE ARM.

3. Global Observing System Studies

3.1 Intercalibration Studies

The primary purpose of the intercalibration project is to compare the infrared window and water vapor channels on geostationary instruments (GOES, Meteosat, and GMS) by using the same polar-orbiting instrument (NOAA AVHRR and HIRS). This work is accomplished by making multiple comparisons at the geostationary sub-satellite points and finding an average brightness temperature difference between the geostationary imager and the polar orbiter.

Comparison of satellite radiances leading to an improved knowledge of calibration is important for various global applications of satellite data where data from more than one instrument are combined for a single purpose. This information has become increasingly important with the emphasis placed on global climate models and the use of satellite data and products in such models. The Coordination Group for Meteorological Satellites (CGMS) has requested satellite operators to regularly perform satellite intercalibration. Routine intercalibration is an ongoing effort at CIMSS and was covered in fiscal year 2003 by other funding under the cooperative agreement.

Between March and October 2003, the following tasks were accomplished. We began testing the effects of using of a different forecast model, with preliminary results showing negligible differences in the results. We did preliminary comparisons between the GOES-12 Imager and NOAA-15 and –16 HIRS 13.3 micron channels, the results of which would be presented at the annual CGMS meeting held October 2003, along with

the other results from routine analysis. We did not receive Meteosat Second Generation (MSG) data and thus have no preliminary results from comparisons with that instrument; however, we have prepared our software for the eventual intercalibration of MSG. This preparation included posting some calibration coefficients for converting radiance to brightness temperature on the ASPT/CIMSS calibration web page (http://cimss.ssec.wisc.edu/calibration/) and preparing a fast forward radiative transfer model with transmittance coefficient files. We are continuing to build an AIRS case study database. We continue to investigate adding MODIS to the realtime intercalibration package.

A paper was accepted for publication: Gunshor, M. M., T. J. Schmit, and W. P. Menzel, 2003: Intercalibration of the Infrared Window and Water Vapor Channels on Operational Geostationary Environmental Satellites Using a Single Polar Orbiting Satellite. Accepted for publication June 2003 in The Journal of Atmospheric and Oceanic Technology (JTECH).

4. GOES Winds Research

4.1 Refine Automated Algorithms for Tracking Winds from Satellite Imagery

The CIMSS winds tracking algorithm is continuously evolving. New science and developments are allowing for additional data characteristics to be carried forward with each vector retrieval. This work has been coordinated with the new winds BUFR file system recently approved by the WMO. The CIMSS winds-tracking software is being modified to allow for easy adaptation to new instruments. Satellite-specific parts of the software are being identified and isolated, thereby minimizing the effort required for adding new satellites and sensors. Additions and adaptations on the near horizon include MSG, MTSAT, INSAT and GIFTS. The PI (Velden) will visit EUMETSAT next spring to exchange scientific ideas with their MSG and winds specialists. This visit will initiate the adaptation of the CIMSS winds code for processing of winds from MSG.

4.2 Support for Field Program and Data Assessment Goals

There was no direct field program support during this 6-month reporting period. However, there was preparation to support The Hemispheric Observing system Research and Predictability EXperiment (THORPEX), which is a newly formed global atmospheric initiative. The primary goals of this 10-year program are to assess the optimal configuration of our observing system and develop advanced data assimilation methodologies to more effectively utilize the observations to improve high impact weather forecasting. Since the initial field phases of this program are focused on oceanic regions (and eventually a global experiment), satellite observations will be an important contributor to the data impact assessments (see figures below for the first field test domain and milestone plan).

In support of the first field phase of THORPEX in late 2003, CIMSS will collect and process datasets from GOES. NESDIS will employ a scanning strategy for GOES that will include a series of rapid scans (RS), allowing for the generation of high-quality satellite wind sets at CIMSS (some of this activity may be supported under other NOAA funding). The increased temporal resolution of these satellite wind products offers significant potential for a positive impact in rapidly developing 4D assimilation systems that provide the initial conditions for NWP. Efforts during this reporting period include the securing of this GOES schedule, and the setting up of the processing code/scripts to accomplish the dataset retrieval. CIMSS will refine the RS processing methods to optimize the vector output, and work with THORPEX scientists and the data assimilation community towards validating the quality and usefulness of the RS satellite wind products.

4.3 CIMSS Researcher Apprenticeship at UK Met Office

The effective assimilation of satellite winds into numerical weather prediction (NWP) models is an ongoing effort. Coordination between data providers and users (NWP) is an essential element of achieving optimal assimilation strategies. CIMSS researcher Howard Berger is currently stationed at the UK Met Office in Bracknell, England with the primary task of working with UK Met scientists on satellite winds assimilation methods. Preliminary work has focused on improving data thinning methods. Experiments have been designed to reduce the correlated error within the winds by averaging the observations and co-located backgrounds within a box into a superobservation. The new superobbing algorithm and related issues of observation error and quality control should reduce the vector random error and result in improved assimilation of the satellite winds (see figure 14 below for a case study example). Model forecast impact studies are underway and will be evaluated. If the results are positive, we plan to port the methodology to the Joint Center for Satellite Data Assimilation for testing in their analysis system.

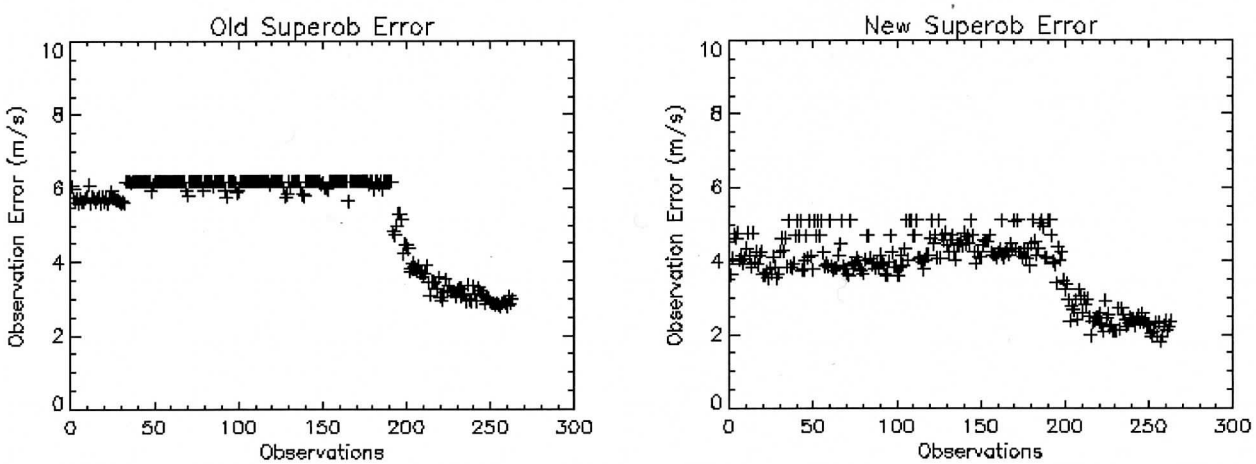

Figure 14. 00z 10 June 2003 (20 N - 40 N) (0E 30 E). Results of Superob improvements.

4.4 Research and Development Items as Identified by the Winds Product Oversight Panel

The Winds POP met to discuss and list items that are high in priority for R&D needs. Current and ongoing topics include product quality assurance and science support, analysis and validation of improved height assignment methods for satellite wind tracers, rapid-scan wind demonstrations, and collaboration with NWP scientists to optimize the assimilation of satellite winds. These topics help guide the CIMSS R&D efforts.

4.5 Investigation of Image Morphing Techniques

This novel approach to applying image "morphing" tools to GOES imagery is in the conceptual stages. The strategy includes creating an image that is interpolated to a time in between the times of two given images, or creating a "projection" of a satellite image into the near future. In many cases, the near future product could be, in fact, a real-time product generated from "near-real-time" imagery. This kind of product could have applications to nowcasting and short-term weather forecasting, as well as in research. The concept is illustrated in Figure 15. Up-to-the-minute estimations of regional satellite imagery would help eliminate the guesswork in directing atmospheric aircraft measurements, or interpreting the measurements afterward. This is especially true when images are missing, or when the work is done in sectors that are viewed by the satellite less often.

Some features of the GOES wind-tracking algorithm are related to the operations used in the field of image morphing (interpreting the navigation of the image, feature tracking, and automated quality control). In fact, morphing is an extension of previous wind-vector determination work. The GOES wind vector results could be an intrinsic part of the morphing process. Morphing requires the identification of control points between successive images, and the wind vector algorithms already have this issue resolved. Furthermore, the wind vectors could be an important guide for the "projection" or "extrapolation" of a near-real-time image into the future. We are beginning to explore these tools and applications.

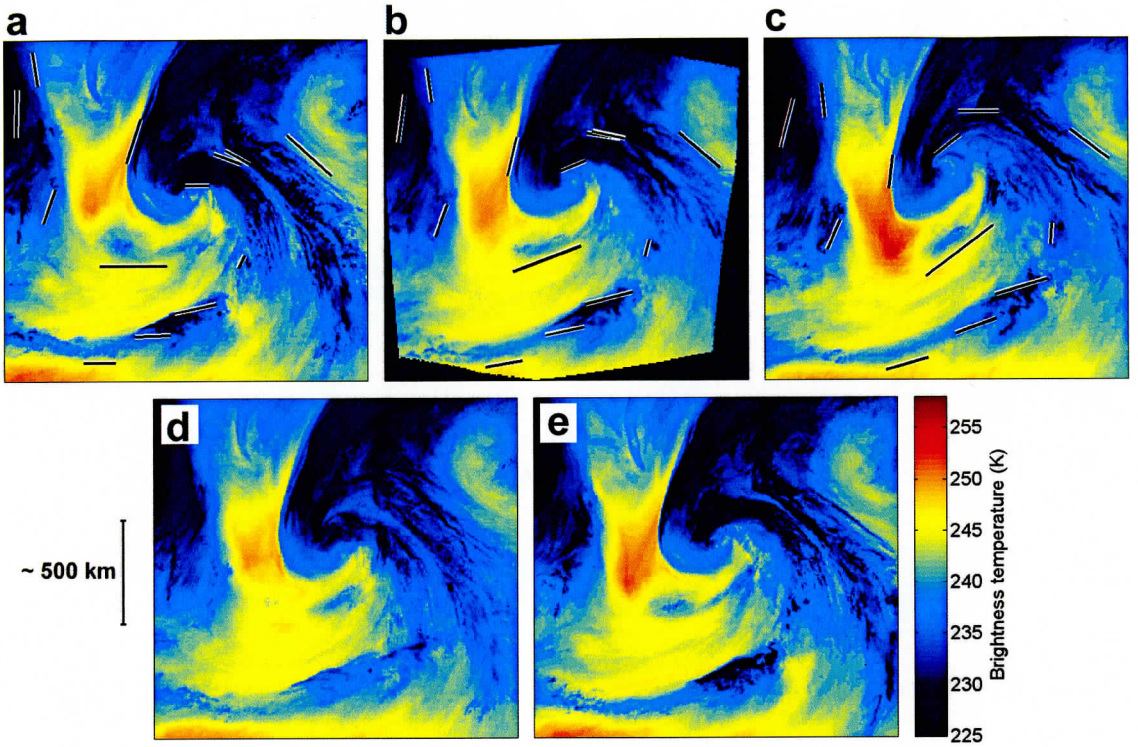

Figure 15. Detail of a mature cyclone in the North Pacific with dry slot (located center-left, in orange and yellow) and comma cloud (located center-right, in blue) from the GOES-W water vapor channel, 9 April 2000. a) Actual image, 0000 UTC, b) Morphed image for 0300 UTC, c) Actual image, 0600 UTC, d) "Cross-dissolve" product, obtained by averaging the pixels from 0000 and 0600 UTC, e) Actual image at 0300 UTC. Black lines on a, b and c are the "guide lines" that control the morphing process. An animation of the morph between 0000 UTC and 0600 UTC is available at http://www.people.virginia.edu/~ajw7g/wvcmorph/

5. GOES Tropical Cyclone Applications

5.1 R&D on Diagnostic Fields Derived from GOES Winds Analyses

An experimental tropical cyclone (TC) diagnostic product was developed in 2002 based on analyses of GOES satellite-derived winds. Fields of vertical wind shear are calculated in the environment of TCs and used to predict short-term intensity changes (see example shear charts below). The diagnostic product derived from the shear charts was run in real time during the 2002 and 2003 Atlantic hurricane seasons (see example below), and results are being evaluated against in situ aircraft observations of TC intensity. Modifications to the algorithm will be based on the quantitative post analysis.

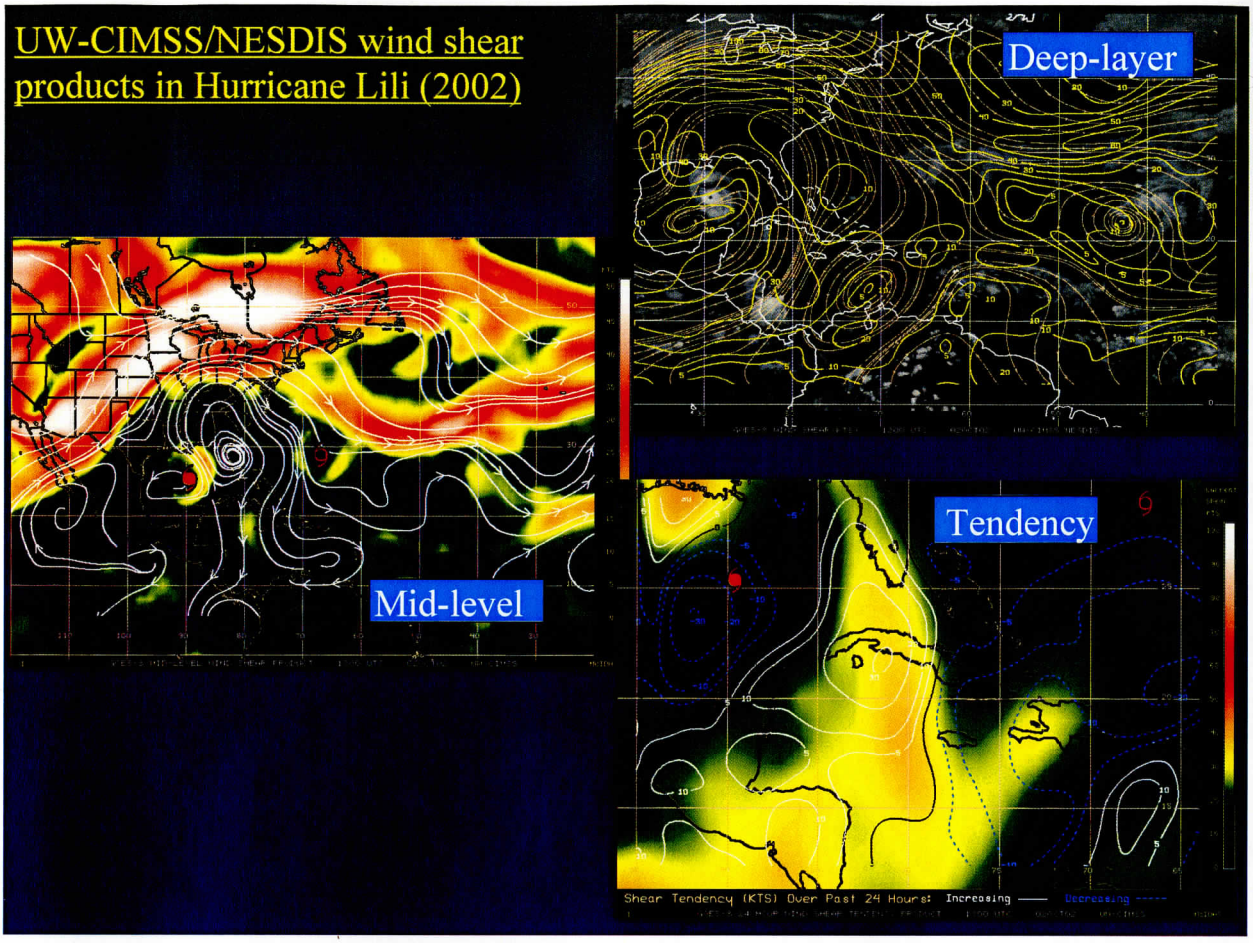

Figure 16. Example of Wind Shear product for Hurricane Lili.

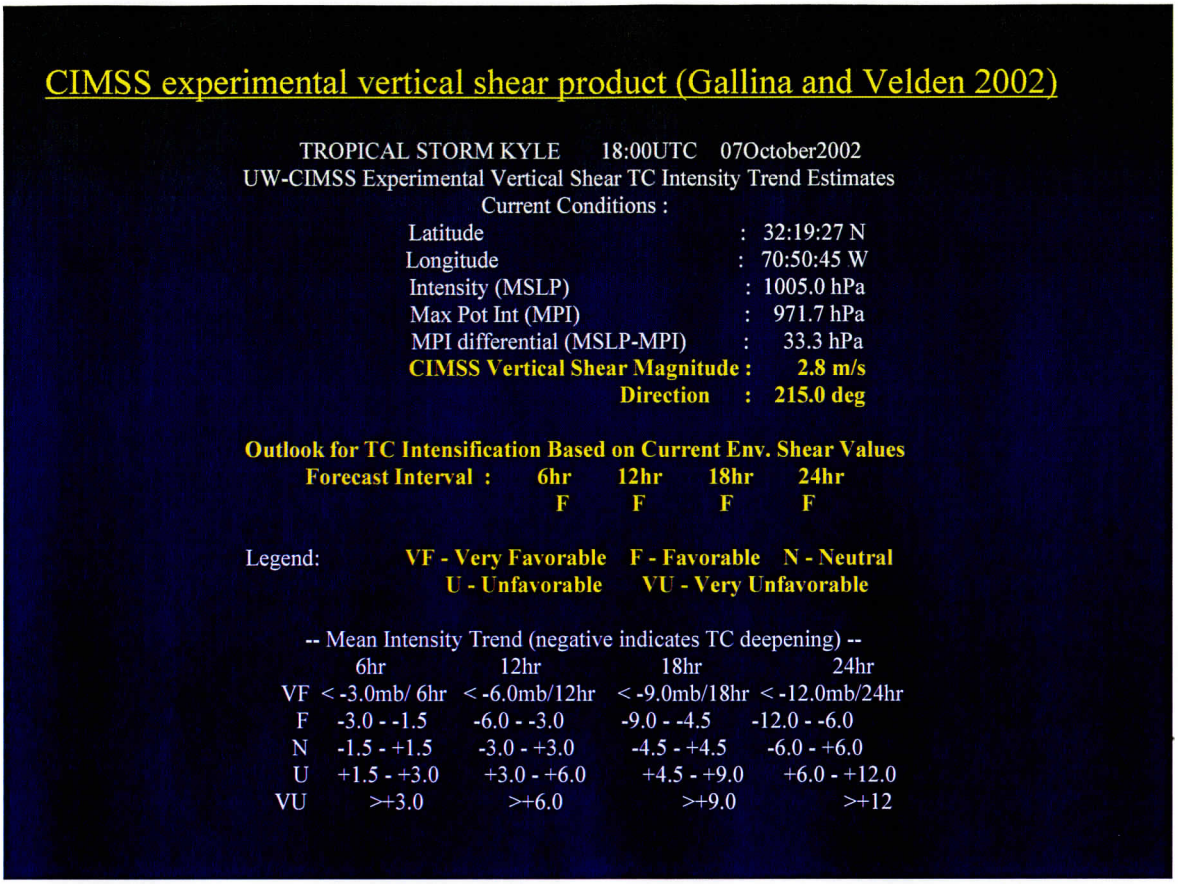

Figure 17. New CIMSS tropical cyclone diagnostic product, which is an objective analysis of the current shear, and the outlook of TC intensity based on a statistical analysis of the shear vs TC intensity behavior. This product is being disseminated in real time every 6 hours via email distribution to the international TC community for feedback.

5.2 Identifying Saharan Air Layer Influencing TC Genesis from GOES

A promising new tool for diagnosing TC genesis and intensity behavior was tested during the 2002 Atlantic hurricane season. A GOES-8 split window algorithm was used to identify the Saharan Air Layer (SAL) around TCs (see example below). The SAL originates over the dry African continent. Frequent SAL surges are observed in the split window imagery as a result of dust and dry air which accompany the SAL as they move off of the continent and into the maritime Atlantic. If TCs are developing or present, their intensity behavior can be negatively impacted by the SAL surges; however, more study is needed.

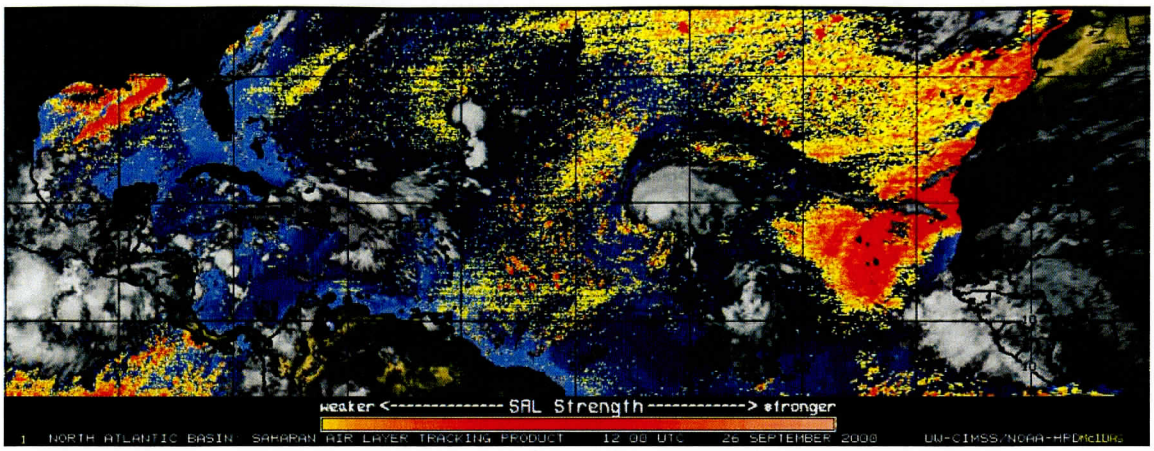

Figure 18. Example of the CIMSS Saharan Air Layer product developed from GOES split-window imagery.

CIMSS has since adapted the product to GOES-12 after it replaced GOES-8. Due to the loss of one of the split-window channels on GOES-12, the product was adapted to use the 3.9 micron channel (daylight applications only). We also hope to explore the use of MSG channels towards this application, once the data become available sometime in 2004. Tropical rawinsondes and special aircraft dropwindsondes are being used to tune and validate the GOES-12 SAL product. Studies are in progress to associate TC behavior with SAL interaction.

5.3 The Advanced Objective Dvorak Technique (AODT)

We continue research studies to improve the AODT algorithm with scientific upgrades focusing on the following primary areas: 1) refinement of the automated TC center finding routine, 2) improvement in the curve-banding scene type analysis for weak systems, 3) evaluation of the rapid intensification cases and AODT performance, and 4) further examination of the automated scene-typing to reduce the need for manual over-rides. Our goal is to complete the evaluation of these upgrades on case studies from the 2003 TC season, and test them during the 2004 season.

6. Biomass Burning Studies

6.1 Biomass Burning Studies

Proposed Work
As part of the GIMPAP research program at CIMSS, the biomass burning monitoring team proposed the following research activities:

- Complete an 8-year trend analysis of fire/smoke/cloud activity in South America as determined with the GOES-8 South American Automated Biomass Burning Algorithm (ABBA) and Merged Automated Cloud/Aerosol Detection Algorithm (MACADA).

- Complete an 8-year comparison of the GOES South American ABBA fire product and the Brazil Instituto Nacional de Pesquisas Espaciais (INPE) Advanced Very High Resolution Radiometer (AVHRR) fire product.
- Continue analyses of the GOES Wildfire ABBA fire product for the Western Hemisphere for applications in hazards, climate change, land-cover/land-use change studies, and fire dynamics modeling.
- Continue collaborations with the atmospheric modeling community to assimilate the GOES Wildfire ABBA fire product into aerosol/trace gas transport models in real time.
- Integrate GOES Wildfire ABBA fire products with satellite derived aerosol and gas phase products.

Accomplishments

CIMSS completed an 8-year (1995-2002) trend analysis of fire, smoke, and cloud activity using the GOES-8 South American ABBA and MACADA. An 8-year comparison of the GOES South American ABBA fire product and the Brazil INPE AVHRR fire product was also completed. Results of these multi-year studies were included in the semi-annual report and will be submitted for publication. For South American fire monitoring, the GOES-8 ABBA has been phased out and replaced with the next generation Wildfire Automated Biomass Burning Algorithm (WF_ABBA). The GOES WF_ABBA is a more robust algorithm allowing for half-hourly fire detection and monitoring throughout the Western Hemisphere. Comparisons of GOES-8 ABBA fire products and the WF_ABBA fire products for South America show that the WF_ABBA has fewer false alarms and is capable of identifying short-lived agricultural fires along the arc of deforestation. The WF_ABBA is also able to detect more of the grassland fires in eastern Brazil. In the state of Acre, Brazil, CIMSS is collaborating with a consortium of international government and university research centers and environmental policy groups to study land cover and land use change and carbon dynamics in the Western Amazon. GOES ABBA fire products are being used to aid in determining land use, deforestation, and fire regimes in the region. The region of Acre, Brazil is the new frontier where land-use and land-cover change has accelerated in recent years along a new road being built across the Andes from Brazil to Peru. Preliminary comparisons of GOES, MODIS, and AVHRR fire products in this region show that the diurnal and high temporal GOES WF_ABBA fire product reports much more fire activity in the region than observed with MODIS or AVHRR with minimal false alarms. Applications of the GOES ABBA and WF_ABBA in South America and comparisons with the Brazilian INPE fire product were presented at the 11th Brazilian Remote Sensing Symposium held in Belo Horizonte, Brazil in April 2003.

The GOES half-hourly WF_ABBA fire product for the Western Hemisphere continues to be produced in near real-time through cost sharing with the NASA Earth Systems Enterprise (ESE) program. The product includes ASCII text files and alpha-blended composite fire imagery. Animations are made available to the user community via the web at http://cimss.ssec.wisc.edu/goes/burn/wfabba.html. The user community includes climate change scientists, the aerosol and trace gas transport modeling community, the land-use and land-cover change detection research community, government agencies,

resource managers, fire managers, international policy and decision makers, educational institutions, and the general public. The GOES WF_ABBA ASCII text files are provided via an anonymous FTP site at CIMSS. The GOES-10/-12 WF_ABBA half-hourly data set provides unique insights into the timing and geographic distribution of wildfires and agricultural burning throughout the Western Hemisphere. Analysis of the Western Hemisphere data set is an extension of the analyses performed in South America with the GOES-8 ABBA.

CIMSS completed a three-year analysis of fire activity throughout the Western Hemisphere as detected by the WF_ABBA in half-hourly GOES-8/-10/-12 data. Results show that the overall distribution of fire activity remains similar in North, Central and South America from year to year with regional differences. During the past year, the relative breakdown of fire activity in North, Central and South America was slightly different than what was observed during the first two years. 82% of all fire pixels detected in the Western Hemisphere were located in South America, while 6% were identified in North America, and 12% in Mexico and Central America (Figure 19). In terms of the percent of the total number of fires detected throughout the Western Hemisphere, this represents a significant decrease for North America and a slight increase for Central America and South America. Overall, the total number of fire pixels detected in Central and South America increased by 12 and 7%, respectively. It decreased by 45% in North America, with a 33% decrease in the number of processed fire pixels, a 52% decrease in the number of saturated pixels, and a 50% decrease in low possibility fire pixels. This change primarily reflects the decrease in wildfire activity in the Western United States after the exceptionally busy wildfire season in 2002. Furthermore, the large decrease in low possibility fire pixels in North America is associated with changes in version 6.0 of the Wildfire ABBA that helped to reduce low possibility false alarms typically observed in North America. Central America fire statistics show a 23% increase in processed fire pixels, an 86% increase in saturated pixels, a 9% increase in low possibility fire pixels and a 99% increase in cloud-covered fire pixels. In South America there was a 14% increase in processed fire pixels, a 15% increase in saturated fire pixels, and 9% decrease in the number of low possibility fire pixels. These results show that both Central and South America saw increases in fire activity during the past year.

CIMSS collaborated with a number of groups in the air quality and atmospheric chemistry user community. As part of the Integrated Program on Urban, Regional, and Global Air Pollution (Massachusetts Institute of Technology), the GOES WF_ABBA fire product is supporting a multinational effort to study air pollution in megacities around the globe. Initial research efforts have focused on Mexico City, including atmospheric modeling; health and risk assessment; and transportation, land-use, and urban development. The Wildfire ABBA fire product is being used to distinguish between air pollution from urban sources and from biomass burning. Within the United States new regulations regarding PM-2.5 (particulate matter with mass median aerodynamic diameter less than 2.5 microns) have resulted in a number of collaborations regarding the impact of biomass burning on air quality. In September and October 2003 CIMSS

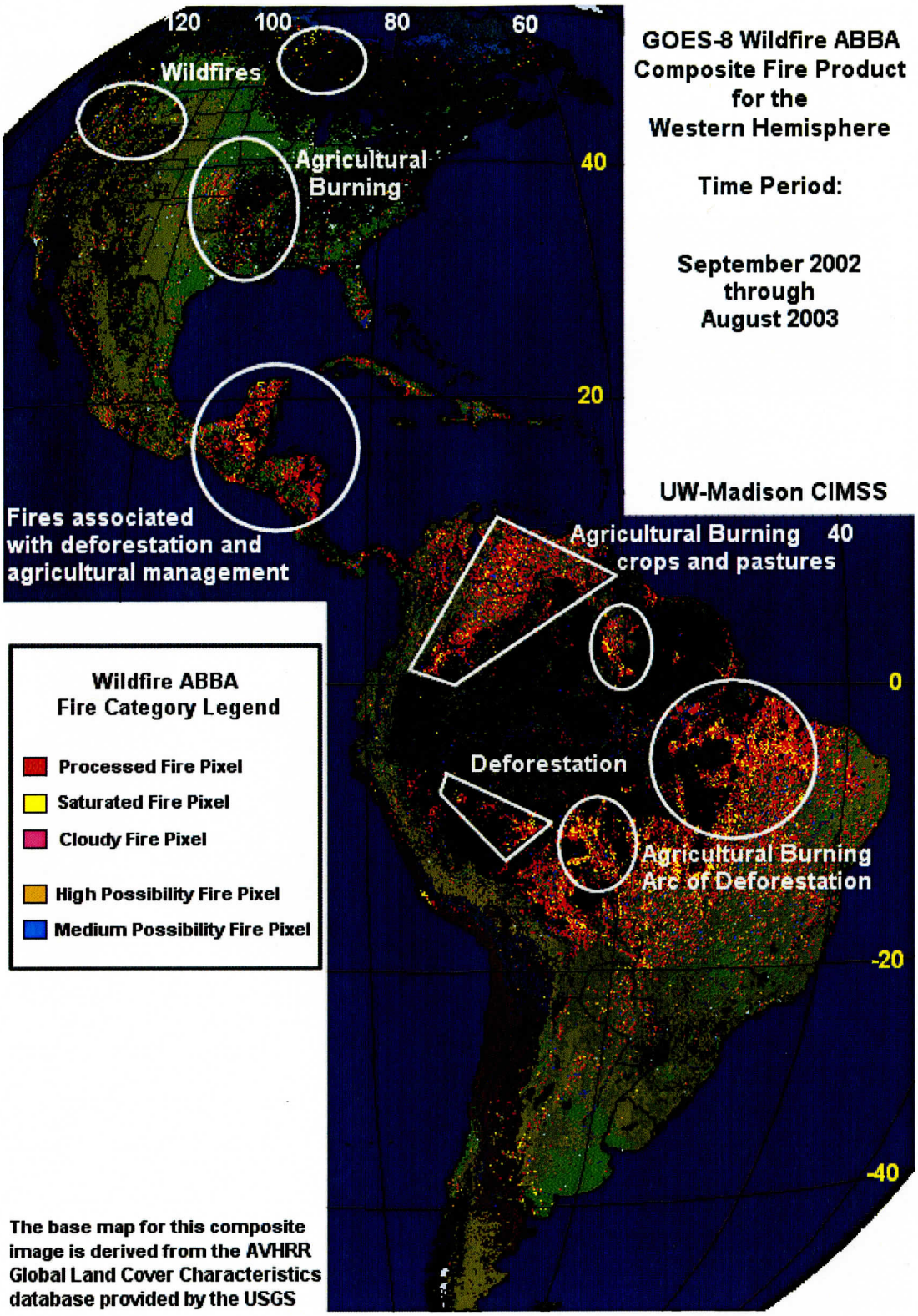

Figure 19. GOES-8/-12 WF_ABBA filtered fire pixel composite for the Western Hemisphere for the time period September 1, 2002 through August 31, 2003. All filtered half-hourly fire product data are represented in this image, except low possibility fires.

participated in an air quality assessment and forecasting demonstration project hosted at NASA Langley. The WF_ABBA fire products were integrated into a real-time web site to provide insight on the impact of fires on regional air quality. This effort is part of the NASA IDEA (Infusing satellite Data into Environmental Applications) program with the goal of improving air quality assessment, management, and prediction by infusing satellite measurements into analyses for public benefit.

CIMSS continues to collaborate with a number of modeling groups who are assimilating GOES Wildfire ABBA fire products into aerosol/trace gas diagnostic and prognostic transport models. CIMSS involvement includes providing the fire products in near real-time and working with the modelers on how to interpret and incorporate the Wildfire ABBA data into their models. The U.S. Navy is assimilating half-hourly GOES-10/-12 ABBA fire products in the NAAPS (Navy Aerosol Analysis and Prediction System) model in real time to analyze and predict aerosol loading and transport. This effort is possible through cost sharing with funding from the NASA ESE program and NASA funding has been extended through 2006. The University of Sao Paulo and the Brazilian INPE CPTEC are assimilating GOES South American Wildfire ABBA fire products to analyze biomass burning emissions such as ozone and CO. Both of these efforts have resulted in accepted peer reviewed manuscripts. There have been a number of new data assimilation collaborations utilizing the Georgia Tech/Goddard Global Ozone Chemistry Aerosol Radiation and Transport (GO-CART) model and the EPA Community Multiscale Air Quality (CMAQ) model to study aerosol transport and regional air quality issues.

The CIMSS biomass burning team continues to investigate how products derived from both operational and research satellites can be used to gain a better understanding of the role of biomass burning on both regional and global air quality and climate change. Much of this work has focused on case studies of biomass burning emissions in North, Central, and South America. CIMSS recently received funding from NASA's EOS/IDS ESE's Modeling and Data Analysis Research program to extend this work to other parts of the globe by comparing global geostationary fire products with other satellite derived aerosol and trace gas products (e.g. Envisat GOMOS (O_3) and SCIAMACHY (O_3, CO); EOS Aqua AIRS (CO); ADEOS-2 POLDER (aerosol); or CALIPSO (aerosol); etc). This effort involves cost sharing with GIMPAP.

6.2 Global Observing System Studies

As part of the GIMPAP research program at CIMSS, the biomass burning team proposed the following research activities.

- Adapt the GOES WF_ABBA for application with METEOSAT Second Generation (MSG).

Initial assessment studies of MSG SEVIRI fire detection capabilities have been completed. Adaptation of the WF_ABBA code for application with MSG will begin with

the release of calibrated/navigated SEVIRI data in McIDAS format.

CIMSS is working in cooperation with the IGOS (Integrated Global Observing Strategy) GTOS (Global Terrestrial Observing System) GOFC/GOLD (Global Observation of Forest and Land cover Dynamics) program on the development and implementation of a global geostationary fire detection system utilizing GOES-E/-W, MSG, and MTSAT-1R.

Publications

Cardosa, M. F., G. C. Hurtt, B. Moore III, C. A. Nobre, and E. Prins, 2003: Projecting future fire activity in Amazonia. *Global Change Biology*, **9**, 1-14.

Freitas, S. R., K. M. Longo, M. A. F. Silva Dias, P. L. Silva Dias, F. S. Recuero, R. Chatfield, E. Prins, P. Artaxo, F. S. Recuero, 2003: Monitoring the transport of biomass burning emissions in South America. Accepted by *Environmental Fluid Dynamics*.

Reid, Jeffrey R., E. M. Prins, D. L. Westphal, C. C. Schmidt, K. Richardson, S. Christopher, T. F. Eck, E. A. Reid, and J. Hoffman, 2003: Real-time modeling of South American smoke particle emissions and transport using a coupled remote sensing/box-model approach. Accepted by *Geophysical Research Letters*.

Weaver, J. F., D. Lindsey, D. Bikos, E. Prins, and C. Schmidt, 2003: Fire Detection using GOES-11 Rapid Scan Imagery. Accepted by *Weather and Forecasting*.

Conference Papers/Posters:

Eck, T. F., B.N. Holben, J.S. Schafer, P. Artaxo, M.A. Yamasoe, A.S. Procopio, E.M. Prins, J. M. Feltz, A. Smirnov, O. Dubovik, and J. Reid, 2002: Inter-annual Variability of Biomass Burning Aerosol Optical Depth in Southern Amazonia, and the Impact of These Aerosols on the Diurnal Cycle of Solar Flux Reduction. AGU Fall Meeting, December 6-10, 2002.

McClaid-Cook, K., D. Selhorst, J. Widson, N. Vidal Pantoja, I. F. Brown, E. M. Prins, J. M. Feltz, A. A. Fonseca Duarte, 2003: Estimation of Amazonian biomass burning events in Acre, Brazil using GOES-8 and AVHRR hot pixel data. The 99th Annual Meeting of the Association of American Geographers, New Orleans, Louisiana, March 5-8, 2003, 8 pp.

Feltz, J. M., E. M. Prins, A. W. Setzer, 2003: A Comparison of GOES-8 ABBA and INPE AVHRR Fire Products for South America from 1995 to 2002. Provided for the XI Brazilian Remote Sensing Symposium Special Session on Satellite-derived fire and burn scar products throughout the Amazon, Belo Horizonte, Brazil, April 7-10, 2003.

Prins, E. M., C. C. Schmidt, J. M. Feltz, J. S. Reid, D. L. Wesphal, and K. Richardson, 2003: A two-year analysis of fire activity in the Western Hemisphere as observed with the GOES Wildfire Automated Biomass Burning Algorithm. Preprints, 12th Conf. on Satellite Meteorology and Oceanography, Long Beach, CA, Amer. Meteor. Soc., CD-ROM, P2.28.

Prins, E. M., C.C. Schmidt, J. M. Feltz, 2003: Fire detection with GOES. Provided for the XI Brazilian Remote Sensing Symposium Special Session on Satellite-derived fire and burn scar products throughout the Amazon, Belo Horizonte, Brazil, April 7-10, 2003.

Reid, J. S., D. L. Westphal, M. Liu, K. Richardson, C. Justice, E. M. Prins, S. Miller, 2003: Detection, modeling, and impacts of biomass and oil fires. Submitted to the Battleship Atmospheric and Cloud Impacts on Military Operations (BACIMO) Conference, Monterey, CA, September 9-11, 2003.

II. PDSI: CIMSS Research in Support of Geostationary and Polar Orbiting Weather Satellite Science Topics

1. Cloud-Drift and Water Vapor Winds in the Polar Regions from MODIS

Geostationary satellite radiance measurements have been used to generate cloud-drift winds in the low- and mid-latitudes of the western hemisphere for more than two decades. Fully automated cloud-drift wind production from the Geostationary Operational Environmental Satellites (GOES) became operational in 1996, and wind vectors are routinely used in operational numerical models of the National Centers for Environmental Prediction (NCEP). Unfortunately, GOES is of little use at high latitudes due to the poor viewing geometry. The objective of this project is to generate wind vectors over the polar regions from polar-orbiting satellites. Of primary interest is the MODIS instrument on NASA's Terra and Aqua satellites. Our goal is to provide an experimental wind product that can be used in numerical weather prediction systems.

The project Principal Investigator at CIMSS is Christopher Velden. David Santek is performing the analyses and oversees the implementation and modification of McIDAS (Man computer Interactive Data Access System) and heritage wind generation software for use with MODIS. Jeff Key, NOAA/NESDIS, works on the project in collaboration with CIMSS scientists, and is the NESDIS point of contact for the project. The project is funded through the NOAA/OSD PSDI process.

Accomplishments

Over the past six months we have continued the real-time generation of the MODIS polar winds product from both Terra and Aqua. The data are made available to users via anonymous ftp. MODIS data are acquired directly from a NOAA computer at NASA Goddard Space Flight Center (thanks to Gene Legg, NESDIS/OSDPD, and Mitch Goldberg, NESDIS/ORA). The lag between the time of the MODIS overpass to the availability of wind vectors is typically 3-5 hours. An example is shown in Figure 20.

We have been working with the NASA Global Modeling and Assimilation Office (GMAO, formerly the Data Assimilation Office) and the European Centre for Medium-Range Weather Forecasts (ECMWF) on the impact of the polar winds on numerical weather prediction (NWP) model forecasts. Both have shown a positive impact in the

Arctic, Northern Hemisphere extratropics, and the Antarctic for a 30-day case study in March-April 2001. The Canadian Meteorological Centre (CMC), the UK Met Office, and the Fleet Numerical Meteorology and Oceanography Center (U.S. Navy) are now also using the real-time winds in their experimental systems. As of January 14, 2003, ECMWF began assimilating the MODIS polar winds in their operational weather forecasting system. (ECMWF understands that this is an experimental product generated by CIMSS for scientific research, not an operational product.)

In October 2003 we held a workshop on polar winds in Fairbanks, Alaska. The polar winds workshop was held as a special session of the "Workshop on Short- to Medium-Range Regional Numerical Weather Prediction (NWP) in the Arctic and Antarctic" at the International Arctic Research Center (IARC), University of Alaska. Speakers for the polar winds workshop were from CIMSS, NOAA NESDIS (J. Daniels and J. Key), the European Centre for Medium-Range Weather Forecasts (ECMWF), the NASA GMAO, the UK Met Office, and the Canadian Meteorological Centre.

Publications

Key, J., D. Santek, C. S. Velden, N. Bormann, J.-N. Thepaut, L. P. Riishojgaard, Y. Zhu, and W. P. Menzel, 2002: Cloud-drift and Water Vapor Winds in the Polar Regions from MODIS. *IEEE Trans. Geosci. Remote Sensing*, **41**(2), 482-492.

Santek, D., J. Key, and C. Velden, 2003: Real-time Derivation of Cloud Drift and Water Vapor Winds in the Polar Regions from MODIS Data. *Proceedings of the 12th Conf. on Satellite Meteorology and Oceanography*, American Meteorological Society, Long Beach, CA, 9-13 February 2003.

Bormann, N., J-N. Thépaut, J. Key, D. Santek, and C. Velden, 2002: Impact of polar cloud track winds from MODIS on ECMWF analyses and forecasts. *Proceedings of the 15th Conf. on Numerical Weather Prediction*, American Meteorological Society, San Antonio, TX, 12-16 August, 2002.

Key, J., D. Santek, C. S. Velden, and W. P. Menzel, 2001: Cloud-drift and water vapor winds in the polar regions from MODIS. Proceedings of the 11th Conference on Satellite Meteorology and Oceanography, American Meteorological Society, Madison, Wisconsin, 15-18 October 2001, 320-323.

Key, J., C. Velden, and D. Santek, 2001: High-latitude cloud-drift and water vapor winds from MODIS. Proceedings of the Sixth Conference on Polar Meteorology and Oceanography, American Meteorological Society, San Diego, 14-18 May 2001, 351-354.

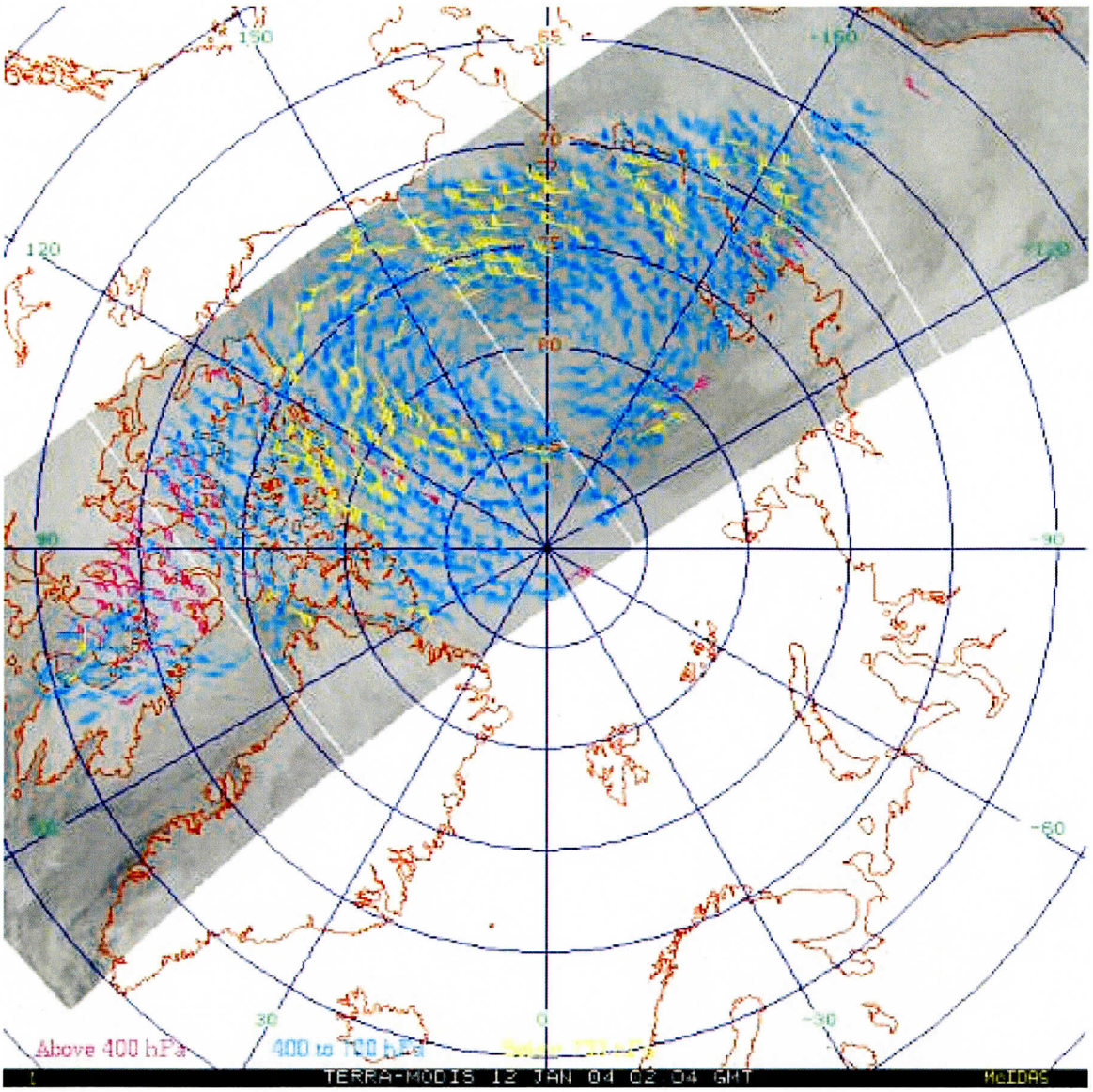

Figure 20. An example of the MODIS polar winds over the Arctic on January 12, 2004. The wind vectors are derived from a triplet of orbits and plotted on the infrared image of the middle overpass. Wind vectors are categorized as low, middle, and high for display purposes.

2. GOES Winds

CIMSS has supported the research and development of the automated satellite winds tracking software for the last 25 years. Under this funding, the CIMSS winds research team is committed to help maintain and advance the winds algorithm science modules and capabilities. This includes any new science advances, validation, and developments for the science community.

The primary accomplishment during this reporting period was the assessment and model impact evaluation of the GOES rapid-scan winds collected and processed during the third GOES rapid-scan WINDs Experiment (GWINDEX-3) conducted in the spring of 2003. The experimental rapid-scan winds were assimilated into the Rapid Update Cycle (RUC) model in case-study mode by the NOAA Forecast Systems Lab research group. Small but encouraging positive impacts were found with short-term model forecasts. Further investigations are underway.

3. GOES Wildfire ABBA

Proposed Work

The CIMSS biomass burning monitoring team proposed the following:

- The current GOES-8/-10 WF_ABBA will be modified for application with subsequent GOES platforms (GOES-11,-12).
- The WF_ABBA will be modified to reduce false alarms and minimize the number of actual fires eliminated by temporal filtering techniques.
- CIMSS will participate in satellite fire product validation and inter-calibration activities.
- CIMSS will produce half-hourly WF_ABBA fire products in real time and make them available via the web and anonymous ftp.

Accomplishments

During the previous 6 months, the WF_ABBA software and processing system was adapted for application with GOES-12 and was implemented in March 2003. The WF_ABBA processing system was also modified to better facilitate transition from one platform to another. In response to requests from the hazards community, the WF_ABBA processing system was modified to reduce the latency. GOES-12 WF_ABBA fire product ASCII files are now available via anonymous ftp within 20-25 minutes of the GOES-12 image time. The alpha-blended composite fire imagery are made available on the web (http://cimss.ssec.wisc.edu/goes/burn/wfabba.html) within approximately 30 minutes. CIMSS also completed a study to investigate the utility and capabilities of a rapid scan GOES WF_ABBA. Using high temporal (rapid scan) GOES-11 data, the WF_ABBA was able to identify several wildfires near or before the initial reported start times during the 2002 fire season, suggesting the need to dedicate resources for rapid WF_ABBA processing and dissemination for early wildfire detection applications in the U.S.

CIMSS is involved in several ongoing WF_ABBA validation and inter-calibration activities. In South America, validation and multi-sensor comparison studies continue in the state of Acre, Brazil. In the North-Central plains, the Nature Conservancy provided information regarding prescribed burns and wildfires observed on Nature Conservancy land during the spring of 2003, primarily in the state of Minnesota. The burned vegetation included prairie/grassland, savanna/woodland, forest and wetland and ranged in size from 45 acres to 12000 acres. Of the 24 reported fires, the WF_ABBA detected

nearly half of them. The WF_ABBA also detected additional fires that were not observed in real-time.

CIMSS completed a validation study in Quebec, Canada in collaboration with M. Moreau (Environment Canada/Meteorological Services/Quebec Region) (Figure 21). During the 2002 fire season (June 18 through July 20, 2002) in Quebec, the Societe de protection des forets contre le feu (SOPFEU) fire agency reported 111 fires for the Quebec region. During this time period the GOES-8 WF_ABBA filtered fire product recorded over 8,000 hot spots in Quebec. Many of these detects represent the same fire. More than 30 individual fires were detected in the restrictive protection zone that were ignored by SOPFEU. In many cases, the WF_ABBA fire report was the first. In one case, the WF_ABBA detected a fire 17 days in advance of the first fire agency report. This fire eventually burned more than 55,000 hectares. Comparisons with ground truth showed that only 3% of the temporally filtered WF_ABBA hot spots were false detects.

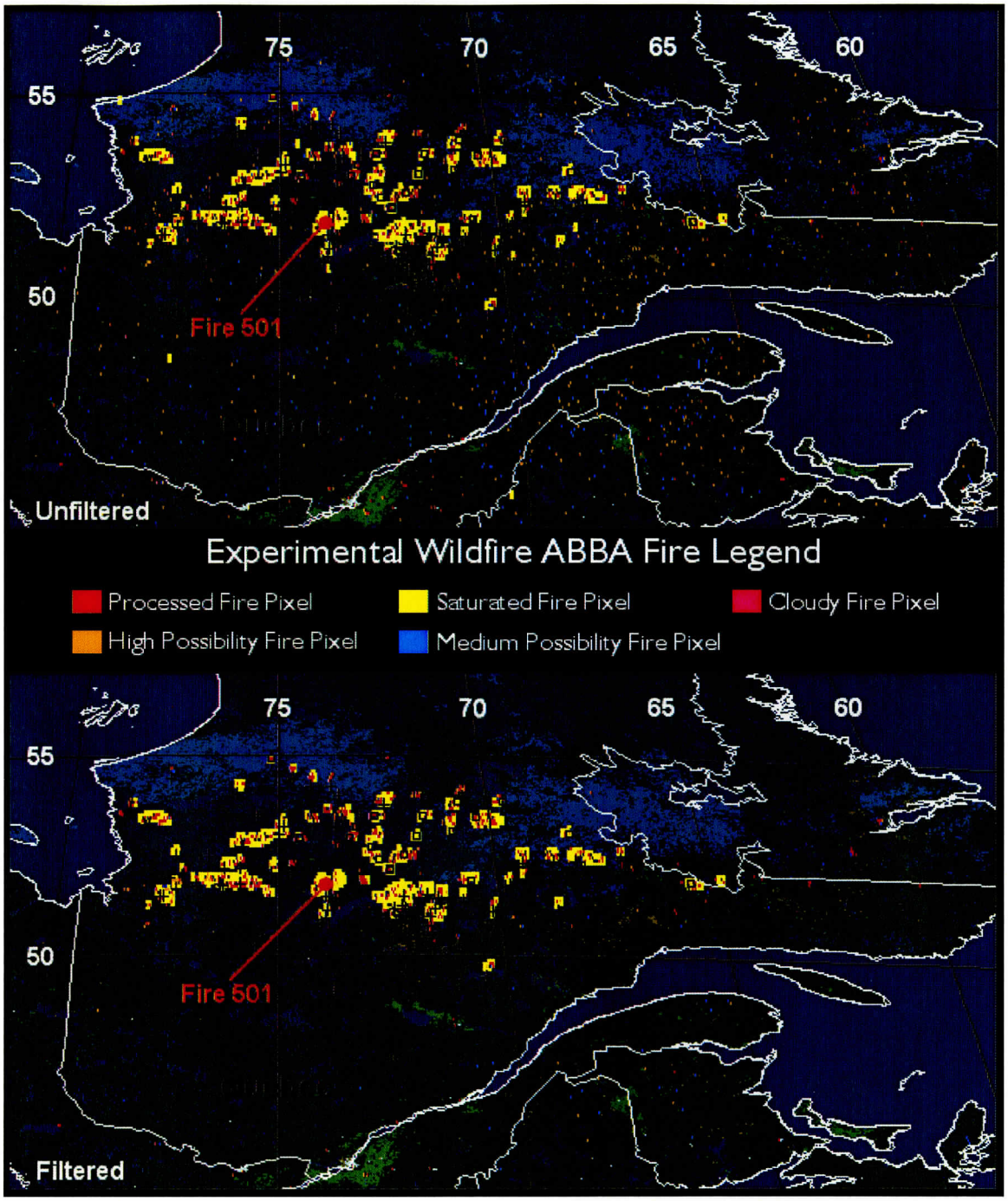

Figure 21. GOES-8 Wildfire ABBA composite of all half-hourly detected fire pixels for the time period June 20 through August 31, 2002. Both the unfiltered (top) and temporally filtered (bottom) analyses are shown. SOPFEU identified fires are indicated in black. Fire 501 was detected 17 days in advance by the WF_ABBA.

4. Clouds from AVHRR (CLAVR-x) Studies

Brief Description of Work Proposed

This project supports the scientific development of the extended Clouds from AVHRR (CLAVR-x) algorithm.

Work Performed from March – September 2003

The CLAVR-x cloud type algorithm was updated during this period. The cloud type algorithm classifies cloudy pixels as low water, super-cooled water, opaque ice, cirrus and overlapped cirrus cloud. This algorithm is part of the operational CLAVR-x system run at NOAA. In addition to developing the algorithm, a validation study was conducted. The results have been accepted for publication.

The cloud mask and resulting cloud amounts were also studied during this period. A paper illustrating the differences in the CLAVR-x and ISCCP cloud products has been submitted for publication. Figure 22 is taken from that study and shows the July – January total cloud amount from ISCCP and CLAVR-x. The agreement in the patterns of the seasonal differences indicates good physical agreement in the two cloud detection methods even though the individual monthly cloud amounts differ significantly.

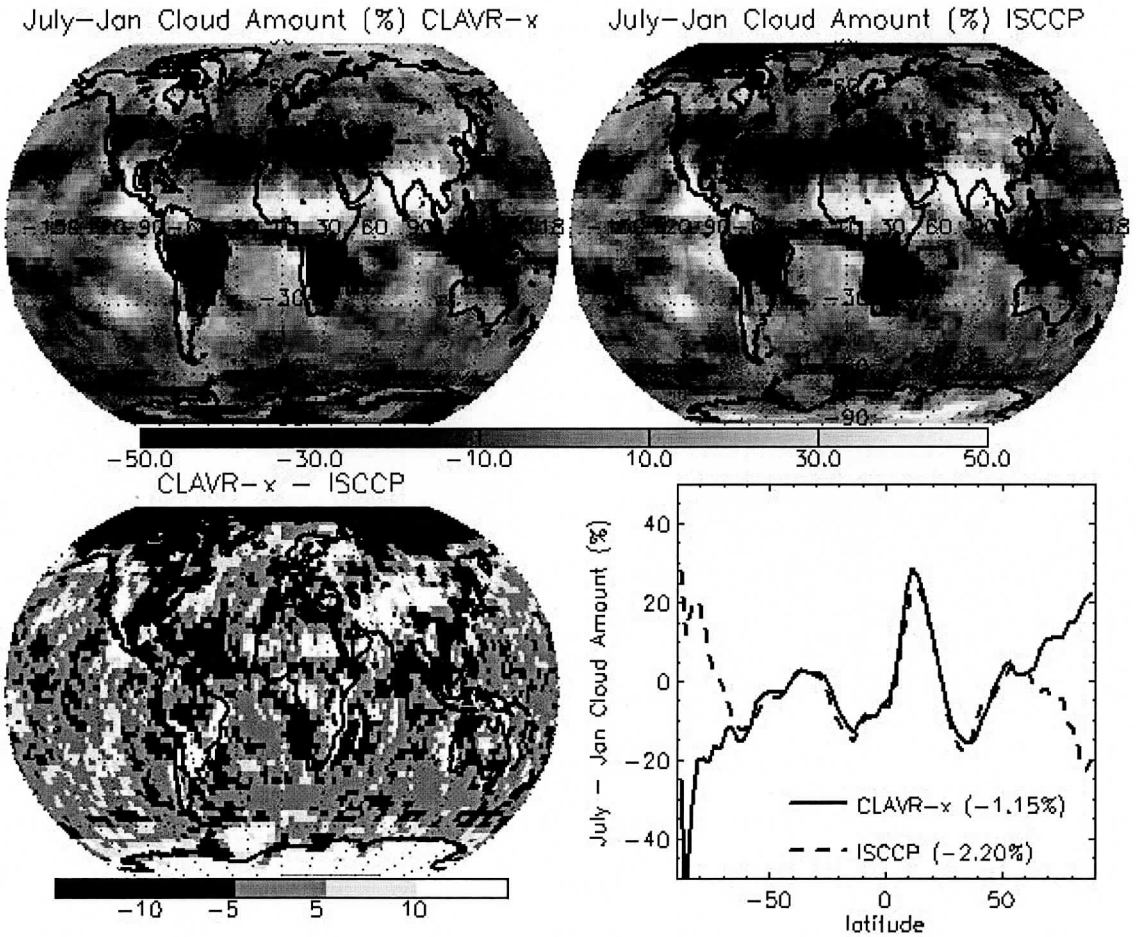

Figure 22. Comparison between the CLAVR-x and ISCCP Seasonal Cycle (July – January) in cloud amount.

5. Intercalibration of GOES/POES

Calibration and instrument intercomparison is the main method by which individual instruments can be validated with each other between the geostationary and polar orbiting platforms. Routine automated intercalibration provides the only picture of how operational geostationary environmental satellites around the globe compare radiometrically. CIMSS has been intercalibrating satellite instruments routinely since late 1999.

The primary purpose of the Intercalibration project is to compare the infrared window and water vapor channels on geostationary instruments (GOES, Meteosat, etc) by using the same polar-orbiting instrument (NOAA AVHRR and HIRS). We make multiple comparisons at the geostationary sub-satellite points and find an average brightness temperature difference between the geostationary imager and the polar orbiter.

Comparison of satellite radiances leading to an improved knowledge of calibration is important for various global applications of satellite data where data from more than one instrument are combined for a single purpose. CGMS (Coordination Group for Meteorological Satellites) has requested satellite operators to regularly perform satellite intercalibration. This request is met at CIMSS through the cooperative agreement with PSDI funding of routine intercalibration.

A secondary, dependent purpose of the project is the support of various, unforeseen calibration issues involving instruments such as GOES imagers and sounders, and POES HIRS, AVHRR, and MODIS among others. In FY03 CIMSS evaluated GOES Imager "midnight corrected" data broadcast in parallel with the regular GOES datastream. This correction was then implemented by NOAA in FY04 (November 2003). In addition, a new satellite processing system (SPS), named the modern SPS (MSPS) was tested with data broadcast in parallel, which were collected by the Space Science and Engineering Center (SSEC) Data Center and evaluated by CIMSS. Problems with the calibration were discovered which led, in part, to delaying implementation of MSPS.

In FY03 GOES-8 was replaced by GOES-12 and GMS-5 was replaced by GOES-9 operationally and in routine intercalibration. Results are updated daily on the world wide web at http://cimss.ssec.wisc.edu/goes/intercal/ and the web page was redesigned in FY03 to include results with NOAA-16 and new time series plots of the results.

6. GOES Sounder Retrieval Research (Single Field of View)

The goal of this project is to conduct research on generating and improving retrieval profiles at full horizontal resolution. Single Field of View (SFOV) GOES Sounder retrievals and associated products are an effort to improve weather analysis and forecasting. Forecasters have shown considerable interest in the SFOV retrieved Total

Precipitable Water (TPW) product, thereby providing good motivation for further development of SFOV retrievals.
It is critical that GOES Sounder products meet current and future user requirements to improve weather services provided to the public.

The current operational NOAA NESDIS GOES Sounder physical retrievals of temperature and moisture are produced at a resolution of 5x5 FOVs, nominally 50km x 50km. As part of the retrieval process, radiance averaging is used as a means of mitigating some of the noise seen in the Sounder data. For a number of years, CIMSS has generated 3x3 FOV GOES Sounder retrievals, also using radiance averaging as part of the retrieval process. Successive Sounders within the GOES I-M series of satellites have demonstrated lower inherent levels of noise, implying there should be less need for radiance averaging. With this in mind, colleagues at FPDT for several years, and more recently, CIMSS personnel also, have produced SFOV retrievals at each of their respective sites.

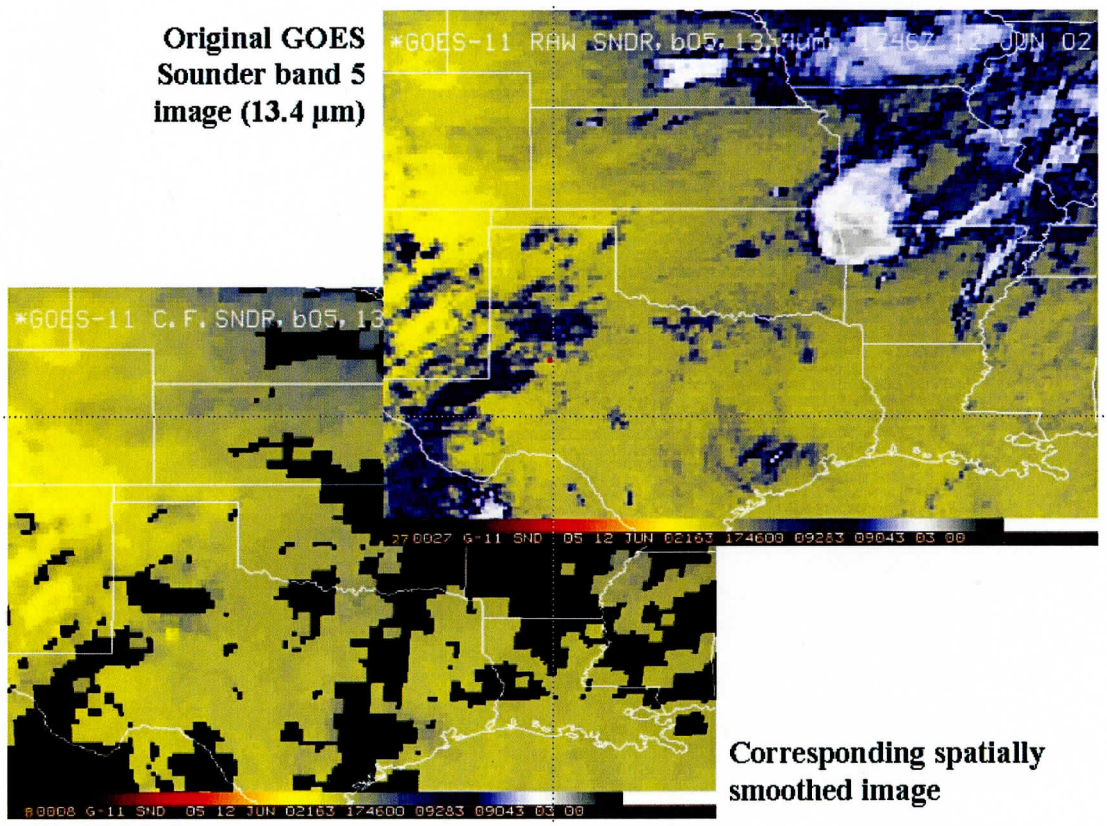

Figure 23. GOES Sounder band 5 (13.4 um) and a (preliminary) spatially smoothed corresponding image.

SFOV algorithm development will take several paths. The SFOV code itself will be enhanced to enable upgrades to the surface emissivity, retrieval first guess, and cloud handling issues, among others. The impact of spatially filtered data will be examined and

validated to determine the accuracy of SFOV Sounder products. Retrievals over low-level clouds will also be examined.

Publications

Feltz, W. F., J. P. Nelson III, T. J. Schmit, and G. S. Wade, 2003: Validation of GOES-8/11 Sounder derived products during IHOP 2002 field experiment. Preprints, *12th Conf. on Satellite Meteorology and Oceanography,* Long Beach, CA, Amer. Meteor. Soc., abstract P4.5.

Schmit, T. J., W. P. Menzel, J. Daniels, Y. Plokhenko, J. P. Nelson III, J. Jung, T. Schreiner and E. Borbas, 2003: 2002 / 2003 Report on NOAA/NESDIS GOES Soundings. CGMS XXXI. Ascona, Switzerland, 3-7 November 2003. EUMETSAT publication.

Wade, G. S., T. J. Schmit, W. F. Feltz, J. P. Nelson III, and A. J. Schreiner, 2003: GOES-11 and GOES-8 Sounders during the International H2O Project (IHOP)-2002 field experiment. *12th Conf. on Satellite Meteorology and Oceanography,* Long Beach, CA, Amer. Meteor. Soc., abstract P4.8.

7. GOES Sounder Spectral Response Functions and Transmittance Files Generation and Implementation

The objective of this task was to obtain new spectral response functions (SRFs) for various satellite instruments and create transmittance files for use in a fast forward radiative transfer model. This work is necessary for the processing of satellite data and tasks such as calculating weighting functions for instrument bands and calculating forward model radiances quickly and relatively easily.

GOES-12 became the operational GOES-East satellite on April 1, 2003. Though not a task specifically named in the original proposal, new GOES-12 Sounder spectral response functions were obtained and transmittance files were tested. Forward model calculations were closer to observed radiances in most of the sounder bands. A technical report on GOES-12, which includes some information on the SRFs, was also published (Hillger, D. W., T. J. Schmit, and J. M. Daniels, 2003: Imager and sounder radiance and product validations for the GOES-12 science test, NOAA Technical Report 115, U.S. Department of Commerce, Washington, DC).

GOES-N Imager and Sounder spectral response functions were obtained and individual detector SRFs were averaged for each band. The mean SRF for each band was used to calculate transmittance files and Planck function coefficients for converting radiance to brightness temperature. Software can now be updated, prior to GOES-N launch for various processes, such as sounder retrievals in preparation for GOES-N check-out.

The primary focus of this task has been on the GOES series of imagers and sounders, but research often involves other remote sensing instruments such as MODIS, Meteosat, and other NOAA instruments such as HIRS and AVHRR. Similar work is performed under this task to maintain similar capabilities with other instruments.

8. Research Product Quality Assurance and Science Maintenance for GOES Imagers and Sounders

The purpose of this work is to support product quality assurance and science maintenance activities for the GOES Imager and Sounder research products. In the event of a problem with one of the GOES Imager or Sounder products, CIMSS will work to identify the source of the problem and take corrective action to resolve the problem. When applicable, parallel processing systems at CIMSS will be utilized to experiment with products or new applications of existing products.

When there are no outstanding science maintenance issues to address, CIMSS will focus efforts on validation work involving current and new products and web page development. Validation efforts will include the use of new ground truth data to validate products through individual case studies, statistical comparisons (bulk statistics and time series), and error analysis.

During the period March through September 2003, several items related either directly or indirectly to the above tasks were accomplished. The switch of the GOES-EAST satellite from GOES-8 to GOES-12 was performed successfully on 1 April 2003 (Figures 24 and 25). Note the similarity between the combined GOES-8 and –10 Total Precipitable Water (TPW) Derived Product Image (DPI) prior to the switch (Figure 24) and the combined GOES-12 and -10 TPW DPI generated after the switch (Figure 25). Furthermore, vital, ongoing oversight of the CIMSS GOES Imager and Sounder processing systems was performed, including monitoring available space on various disk storage systems and removing unnecessary files as needed. In early July, some Office of Research and Applications (ORA) funding was secured to purchase two additional 73 gigabyte disk drives for our Dell PC system that runs the Linux operating system in order to upgrade our GOES computing infrastructure. Near the end of the 6-month period, preliminary logistics work was done prior to the purchase of a Dell rack that will eventually house numerous dual-CPU computer nodes running Linux, that will serve as the "next generation" of GOES Imager and Sounder processing hardware at CIMSS. It should be noted that NOAA/NESDIS operations currently employs PCs running Linux.

In other activities, a daily archive containing 3-4 gigabytes of various Imager and Sounder products, other files related to product processing, and raw satellite imagery was overseen. A comprehensive archive can be very useful for quality assurance, such as determining when a particular product begins to degrade in quality. Moreover, as has been done for several years, files containing collocated GOES Sounder retrieval and radiosonde vertical temperature and moisture profiles continued to be generated and archived. These collocation files are important for subsequent retrieval quality evaluations. In terms of web page development, by March 2003 (and continuing into April), modifications and updates were required on the CIMSS Realtime GOES Page (http://cimss.ssec.wisc.edu/goes/realtime/realtime.html). These changes were necessitated by the addition of Imager products (GOES-10 and -12 Clear Sky Brightness Temperature (CSBT) DPI as well as GOES-12 Imager cloud DPI) and the decision to

solely use the NCEP AVN forecast as the first-guess for both the 3x3 FOV as well as the single FOV (SFOV) Sounder retrievals and DPI, generated at CIMSS.

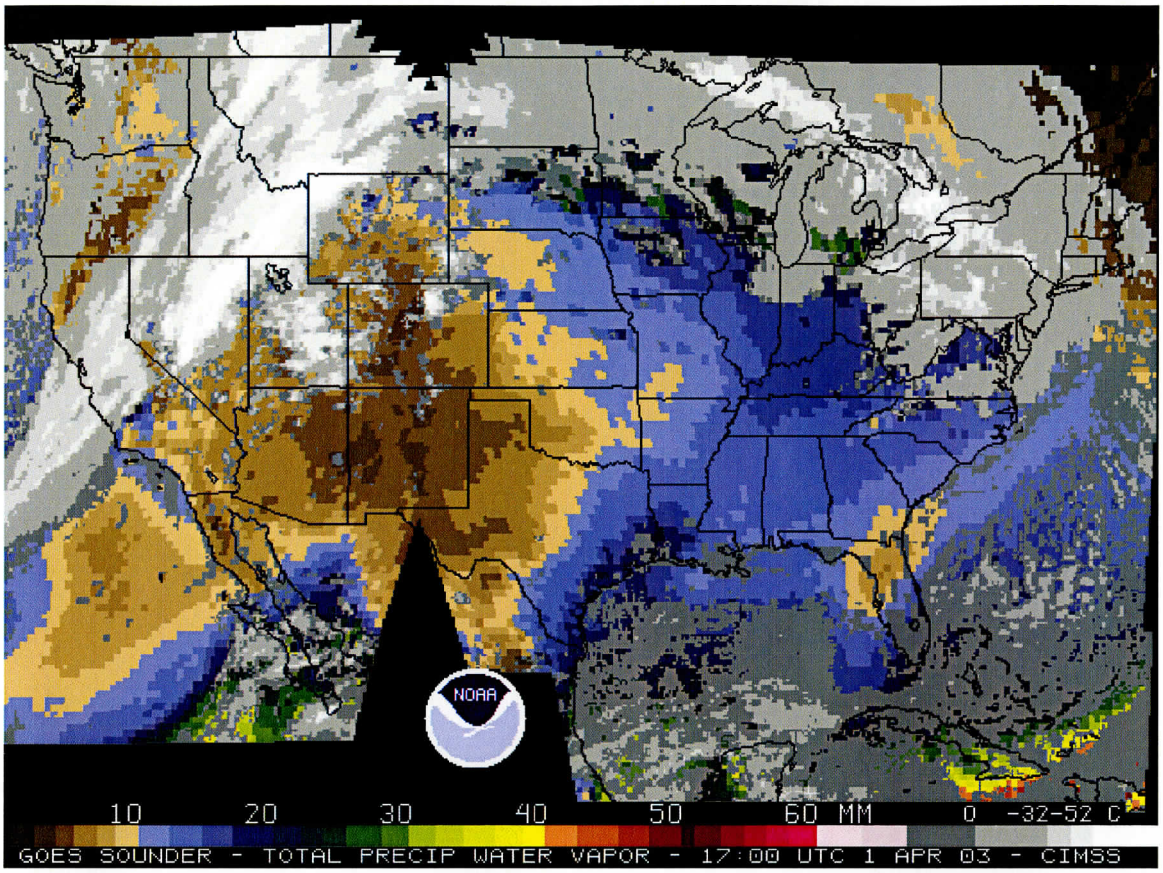

Figure 24. GOES-8 and –10 Sounder Total Precipitable Water valid 17UTC on 1 Apr 2003.

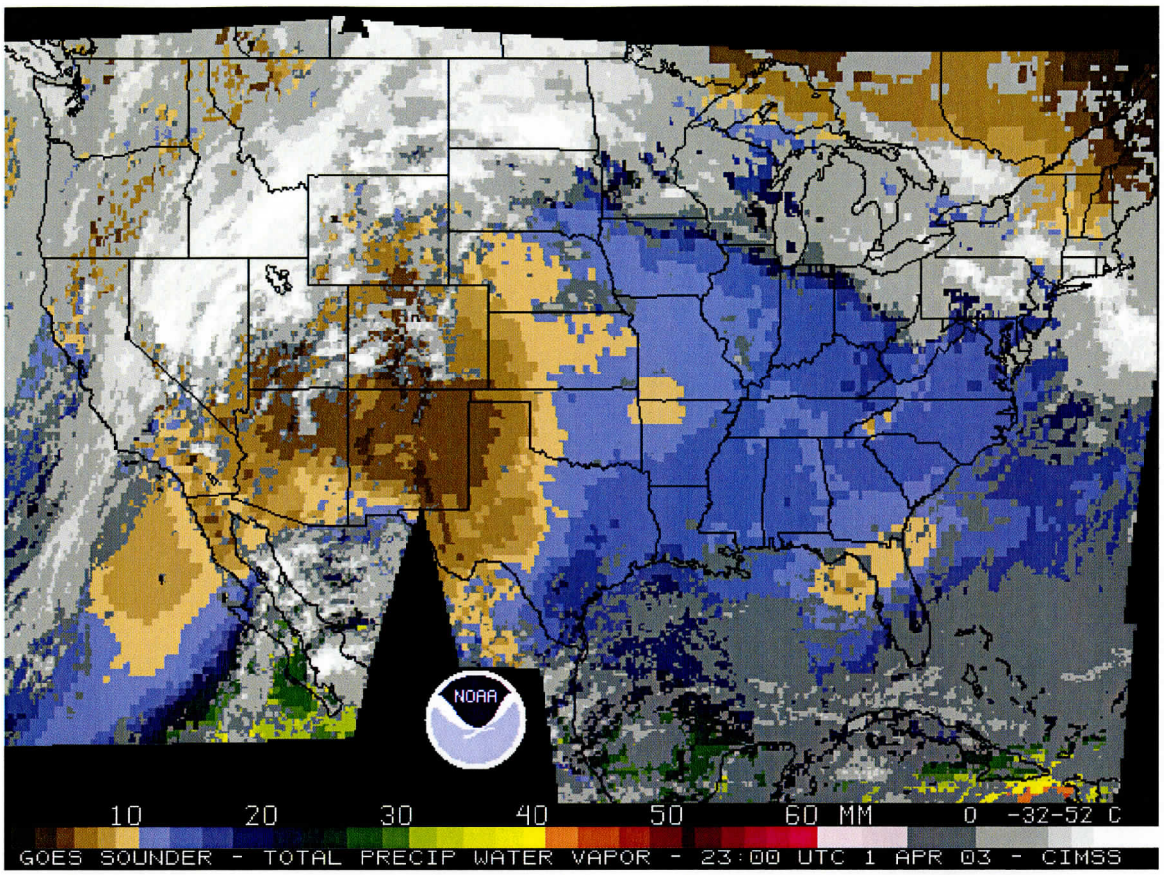

Figure 25. GOES-12 and –10 Sounder Total Precipitable Water valid 23UTC on 1 Apr 2003.

III. CIMSS Research Activities in the NOAA Ground Systems Program

1. GOES –11 Post Launch Data Analysis and Validation from IHOP Operations

Background

The International H2O Project (IHOP) was conducted in the DOE ARM Southern Great Plains (SGP) region of the United States from 13 May – 25 June 2002. Two of the primary goals for the program were to measure water vapor variability at high temporal/spatial resolution and to study the mechanisms for convective initiation. GOES-11 was activated by the National Environmental Satellite and Data Information Service (NESDIS) for part of the IHOP campaign, improving the sounder time resolution to 30 minutes and providing a more vertical scanning position over the IHOP domain. Activation of a spare GOES satellite was unique to a large-scale field program. The IHOP field experiment provides a unique opportunity to validate 1x1 (10x15 km) single field of view (SFOV) GOES sounder derived products. A case study from the IHOP

campaign on 12 June 2002 indicated that the GOES-11 SFOV TPW was successful at retrieving a 1 cm water vapor oscillation as compared to Global Positioning System (GPS) and Atmospheric Emitted Radiance Interferometer (AERI) ground based TPW measurements. GOES-11 SFOV retrievals are currently being recalculated with several improvements. A paper describing these results is currently being written and will be submitted for peer review. A preliminary comparison of the IHOP/DOE ARM data sets to GOES-11 sounder derived products will be conducted.

Accomplishments

Microwave radiometer and radiosonde data from the IHOP and Department of Energy Atmospheric Radiation Measurement (DOE ARM) programs were used to provide preliminary validation of GOES 8/11 total precipitable water (TPW) sounder derived products. A preliminary comparison of coarser spatial resolution 3x3 FOV TPW to the SFOV TPW products for both GOES-8 and GOES-11 was conducted to quantitatively demonstrate the accuracy and utility of the relatively higher spatial resolution data. The GOES SFOV physical retrieval algorithm has been compiled on a LINUX work station and is currently recomputing the GOES-11 SFOV retrieval with techniques to reduce radiance noise and cloud filtering. Figure 26 indicates the advantage of spatial radiance filtering for sounder channels with low signal to noise ratios. A full analysis comparing SFOV vs 3x3 retrievals is underway.

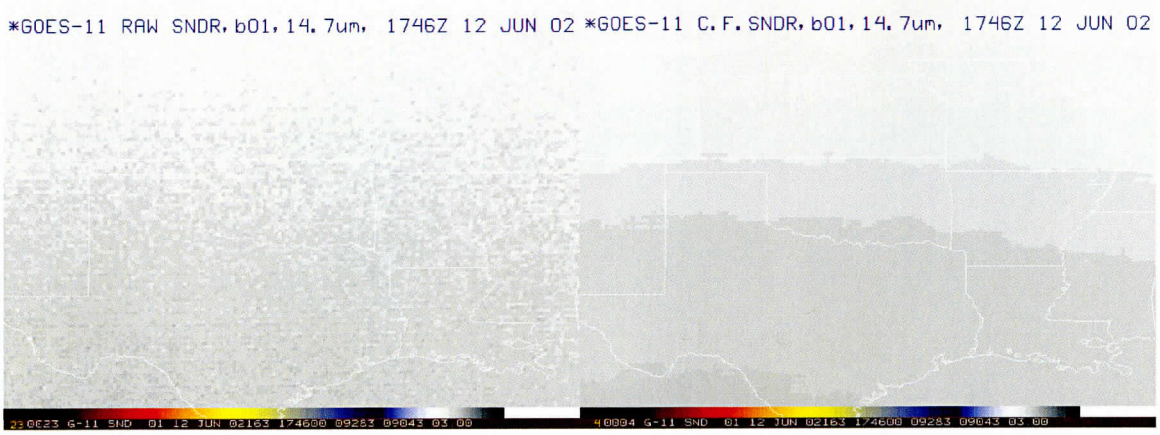

Figure 26. Results of spatial filtering GOES-11 sounder upper troposphere (channel 1) brightness temperature. Spatial averaging resolves the gradient in the upper tropospheric and will be implemented on a channel by channel basis as a preprocessing step prior to input into the GOES physical retrieval algorithm.

Accomplishments include:

- The NOAA FPDT GOES SFOV retrieval algorithm was implemented at SSEC/CIMSS to provide a consistent benchmark to begin improvement of SFOV GOES sounder retrievals.
- Preliminary results indicate that cone filtering (spatial averaging on a per channel basis) significantly reduces pixel to pixel noise in upper tropospheric and mid

tropospheric channels.

- The GOES sounder SFOV algorithm has been transitioned to a LINUX operating system with the goal to reprocess the GOES-11 data and then add cone filtering and cloud clearing.
- SFOV ozone retrieval logic is also being incorporated into the algorithm.

The IHOP program provides the opportunity to conduct an intensive analysis of higher spatial and temporal resolution GOES products. Updated hardware is required to fulfill this validation. The hardware includes a computer workstation and hard drive disk array to archive the various ARM and GOES data sets for the validation project and to supply a resource for future GOES-12 validation. A cluster of Dell workstations have been purchased and is currently being used to improve the GOES SFOV retrievals using GOES-11 IHOP datasets and will be then used to provide real-time GOES derived product validation. The computer assets have provided a means for timely calculations and automation of near real-time validation.

Publications

Feltz, W. F., J. P. Nelson, III, G. S. Wade, and T. J. Schmit, 2003: An evaluation of GOES-11 sounder derived products during IHOP 2002 field experiment. IHOP Science Workshop Boulder, Colorado 24-26 March 2003.

2. GOES –GOES 9 Data Processing (preparation)

Since May of 2003, the GOES-9 satellite has been operating over the western Pacific ocean, centered over the equator at 155 degrees east longitude. Each hour, radiances from the Sounder instrument are received and utilized to generate meteorologically-useful products, such as retrieved atmospheric temperature and moisture profiles and retrieved cloud parameters, as well as various associated Derived Product Images (DPI). Continued GOES-9 Sounder product generation is important, because sounding the atmosphere from geostationary orbit has never before been possible over this portion of the globe.

Significant progress has been made on a number of items. For example, GOES-9 DPI imagery has been posted to the Web. The DPI imagery currently available are total precipitable water (TPW) and cloudtop pressure (CTP), and can be seen at: *http://cimss.ssec.wisc.edu/goes/realtime/grtmain.html#g3pw*

Examples of these unique, experimental DPI have been made available. Furthermore, progress has been made toward making the atmospheric temperature and moisture profiles available in Binary Universal FoRm (BUFR) format. In addition, the TPW and CTP DPI imagery, as well as the Lifted Index, Surface Skin Temperature, and Effective Cloud Amount DPI imagery, are available via the McIDAS Abstract Data Distribution Environment (ADDE), as are the retrieved atmospheric temperature and moisture profiles themselves. The retrievals have also been validated against co-located radiosonde data, although there are only a few radiosondes. Comparisons of the GOES CTP and the

surface measured microwave/radar determined cloud heights at the DOE CART site in the Western Pacific are being conducted.

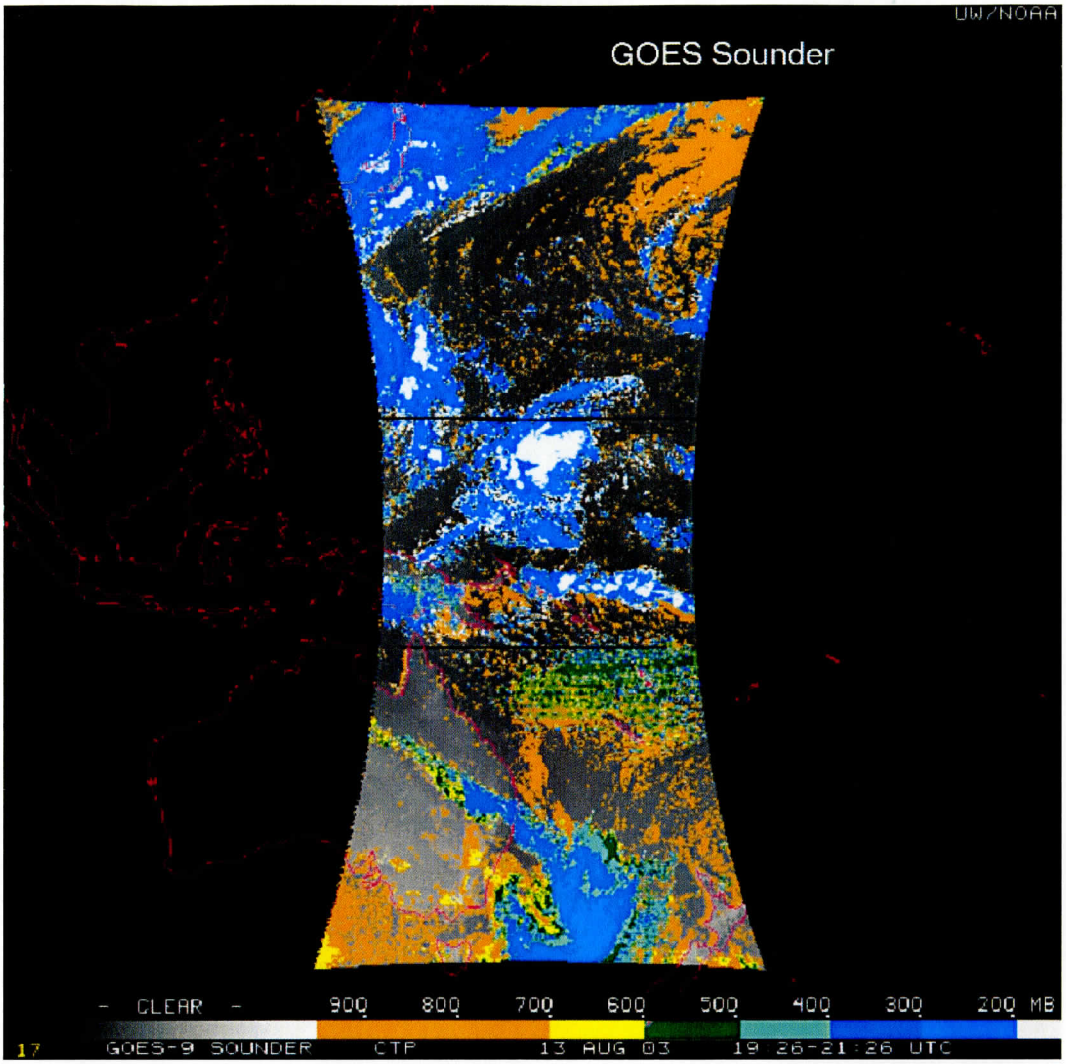

Figure 27. GOES-9 Sounder Cloud-Top Pressure from the three routine sounder sectors over the Western Pacific.

Publications

Nelson, J. P. III, G. S. Wade, A. J. Schreiner, T. J. Schmit, W. F. Feltz, and C. C. Schmidt, 2004: A study of data and products from the GOES-9 Imager and Sounder over the western Pacific Ocean. Preprints, *20th Intl. Conf. on Interactive Information and Processing Systems (IIPS) for Meteorology, Oceanography and Hydrology*, Seattle, WA, 11-15 January 2004, Amer. Meteor. Soc.

3. Geostationary Winds Processing System for GOES –12, Meteosat Second Generation (MSG), and MTSAT

As new satellites are launched, the CIMSS/NESDIS automated winds processing code needs to be updated and modified to handle the inputs. For example, in 2003 the GOES-12, with a CO2 channel and upgraded H2O channel, needed algorithm validation after activation. Also in 2003, GOES-9 was repositioned over the western Pacific Ocean and was activated upon failure of GMS-5. The winds algorithm was updated to process and derive products and optimize their quality upon activation.

Upon failure of the Japanese GMS satellite, modifications to the CIMSS satwinds processing code were enabled to adapt to the GOES-9 replacement; Full-disk WV and IR GOES-9 winds are now running routinely after being evaluated for quality. The GOES-9 satellite automated navigation stabilizer had to be turned off by NESDIS in AugustA 10-15% degradation in number of vectors was the result. CIMSS helped to resolve this problem by invoking the image-to-image self registration and correction module in the CIMSS processing package.

Also, final code modifications were added to process the new GOES-12 satellite data into winds. The addition of the 13 micron CO2 channel will allow better vector height assignments.

4. CLAVR –x Development for METOP

Brief Description of Work
CLAVR-x will be included in the front-end processing of METOP/AVHRR data. This project performs research to optimize the CLAVR-x cloud mask performance for the METOP era.

Several activities were undertaken. First the CLAVR-x code was modified to process 1km AVHRR data (HPRT and LAC) because 1 km METOP data is not available yet. We also began developing a system to automatically process all HRPT over the conterminous USA. These 1km products will then be compared to the 4 km results from GAC data. These studies will reveal the expected difference in NOAA products when processing of the global 1km METOP data begins in 2005.

IV. CIMSS Research in Satellite Data Assimilation

1. An Ongoing Evaluation of Data Impact studies in NCEP's NWP Models

A forecast impact study of in-situ rawinsonde data and remotely sensed geostationary and polar orbiting satellite data used in NCEP's Eta Data Assimilation/Forecast System (EDAS) has recently been completed for 15-day periods during all four seasons. This basic research should be of interest to NCEP personnel for several reasons. First, the

study uses the same model resolution (32 km, 60 layers), assimilation scheme, data sources and model algorithms as the NCEP parallel runs. As such, the impact results are directly applicable to the NCEP parallel development suite. Second, the study provides a detailed assessment of the impact of satellite radiances in the Eta model by examining the contribution from individual observing systems such as GOES, AMSU, MSU and HIRS. The results of this data denial study should also be interesting to NWS field forecasters which are trying to identify the overall forecast impact of traditional land based rawinsonde data sources with remotely sensed satellite data sources that exist domain wide.

The four season results (spanning Fall 2001 through Summer 2002) of this study are summarized in Figure 28, and show that a positive forecast impact is achieved from all three combined data sources (labeled RAOB, GOES and POES), as well as the nine individual components. Cumulatively, the rawinsonde data has the largest positive impact. However, GOES data demonstrates the largest positive forecast impact for several fields, especially moisture during summer and fall. In general, GOES data also provides larger positive forecast impacts than POES data over both CONUS and the entire domain, especially for the wind components and moisture. Two additional findings from this study are also important. The first is that the forecast impact of all data types drops by at least a factor of two during all seasons between 24- and 48-hrs. The second is that GOES data provides nearly equal forecast impacts to the 0000 and 1200 UTC forecast cycles, while RAOB and especially POES data provide biased forecast impacts between 0000 UTC and 1200 UTC, with larger forecast impacts at 1200 UTC.

Subsequent to completion of the EDAS denial studies, further research includes duplicating the regional EDAS data denial studies in the NCEP global GFS system. Experiments currently underway include a winter/summer investigation of HIRS, AMSU and GOES data. At the request of NCEP personnel, the global denials span a six week time window, with diagnostics performed on the last four weeks. Similar to the EDAS results discussed above, these denials use the latest version of the NCEP GFS at the operational resolution (T254L64). This basic research study will benefit the global branch of NCEP's modeling community, just as the EDAS denials benefit the mesoscale branch.

Publications

Zapotocny. T. H., W. Paul Menzel, J. A. Jung, and J. P. Nelson III, 2003: A four season impact study of rawinsonde, GOES and POES data in the Eta data assimilation system. Part I: The total contribution. Submitted to *Wea. Forecasting.* October 2003.

Zapotocny. T. H., W. Paul Menzel, J. A. Jung, and J. P. Nelson III, 2003: A four season impact study of rawinsonde, GOES and POES data in the Eta data assimilation system. Part II: Contribution of the components. Submitted to *Wea. Forecasting.* October 2003.

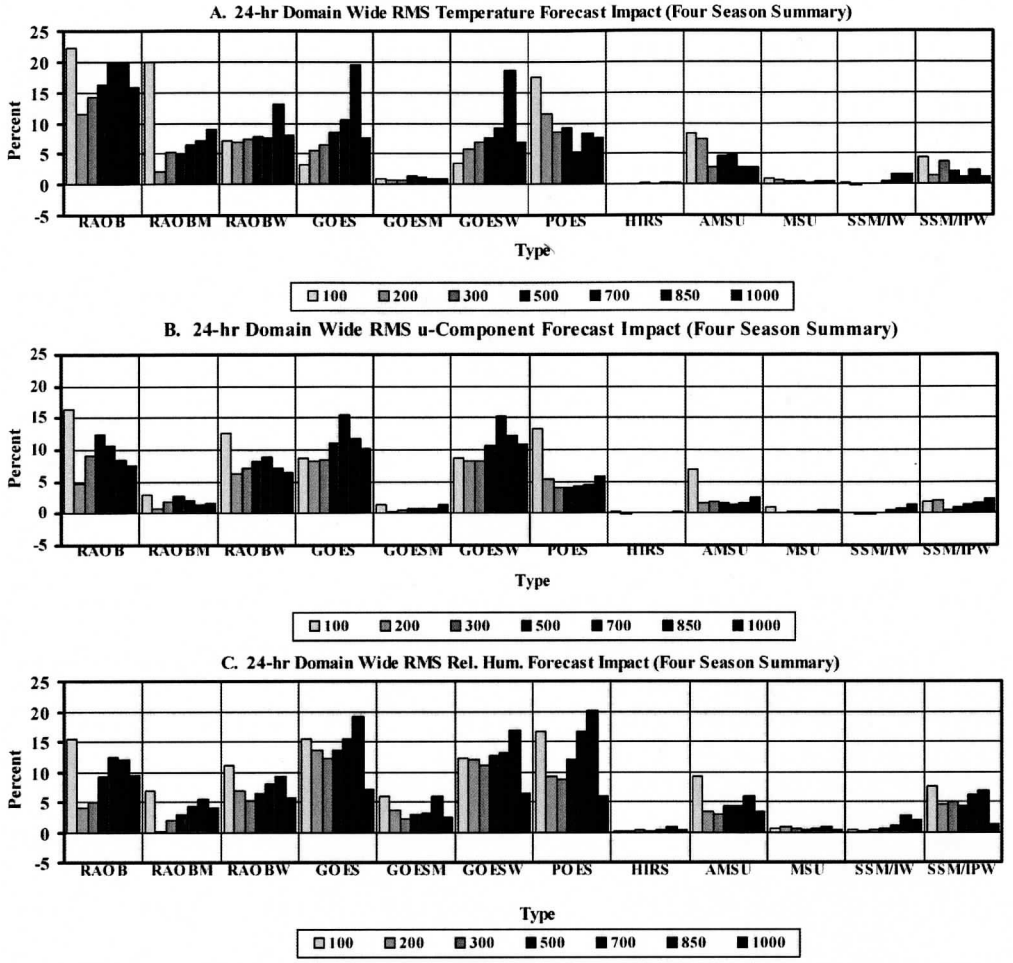

Figure 28. The four season summary of RMS forecast impact (%) on the 104 grid for (a) temperature, (b) u-component, and (c) relative humidity, after 24-hrs of Eta model integration. Both the three aggregate denials (RAOB, GOES, and POES) and the nine individual denials are shown. Data types ending in "W" are wind observation; data types ending in "M" are mass observations; and data types ending in "PW" are precipitable water observations.

2. JCSDA: Data Assimilation experiments

The latest version of the Eta Data Assimilation System (EDAS) has been successfully ported to the NESDIS/JCSDA computer. Some main changes in this version include GOES-12 data assimilation and several modifications to the radiance assimilation. The only difference between this version of the EDAS and NCEP's operational EDAS is that we use 32km horizontal resolution instead of 12km.

The satellite wind's assimilation work with Jaime Daniels, (NESDIS), Dennis Keyser (NCEP), Dave Parrish (NCEP) and Eric Rogers (NCEP) continues. We have tried several different assimilation techniques and various combinations of these techniques.

We are currently testing a speed bias correction with a best fit to the model height adjustment. The speed bias correction is based on rawinsonde and satellite wind co-location data for 1 Jan 2002 through 31 Dec 2002. In all cases the U and V components of the satellite winds are slower than the rawinsonde winds. We are testing a height adjustment or height reassignment technique which is presently being used by NESDIS for quality control. It uses a penalty function based on mean vector difference and pressure to determine where the observation agrees with the model the best. A similar technique is also being tested by NASA DAO (Lars Peters).

NESDIS is in the process of changing how they generate their GOES Sounder products. They are testing a single field of view product to replace a 5X5 pixel averaged product. Work is ongoing with Jaime Daniels (NESDIS) and Gary Gray (Raytheon) assimilate the GOES Sounder single field of view radiance products into the EDAS. Most of the preliminary work is done; we are currently waiting on the data stream. We will specifically look for cloud contamination and ways it can be eliminated. We also plan to look at biases from each of the 4 detectors to see if a specific detector bias correction should be generated. The impact of using some of the radiances over land will also be investigated if time permits.

3. Assimilation of Moisture and Winds (Bill Raymond's Final Projects)

A new method for incorporating upper tropospheric moisture and winds in NWP models has been demonstrated by using direct assimilation of GOES brightness temperatures. This study uses GOES Imager channel 3 (6.7 μm) data from both clear and cloudy regions, a forward radiative transmittance model, and a numerical optimization procedure to modify middle to upper tropospheric moisture and winds.

The newly developed scheme was used in a series of 10 day tests during September 2000. The initial conditions were supplied by NCEP's EDAS, after which the model initial atmosphere was modified to include the new GOES brightness temperature data. Modifications made with observed brightness temperature data from GOES channel 3 to the initial model atmosphere for an individual time period are illustrated in Figure 29. GOES data adjusted the model atmosphere closer to "truth" in many locations: especially southwest of California, west of the U.S. west coast (125-130W), near Lake Superior, and western Mexico. In addition, forecast correlation results of brightness temperature showed that the new scheme improved the forecast for all 10 days of the study at 24-hrs and 8 of the 10 days at 48-hrs.

The water vapor weighting functions (such as for channel 3) can also be used to modify/adjust a first guess wind field. GOES water vapor wind observations have been compared to weighted average wind components from an initial model forecast field to provide potential adjustments/corrections to the model data. Studies similar to the 10 day brightness temperature discussed above have also been evaluated for the water vapor weighting functions.

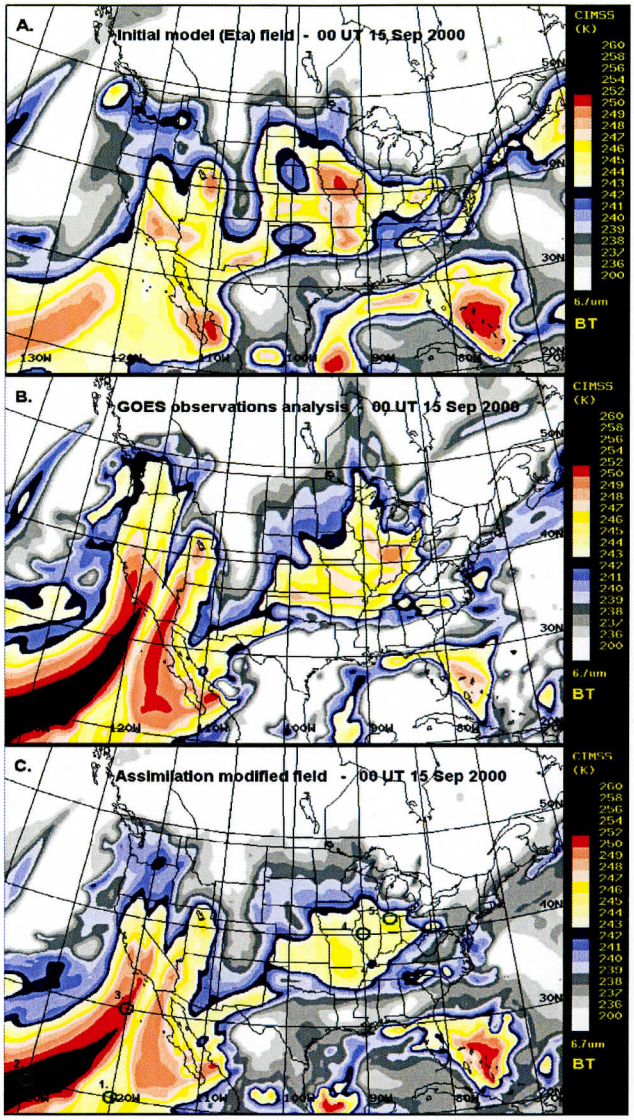

Figure 29. Upper tropospheric water vapor (GOES channel 3, 6.7mm) brightness temperatures for 0000 UTC 15 Sep. 2000 from the (a) forward radiative transmittance model calculations (RTTOVS) using smoothed Eta background fields that have been sharpened by an analysis of in situ upper air and surface data (b) GOES channel 3 observations analyzed to a 40-km grid by a recursive filter, and (c) the moisture field as modified by GOES channel 3 observations using the proposed assimilation scheme. Note that some key features from (b) missing in (a) are present in (c).

Publications

Raymond, W. H., G. S. Wade, and T. H. Zapotocny, 2004: Assimilating GOES brightness temperatures. Part 1: Upper tropospheric moisture. *J. Appl. Meteor.*, **1**, 17-27.

Raymond, W. H., G. S. Wade, and T. H. Zapotocny, 2004: Assimilating GOES brightness temperatures. Part 2: Assigning water vapor wind heights directly from weighting functions. Conditionally accepted for publication in *J. Appl. Meteor.*

V. A CIMSS Research Study of the Advanced Baseline Sounder (ABS) / Hyperspectral Environmental Suite (HES) Data Compression

1. ABS/HES data cube preparation for compression studies

The proposed ABS/HES is either a 2-band interferometer (GIFTS like) or a 3-band grating sounder (AIRS like). Figure 30 shows the proposed spectral coverage and resolution that provide useful temperature, water vapor, ozone, clouds, and carbon dioxide information. ABS/HES prime (ABS′) is an alternative proposal to improve spatial resolution from the baseline 10 km to 4 km and adopt a spectral range and resolution more closely paralleling that of the GIFTS instrument. For comparison the current GOES-8 spectral coverage is also shown.

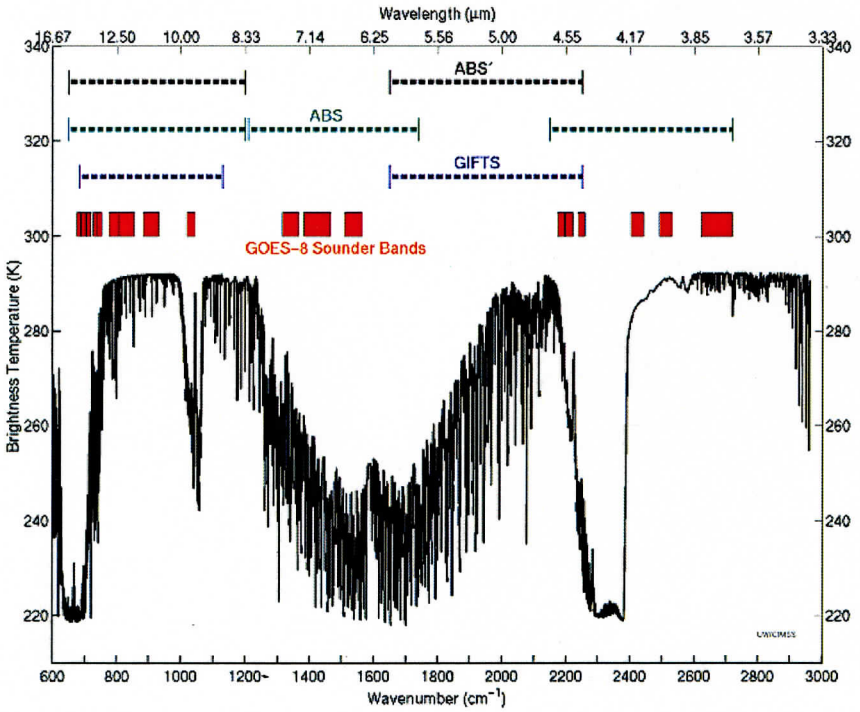

Figure 30. A comparison of GOES-8 sounder bands and the proposed ABS/HES baseline, ABS/HES prime, GIFTS spectral coverage and resolution superimposed over a typical atmospheric spectrum.

For grating-type ABS/HES compression studies we have adopted and modified the NASA AIRS radiance observations from 6 September 2002. The AIRS instrument aboard

NASA's Aqua spacecraft employs a 49.5 degree cross-track scanning with a 1.1 degree instantaneous field of view to provide twice daily coverage of essentially the entire globe in a 1:30 PM sun synchronous orbit. The AIRS data includes 2378 infrared channels in the 3.74 to 15.4 μm region of the spectrum. A day's worth of AIRS data is divided into 240 granules, each of 6 minute durations. Each granule consists of 135 scan lines containing 90 cross-track footprints; thus there are a total of 135 x 90 = 12,150 footprints per granule. The 16-bit raw radiances are converted into the brightness temperatures, and then scaled as unsigned 16-bit integers. To make the tested hyperspectral sounding data generic, 270 bad channels in the original observations are excluded assuming that they occur only in the AIRS sounder but not in other hyperspectral sounders. Each resulting granule is saved as a binary file, arranged as 2108 channels, 135 scan lines, and 90 pixels for each scan line. Ten granules, five daytime and five nighttime, are chosen from different geographical regions of the Earth. Their locations, UTC times and local time adjustments are listed in Table 1.

Table 1. Ten selected AIRS granules for hyperspectral sounding data compression studies.

Granule 9	00:53:31 UTC	-12 H	(Pacific Ocean, Daytime)
Granule 16	01:35:31 UTC	+2 H	(Europe, Nighttime)
Granule 60	05:59:31 UTC	+7 H	(Asia, Daytime)
Granule 82	08:11:31 UTC	-5 H	(North America, Nighttime)
Granule 120	11:59:31 UTC	-10 H	(Antarctica, Nighttime)
Granule 126	12:35:31 UTC	-0 H	(Africa, Daytime)
Granule 129	12:53:31 UTC	-2 H	(Arctic, Daytime)
Granule 151	15:05:31 UTC	+11 H	(Australia, Nighttime)
Granule 182	18:11:31 UTC	+8 H	(Asia, Nighttime)
Granule 193	19:17:31 UTC	-7 H	(North America, Daytime)

The data is available via anonymous ftp (ftp://ftp.ssec.wisc.edu/pub/bormin/HES) for other ABS/HES compression teams and the IEEE data compression society. Figure 31 shows the AIRS radiances at wavenumber 900.3 cm^{-1} for the 10 selected granules on 6 September 2002.

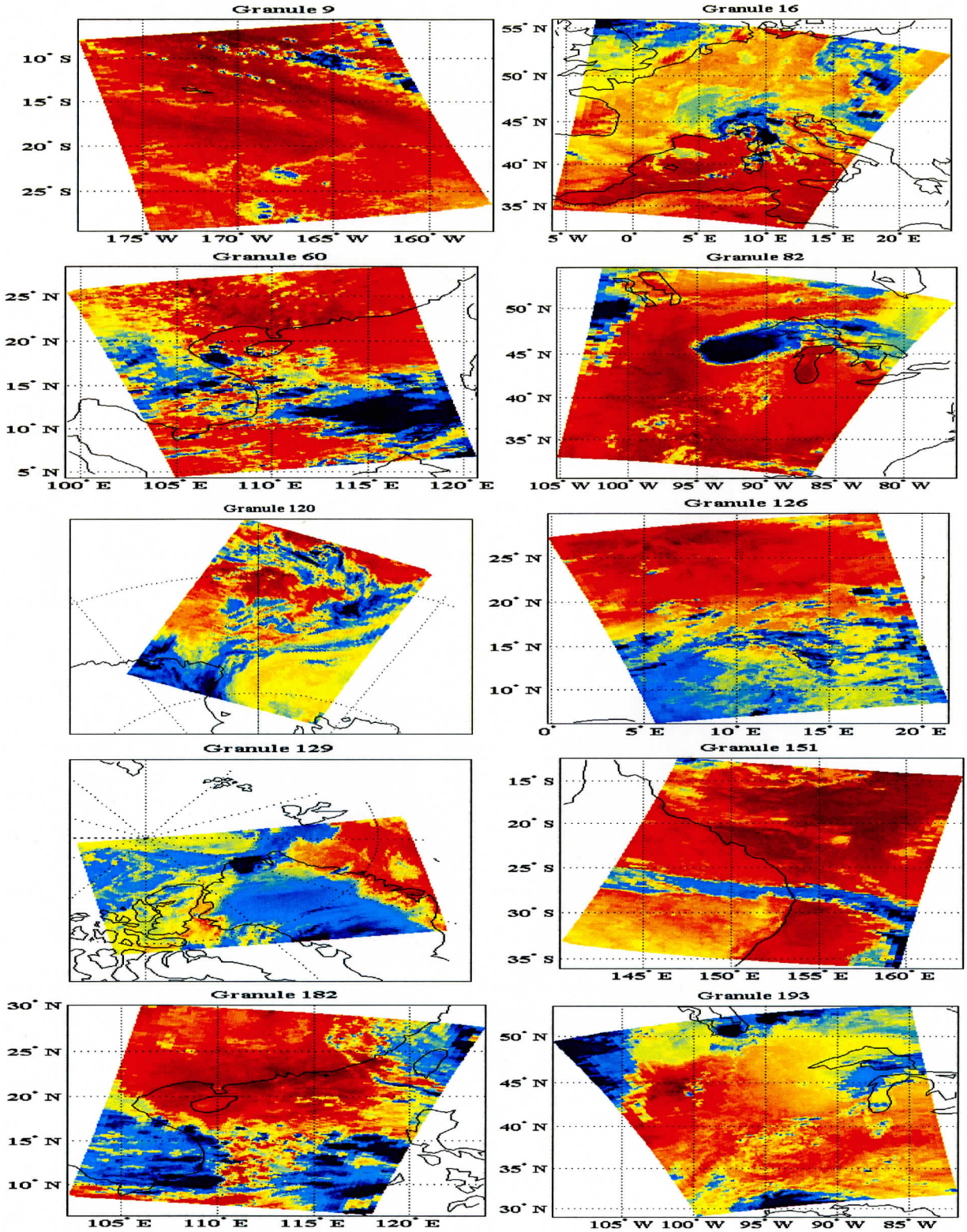

Figure 31. Spatial distribution of AIRS radiance at wavenumber 900.3cm^{-1} for the 10 selected granules on Sept. 6, 2002.

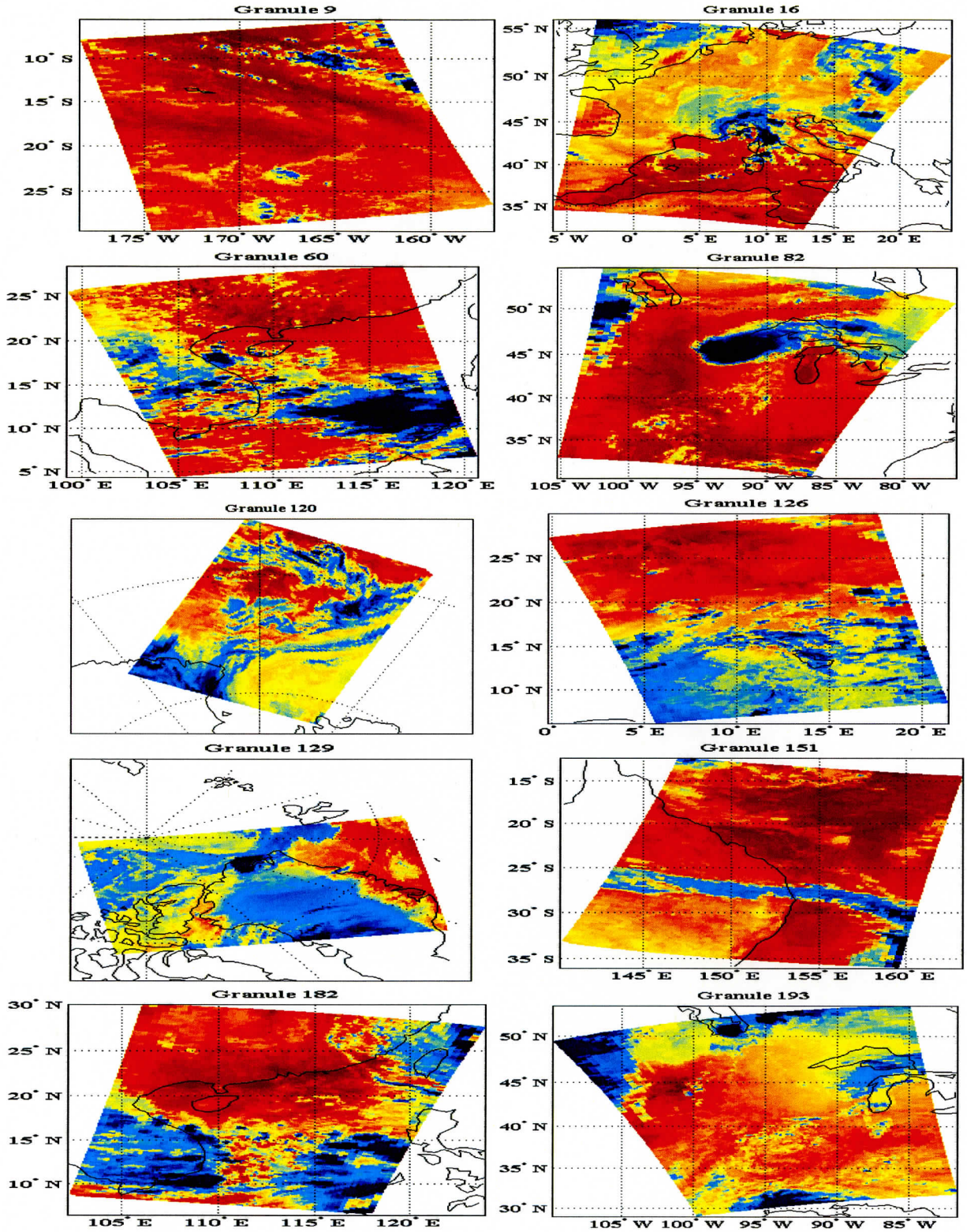

Figure 31. Spatial distribution of AIRS radiance at wavenumber 900.3cm^{-1} for the 10 selected granules on Sept. 6, 2002.

In these granules, coast lines are depicted by solid curves and multiple clouds at various altitudes are shown as different shades of colored pixels. Figure 32 shows all 12150 radiance spectra (135 scan lines x 90 pixels) in granule 82. For comparison Figure 32b shows the calibrated noise spectrum converted from the noise equivalent temperature provided in the AIRS channel properties file. Each infrared spectrum spans several orders of magnitude in radiance ranging from longwave to shortwave infrared regions and has various degrees of signal-to-noise ratios.

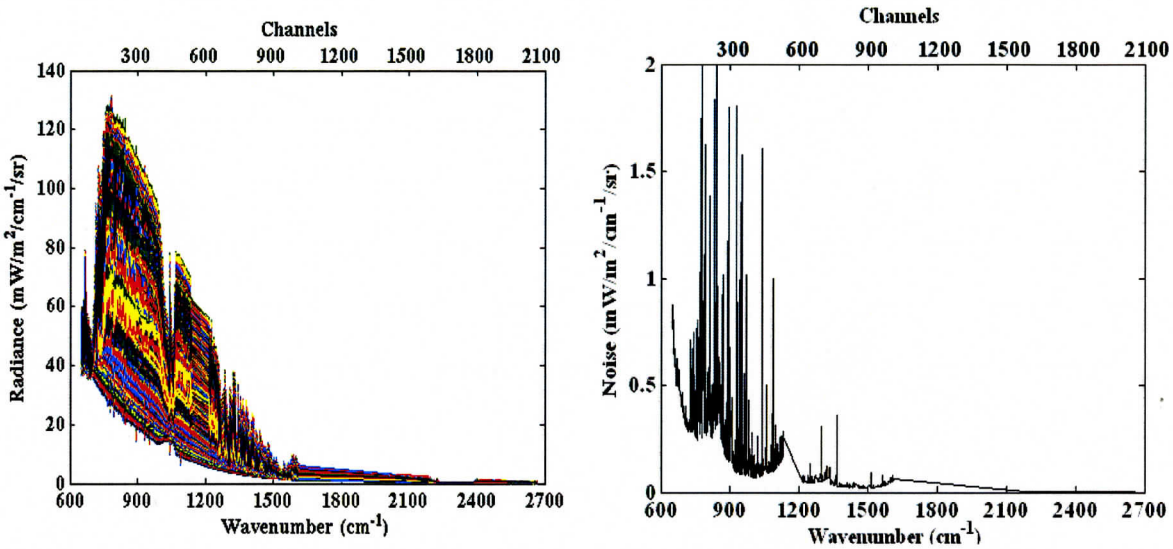

Figure 32. (a) 12150 observed AIRS radiance spectra in granule 82 from 6 September 2002. For generic hyperspectral sounder data compression studies, 270 bad channels out of the original 2378 AIRS channels have been removed. (b) AIRS calibrated noise spectrum in granule 82.

2. ABS/HES lossless wavelet compression studies

The wavelet transform has been a successful tool in data compression. It features multi-resolution analysis with compact support and linear computation times. As a technique for image compression, the transform consists of a set of basis functions onto which the image is projected, and the resultant coefficients are then encoded. Wavelet compression exploits redundancies in scale to reduce the information stored in the wavelet domain. Invertible wavelet transforms that map integers to integers are reversible in finite-precision arithmetic and hence have important applications in lossless data compression.

Wavelet Transforms

The wavelet transform may be classified by a pair of vanishing moments $(n, \tilde{n})$, where n and $\tilde{n}$ represent the number of vanishing moments of the analysis and the synthesis high pass filters respectively. Additionally, we use the notation $L / \tilde{L}$ to represent the length of the low pass and high pass filters respectively. The discrete wavelet transform can be

implemented with the use of the lifting scheme. The lifting scheme has several desirable advantages that include low complexity, linear execution time and in-place computation, and it can be used on signals with an arbitrary length. The integer wavelet transform can be obtained via the lifting scheme combined with some rounding-off operation. It consists of three steps:

1) the lazy wavelet transform:

$$h_0[n] = x[2n+1],$$
$$l_0[n] = x[2n].$$

2) one or more dual and primal lifting steps:

$$h_i[n] = h_{i-1}[n] - \left\lfloor \left(\sum_k s_i[k]\, l_{i-1}[n-k] \right) + \frac{1}{2} \right\rfloor,$$
$$l_i[n] = l_{i-1}[n] - \left\lfloor \left(\sum_k t_i[k]\, h_i[n-k] \right) + \frac{1}{2} \right\rfloor.$$

where the filter coefficients $s_i[k]$ and $t_i[k]$ are computed by factorization of a polyphase matrix of any perfect reconstruction filter bank.

3) rescaling:

$$l[n] = \frac{l_N[n]}{K},$$
$$h[n] = K \cdot h_N[n].$$

The inverse is obtained by reversing the lifting and dual-lifting steps with the corresponding sign flips as:

$$l_{i-1}[n] = l_i[n] + \left\lfloor \left(\sum_k t_i[k]\, h_i[n-k] \right) + \frac{1}{2} \right\rfloor,$$
$$h_{i-1}[n] = h_i[n] + \left\lfloor \left(\sum_k s_i[k]\, l_{i-1}[n-k] \right) + \frac{1}{2} \right\rfloor.$$

The filter coefficients need not be integers, but are generally rational with power-of-two denominators allowing all divisions to be implemented using binary shifts. Figures 33 and 34 show the forward and inverse wavelet transforms using the lifting scheme, respectively.

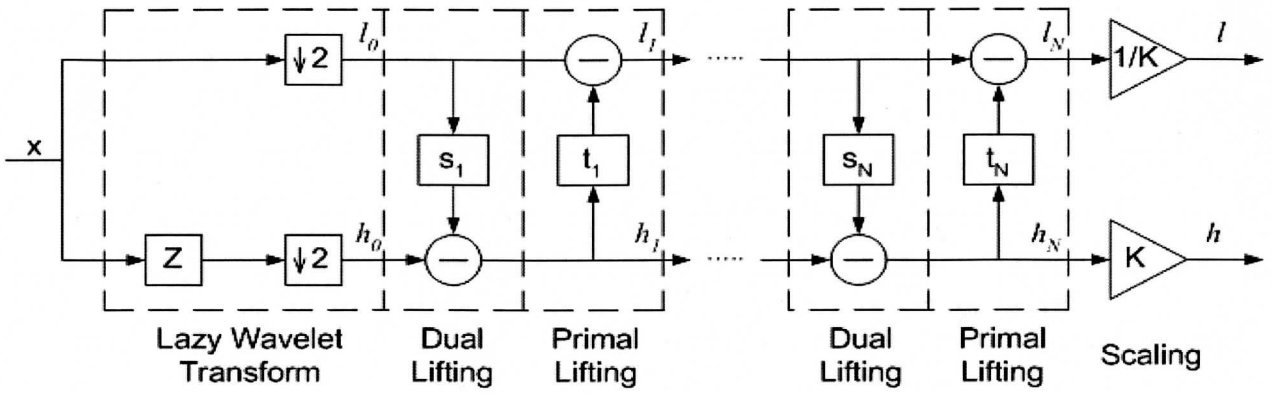

Figure 33. Forward wavelet transform using the lifting scheme.

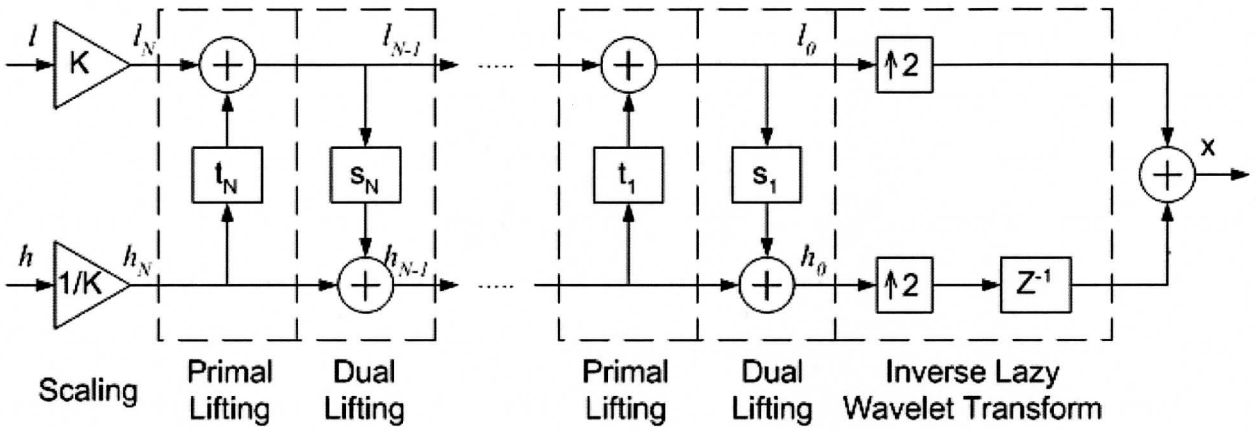

Figure 34. Inverse wavelet transform using the lifting scheme.

Three-dimensional Zerotree Coding

After the wavelet transform, the coefficients can be represented by use of a tree structure. Both the embedded zerotree wavelet (EZW) scheme and the Set Partitioning in Hierarchical Trees (SPIHT) take advantage of this structure for better compression.

Different levels in the hierarchical subbands, but at the same spatial orientation, display similar characteristics. EZW uses this characteristic of multi-level wavelet transforms to efficiently encode the DWT coefficient by defining the parent-child interband relationships in the decomposition structure. SPIHT is a refinement of the EZW scheme which provides a better compression while also having faster encoding and decoding times. It uses spatially oriented trees to describe the relationship between the parents on higher levels to the children and grandchildren on lower levels. These spatial relationship trees are common for both SPIHT and EZW and can be seen in the 2D wavelet decomposition of Figure 35.

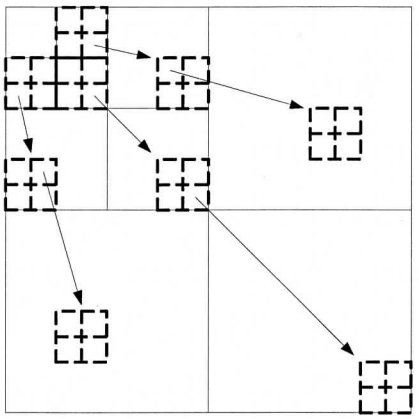

Figure 35. Parent-child interband relationship for zerotree coding.

Special Consideration for 3D Irregular Data

Special consideration needs to be given when applying SPIHT or EZW to the hyperspectral sounding data that is not regular i.e. the boundaries of the data set are not divisible by 2^N, where N is the number of levels of wavelet decomposition. The number of children varies for each parent node and not all combinations of child nodes are possible for an irregular data set. It can be shown that {1, 2, 3, 4, 6, 9} are the allowable child combination set for 2D irregular data whereas {1, 2, 3, 4, 6, 8, 9, 12, 18, 27} for 3D irregular data. In contrast, the allowable numbers of children for 2D and 3D regular data are {4} and {8} respectively. Figure 36(a) shows {1, 2, 3, 6, 9} as the possible numbers of children for 2D irregular data whereas Figure 36(b) shows {1, 2, 4}. We will present results for both the regular and irregular size hyperspectral sounder data. The SPIHT scheme for irregular data requires significant amount of additional memory storage or CPU time to do the bookkeeping of parent-child relationships.

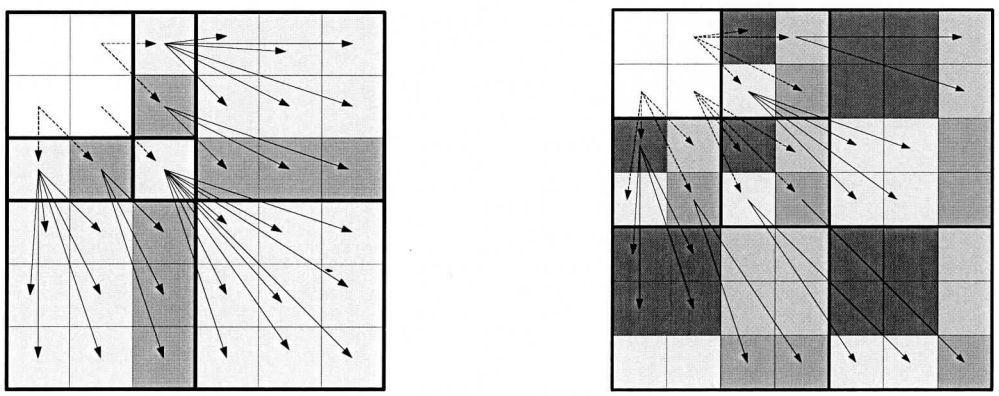

(a) (b)

Figure 36. Examples of allowable parent-child relations for 2D irregular data.

JPEG2000

This algorithm is published as a standard of ISO/IEC, as well as an ITU-T recommendation. Its rich feature list includes progressive transmission by quality, resolution, component, or spatial locality, lossy and lossless compression, region of interest coding by progression, and limited memory implementations, to name a few.

The JPEG2000 encoder consists of three main stages: discrete wavelet transform, scalar quantization, and block coding. After the DWT stage, embedded scalar quantization is performed with the quantization step size possibly varying for each subband. The block coder is based on the principles of Embedded Block Coding with Optimized Truncation (EBCOT) and includes an arithmetic coder coupled with a rate-distortion optimization algorithm to achieve the optimal bitrates.

3. ABS/HES lossless predictor-based compression studies

CALIC and JPEG-LS are the state-of-the-art lossless compression schemes that belong to this class of compression schemes. Both of these are characterized by prediction of the current pixel value using some of its previous neighbors, and then entropy coding of the error between the predicted value and actual pixel value.

JPEG-LS

The ISO/IEC working group released a new standard for the lossless/ near lossless compression of continuous-tone images in 1999, popularly known as JPEG-LS. Near lossless compression is controlled through an integer valued threshold representing the maximum permissible absolute difference between each original pixel value and its decompressed value. As shown in Figure 37, the JPEG-LS encoder is composed of four main stages: prediction, context modeling, error encoding, and run mode. A brief description of these stages follows.

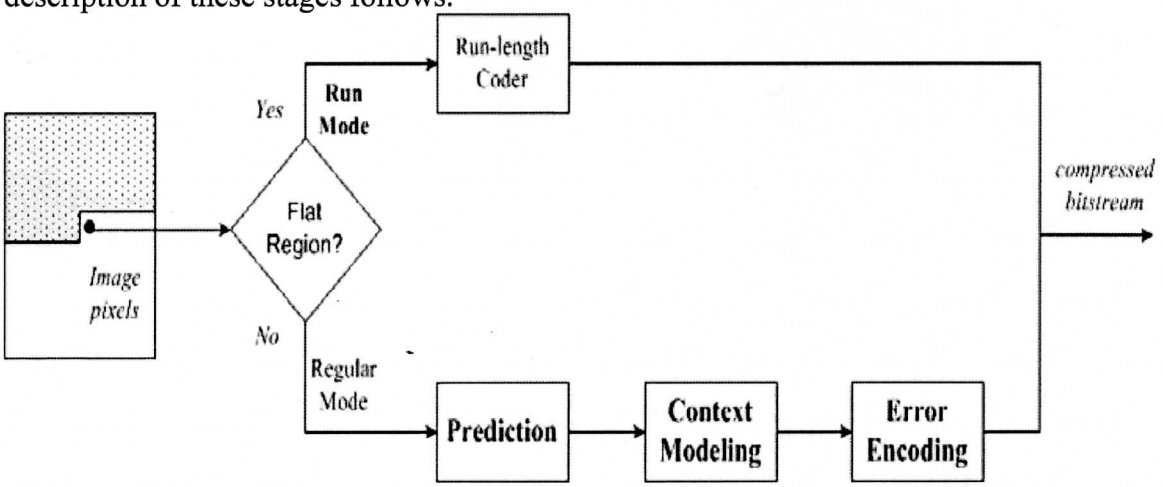

Figure 37. Schematic diagram of JPEG-LS encoder

Prediction

The nonlinear predictor $P(x)$ is a function of the neighborhood values shown in Figure 38, denoted as *a, b, c* and *d*.

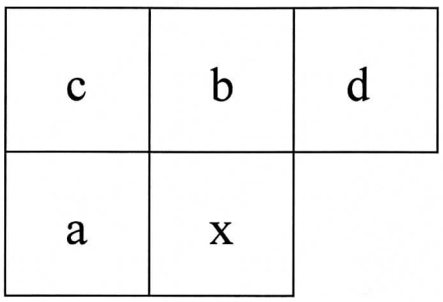

Figure 38. Causal Neighborhood of JPEG-LS.

It is based on the principle of edge detection and is given by

$$P(x) = \begin{cases} \min(a,b) & \text{if } c \geq \max(a,b) \\ \max(a,b) & \text{if } c \leq \min(a,b) \\ a+b-c & \text{otherwise} \end{cases} \quad (1)$$

Context Modeling

Three local gradients are used to determine the contexts for characterizing the neighborhood of the pixel being predicted. They are given by

$$\Delta_1 = d-b, \qquad \Delta_2 = b-c, \qquad \Delta_3 = c-a. \quad (2)$$

To further reduce the context model, each of these local gradients Δ_i, is quantized to obtain 9 quantization indices $Q_i \in \{-4,4\}$. These contexts are used later in Golomb coding for better compression.

Error Encoding

The error, $e(x) = x - P(x)$, is encoded instead of the image pixel x. A bias term is also added to this error for efficient coding. These errors are represented by a Golomb code with parameter $m = 2^k$ and are mapped to a nonnegative quantity $e'(x)$. The Golomb code is optimal for one-sided geometric distribution of non-negative integers. The parameter k depends on the context and hence is determined adaptively and updated each time a pixel with that context is found. To avoid excessively large code words from being produced, JPEG-LS employs a length-constrained Golomb code.

Run Mode

To capture local redundancy in homogeneous regions, JPEG-LS supports a run mode. It enters this mode whenever all the neighborhood samples are the same. In this mode, the value of the current pixel x is run-length encoded by counts the number of consecutive pixels that are all identical to the reference value. This mode is terminated either when a sample value is not equal to the reference value, or the end of line is reached.

CALIC

The Context-Adaptive Lossless Image Codec (CALIC) scheme is considered as a benchmark for lossless compression of continuous tone images. It works on the principle of a context-adaptive non-linear predictor which adjusts to the local gradients around the current pixel. The algorithm itself is guided by the idea of universal context modeling (UCM). A schematic description of the coding algorithm from the original paper is shown in Figure 39.

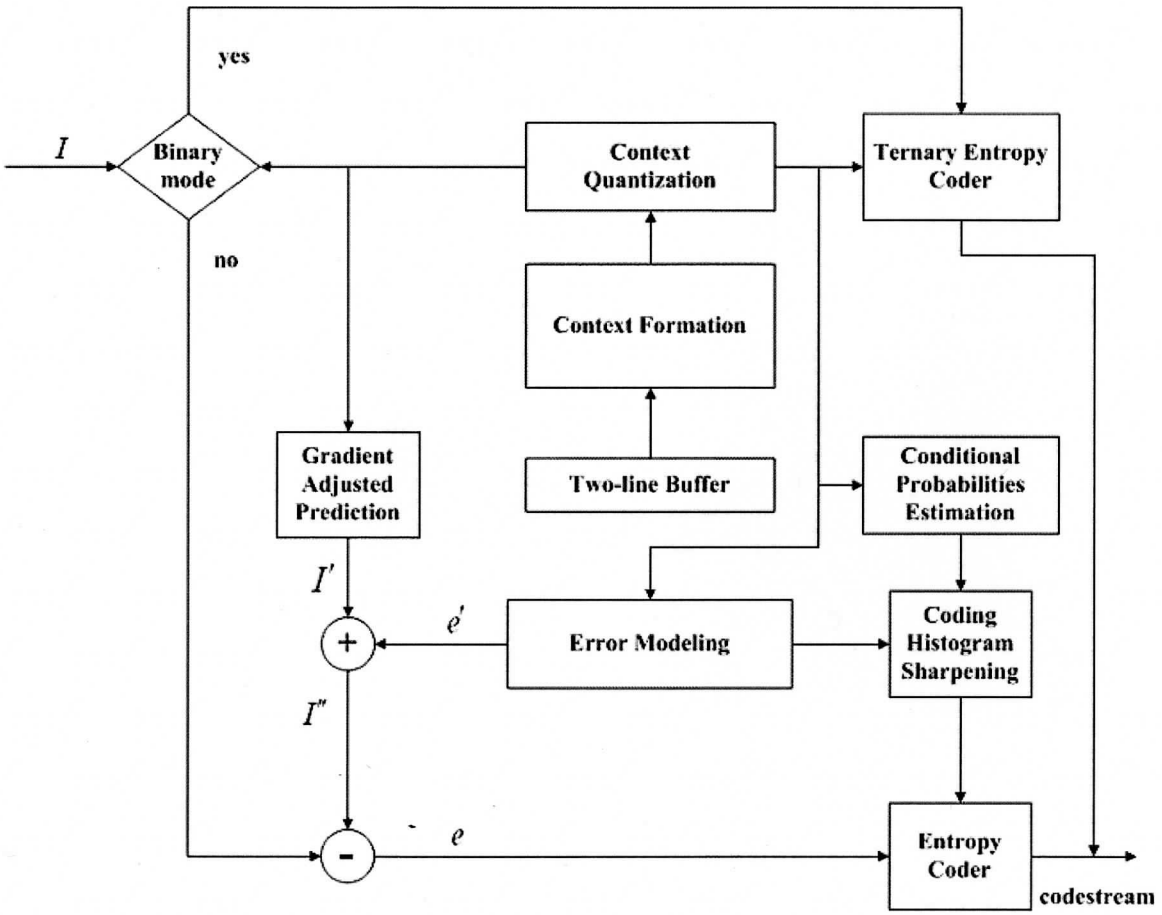

Figure 39. Schematic description of CALIC's encoder.

The algorithm operates in the binary or continuous modes. The binary mode codes the regions of the image in which the intensity value is no more than two. In the continuous mode, the system has four major components: gradient-adjusted prediction, context

selection and quantization, context modeling of prediction errors, and entropy coding of prediction errors. A brief description of these major components follows.

Gradient-Adjusted Prediction

This is an adaptive nonlinear predictor that adapts to the intensity gradients near the predicted pixel. It utilizes the pixels in the current and previous two scan lines of the current pixel being predicted, as shown in Figure 40.

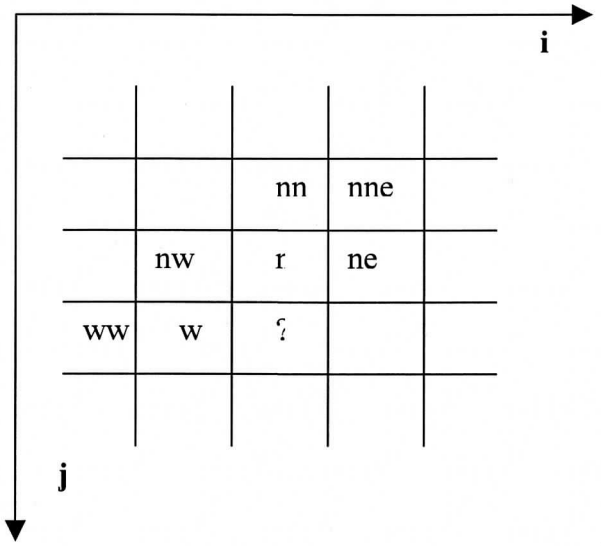

Figure 40. Neighboring pixels used in prediction and modeling.

The gradients of the pixels calculated in the horizontal and vertical are given by

$$d_h = |I[i-1,j]-I[i-2,j]|+|I[i,j-1]-I[i-1,j-1]|+|I[i+1,j-1]-I[i,j-1]| \quad (1)$$

$$d_v = |I[i-1,j]-I[i-1,j-1]|+|I[i,j-1]-I[i,j-2]|+|I[i+1,j-1]-I[i+1,j-2]| \quad (2)$$

These gradients are used to weight the neighboring pixels of $I[i,j]$ to form the first prediction I' of $I[i,j]$ according to an empirically chosen formula.

Context Selection and Quantization

For further decorrelation, an energy estimator Δ is calculated from the above gradients and the prediction error of the previous pixel. This is given by

$$\Delta = a\, d_h + b\, d_v + c\,|e_w| \quad (3)$$

where the values of a, b and c are empirically chosen and e_w is the prediction error of the previous pixel. This energy estimator is quantized into eight bins for time and space efficiency denoted by Δ'. To separate the prediction errors into classes of different variances, the error distribution is conditioned on this energy estimator. Thus the entropy

coding of errors using the conditional error probability $p(e \mid \Delta')$ improves coding efficiency over using just the probability $p(e)$.

Context modeling of prediction errors

Context modeling is used to achieve further compression gains by feeding back an error term to correct the bias in the fist prediction. Hence we have

$$I'' = I' + e', \tag{4}$$

where I'' is the second prediction and e' is the feedback error.

Entropy coding of prediction errors

The new prediction error $\varepsilon = I - I''$ is entropy coded using the conditional error probabilities $p(e \mid \Delta')$. In the binary mode, a simple ternary adaptive arithmetic coder is used along with 32 different contexts for which a frequency count is maintained. In the continuous-tone mode, an *m*-ary arithmetic coder based on the work of Moffat, Neal and Witten is used.

To apply the CALIC algorithm to the 3D hyperspectral sounding data, the data needs to be converted into two dimensions. This can be done by converting the 2D spatial domain into one dimension. Although the raster scan can serve this purpose, a continuous scan will smooth the transition of data samples from one line to another. Examples of continuous scans are horizontal, vertical and diagonal zigzag scans, spiral scan, and the Peano scan.

4. Bias Adjusted Reordering for ABS/HES lossless compression studies

CALIC, JPEG-LS, and JPEG2000 are the state-of-the-art lossless compression algorithms but they only support compression of 2D data. Therefore to apply these algorithms to the 3D hyperspectral sounding data, one can process the data framewise or make the data two-dimensional by converting the two spatial dimensions into one dimension by a continuous scan. The disadvantage to the first approach is that it does not explore the correlation between different spectral channels whereas the second approach explores it little via predictive techniques (JPEG-LS, CALIC) or the wavelet transform (JPEG2000). To remedy these situations in order to improve the JPEG-LS compression on the hyperspectral sounding data, we develop a bias-adjusted reordering (BAR) scheme for converting the 3D data into 2D with the highest correlation channels rearranged together. The BAR scheme takes advantage of the unique spectroscopic characteristics of the hyperspectral sounding data that features the strong correlations in disjoint spectral regions affected by the same type of absorbing gases at various altitudes. It can also explore the spatial correlations of the data due to similar absorbing gases and clouds scattered across the geographical domain. The BAR scheme is geared towards exploiting these correlations along different dimensions. When applying the BAR scheme in the spectral dimension, channels with similar dynamical range but different radiance values due to each channel's altitude preference are bias aligned together for finding the highest correlated spatial vector as the nearest neighbor of each reordered channel. Similarly, when applying the BAR scheme to the spatial dimension, pixels with similar dynamical

range but different radiance values due to different amount of absorption from the same kind of absorption gases or clouds are bias aligned together for finding the highest correlated spectral vector as the nearest neighbor of each reordered pixel.

The bias-adjusted reordering scheme can explore the correlation among disjoint spectral regions and disjoint spatial regions affected by the same type of absorbing constituents at similar altitudes. Consider a 3D hyperspectral data cube of size n_c by n_x by n_y. For JPEG2000 compression, it is reshaped into a 2D data of size n_c by n_s via a continuous scan, where $n_s = n_x \times n_y$. When data is spectrally reordered, there are n_c vectors, each with n_s components. Each vector $V = \left(v_1, ..., v_{n_s}\right)$ represents a point in the $\mathbb{R}^{n_s}$ space. Let S be the pool of the vectors not yet reordered. In the bias-adjusted reordering scheme along the spectral dimension we start with a reference vector, and each vector $V \in S$ is optimally bias-adjusted by a constant scalar b for better match with the reference vector. The best matched bias-adjusted vector is the nearest neighbor of the reference vector in the $\mathbb{R}^{n_s}$ space. It becomes a new reference vector and its associated unadjusted vector is removed from S. The process is repeated until the pool S becomes empty.
Mathematically, given the *i-th* reordered vector $\tilde{V}^i$, we are seeking V^* and b^*, the minimum norm solution of

$$\min_{\substack{V \in S \\ b \in \mathbb{R}}} f^i(V, b), \tag{3}$$

where the cost function is

$$f^i(V, b) = \left\| \tilde{V}^i - V - b \right\|^2 = \sum_{k=1}^{n_s} (\tilde{v}_k^i - v_k - b)^2 . \tag{4}$$

Then the $(i+1)$-*th* reordered vector is simply

$$\tilde{V}^{i+1} = V^* + b^* .$$

The optimal value b^* is obtained by

$$\left. \frac{\partial f^i(V, b)}{\partial b} \right|_{b=b^*} = 0, \tag{5}$$

which yields

$$b^* = \frac{\sum_{k=1}^{n_s} (\tilde{v}_k^i - v_k)}{n_s} = \langle \tilde{V}^i \rangle - \langle V \rangle , \tag{6}$$

where $\langle\ \rangle$ is the mean of a vector over its components. The b^* represents the bias between the two vectors $\tilde{V}^i$ and V.

Applying Eq. (6) to Eq. (4) yields the following cost function

$$f_{b^*}^{i}(V) = \sum_{k=1}^{n_s} (\tilde{v}_k^i - v_k)^2 - \frac{1}{n_s}\left[\sum_{k=1}^{n_s} (\tilde{v}_k^i - v_k)\right]^2, \tag{7}$$

or

$$f_{b^*}^{i}(V) = \left\|\tilde{V}^i - V\right\|^2 - n_s\left(\langle\tilde{V}^i\rangle - \langle V\rangle\right)^2, \tag{8}$$

and the bias-adjusted reordering problem is reduced to finding the minimum norm solution V^* of

$$\min_{V \in S} f_{b^*}^{i}(V). \tag{9}$$

For lossless compression, the b^* is rounded to the nearest integer $[\![b^*]\!]$. Similarly, the bias-adjusted reordering scheme can be applied along the spatial dimension.
For the ABS/HES data compression studies, we have implemented various 3D wavelet transforms via lifting schemes and performed compression on the ten granules for the 3D EZW and 3D SPIHT compression algorithms. These results are shown in Figures 41-44.

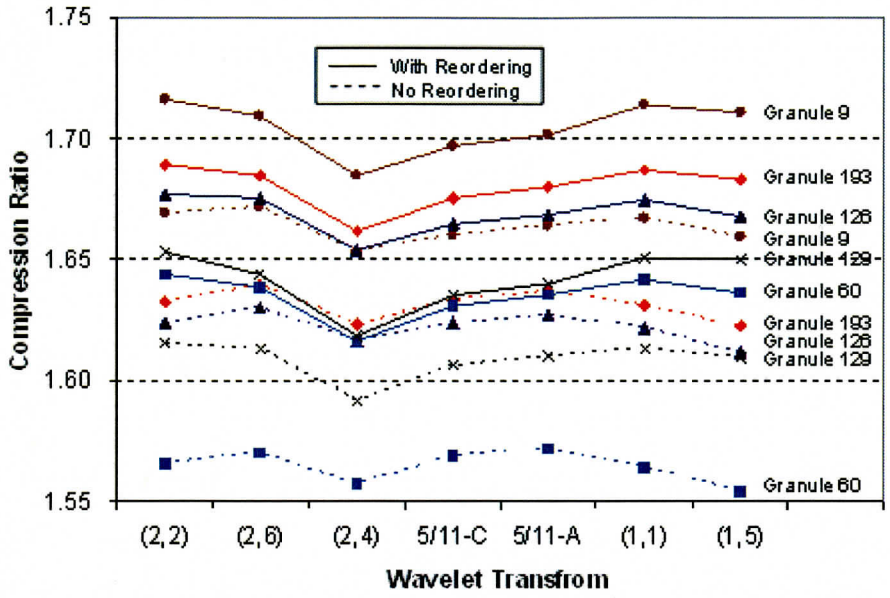

(a)

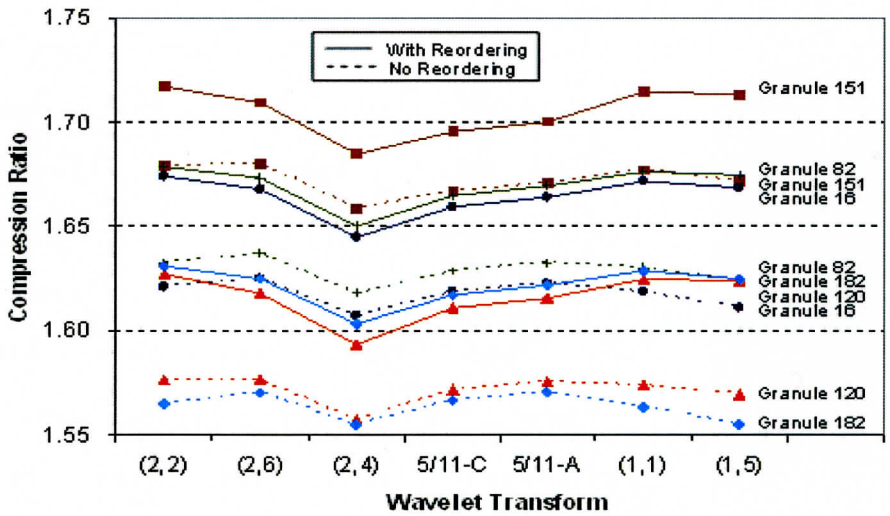

(b)

Figure 41. (a) Compression ratios for daytime granules by use of EZW and different wavelet transforms with and without original reordering. (b) Compression ratios for nighttime granules by use of EZW and different wavelet transforms with and without original reordering.

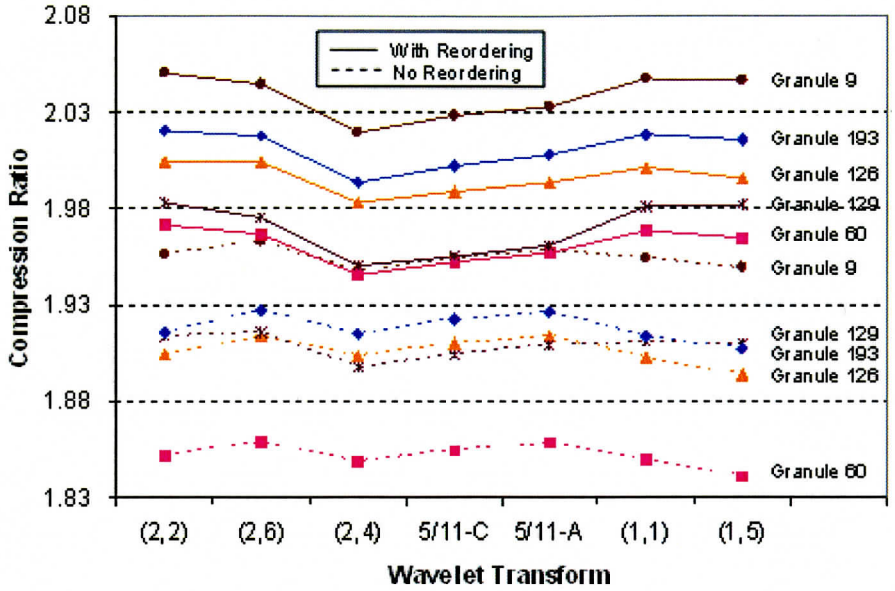

(a)

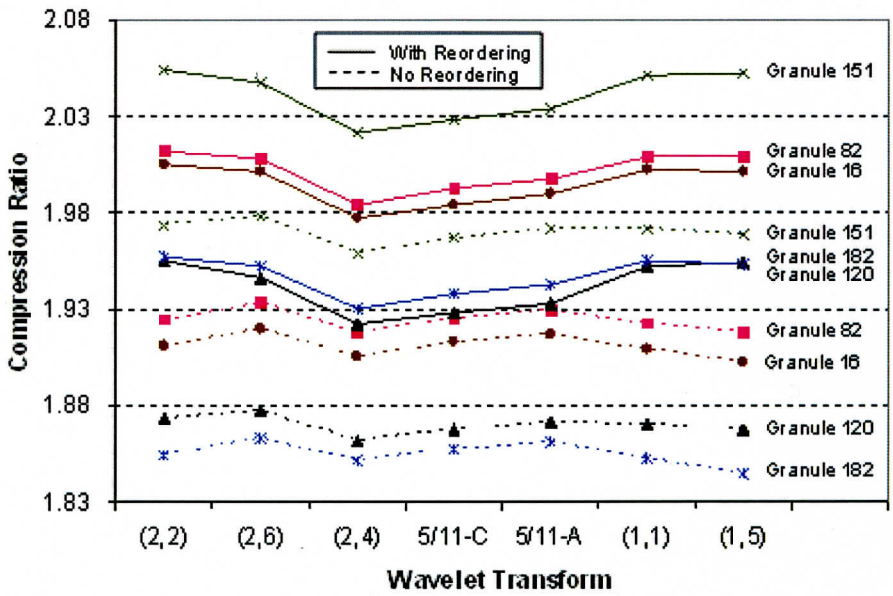

(b)

Figure 42. (a) Compression ratios for daytime granules by use of SPIHT and different wavelet transforms with and without original reordering. (b) Compression ratios for nighttime granules by use of SPIHT and different wavelet transforms with and without original reordering.

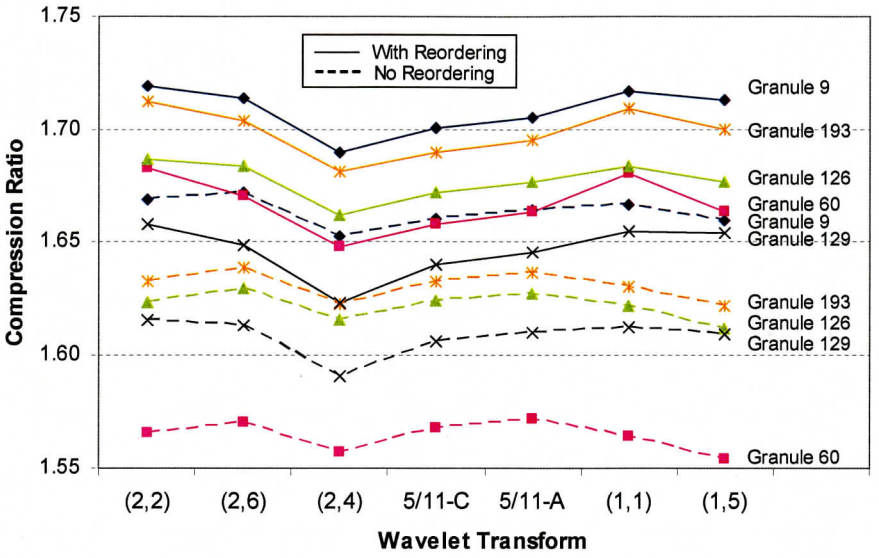

(a)

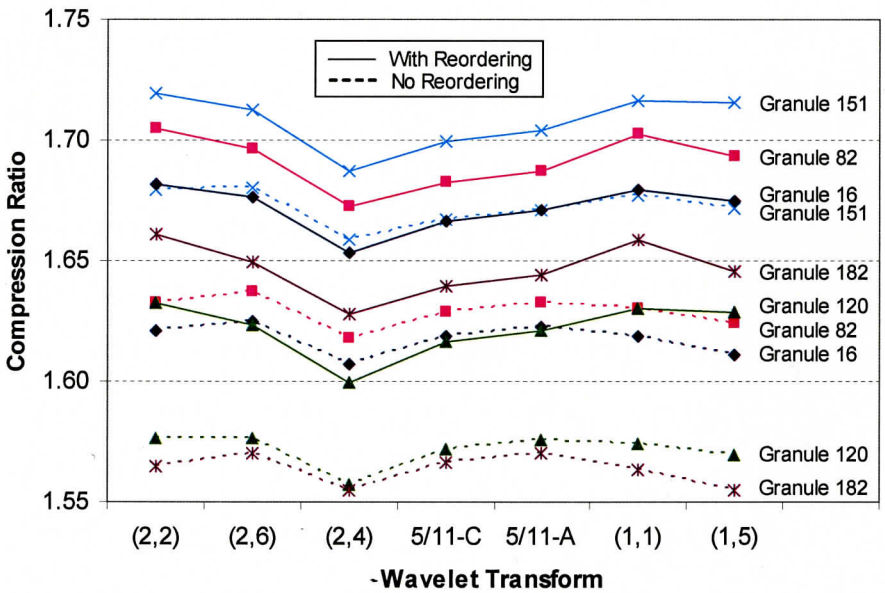

(b)

Figure 43. (a) Compression ratios for daytime granules by use of EZW and different wavelet transforms with and without BAR. (b) Compression ratios for nighttime granules by use of EZW and different wavelet transforms with and without BAR.

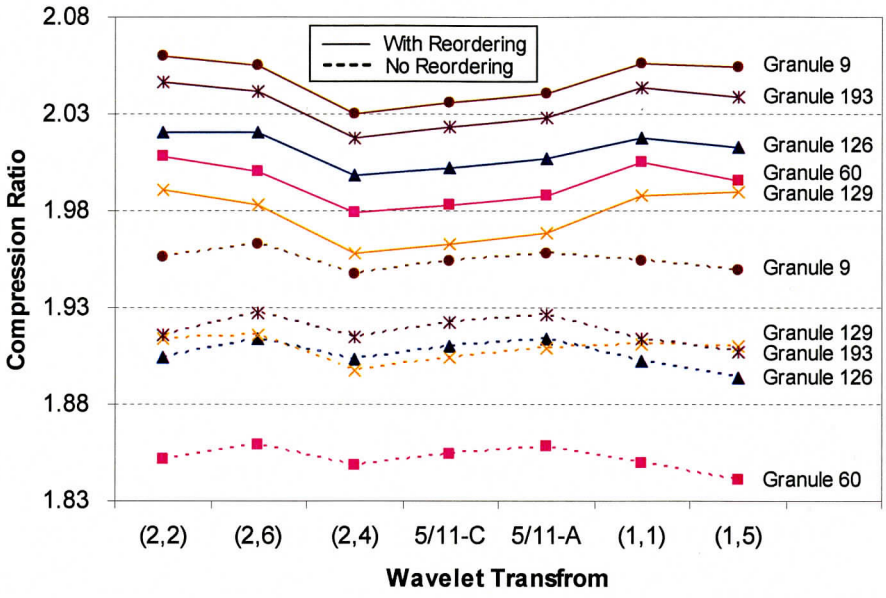

(a)

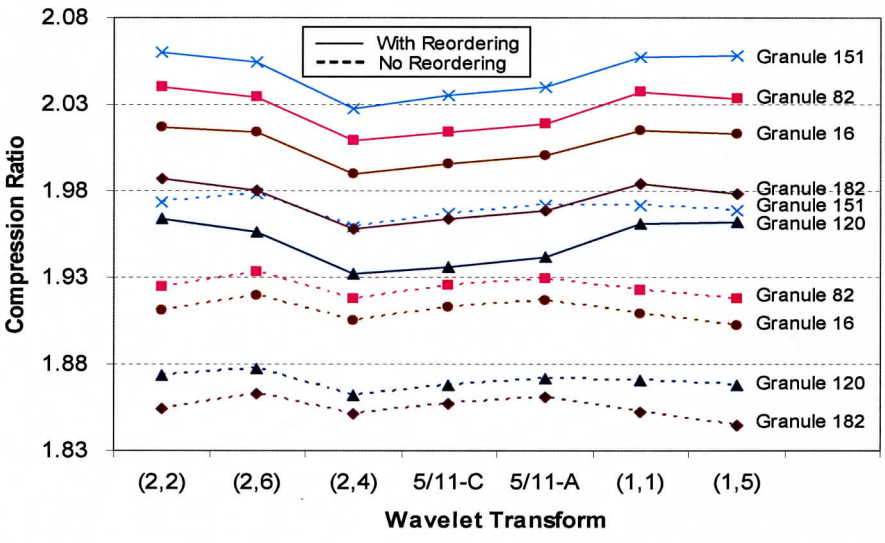

(b)

Figure 44. (a) Compression ratios for daytime granules by use of SPIHT and different wavelet transforms with and without BAR. (b) Compression ratios for nighttime granules by use of SPIHT and different wavelet transforms with and without BAR.

The results for the different compression schemes including CALIC, JPEG-LS and JPEG2000 with the BAR scheme are given below in Figure 45. For a comparison, we also include the compression ratios obtained for the reordering without bias-adjustment.

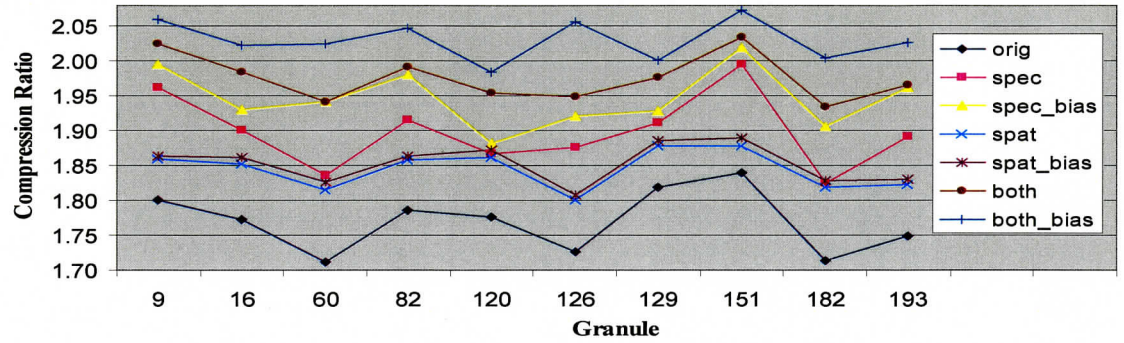

(a)

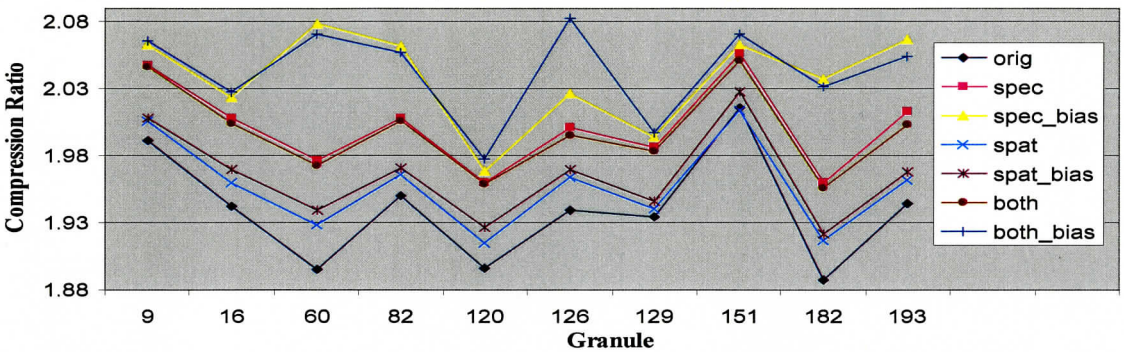

(b)

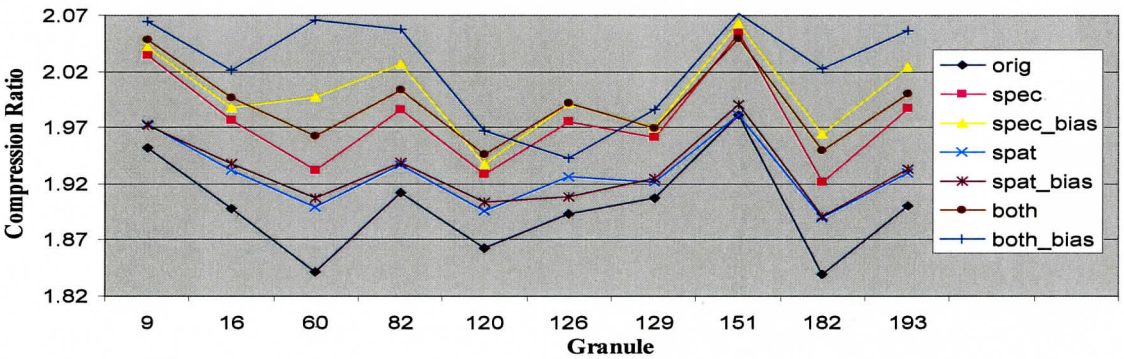

(c)

Figure 45. (a) Compression ratios for CALIC compression with and without reordering for the 10 tested granules. (b) Same as (a) except for JPEG-LS compression. (c) Same as (a) expect for JPEG2000 compression.

Furthermore, we give a comparison for all five compression schemes for bias-adjusted spectral reordering as shown in Figure 46.

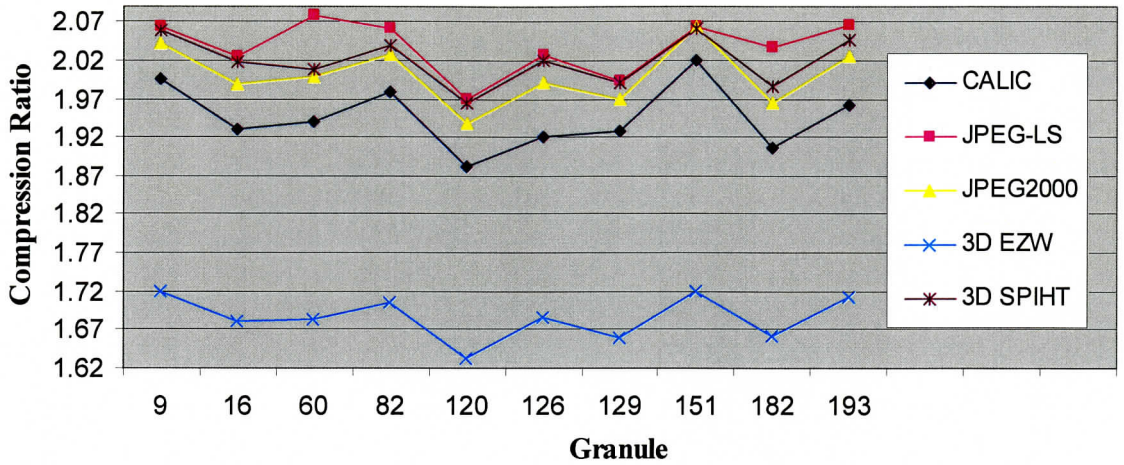

Figure 46. Compression ratios for different schemes with spectral bias adjusted reordering on 10 granules.

The figure shows that JPEG-LS outperforms all the other schemes in terms of compression ratios. 3D EZW produces the smallest compression ratios, whereas 3D SPIHT and JPEG2000 have similar compression ratios.

VI. CIMSS Studies on Next-Generation GOES Sounder (HES) and Imager (ABI) on GOES-R and Beyond

1. Proposed Research Activities in 2003

- Continue channel selection for ABI based on the users' requirement and cost to benefit. Trade-off ABI channel selection using MODIS data to demonstrate the impact by adding or removing 2.26 and 3.7 micron bands.
- Continue to do trade-off studies of the HES instrument design. Information comparison between 2-band interferometer option and 3-band AIRS like option will be conducted. In addition, information comparison between AIRS 2-band option (Longwave + Midwave) and AIRS 3-band option (Longwave + Midwave + Shortwave) will also be conducted. These trade-off studies will support the instrument design base on the users' requirement and cost to benefit.
- Investigate the improved and new products from ABI and study the utility of those products on weather monitoring and forecasting. Compare the capability of ABI and current GOES imager. Demonstrate the advantages and benefits of ABI on future weather monitoring and forecasting.
- Continue to investigate vertical and spatial resolutions achievable from HES/ABI measurements.
- Combine HES/ABI for cloud detection and classification, optimal sounding under clear and cloudy skies, better cloud property retrieval under cloudy skies.

Demonstrate the advantages of products from HES/ABI combination over that from either HES or ABI alone.

- Trace gas (ozone, CO etc.) study from combination of HES/ABI.
- Use AIRS/MODIS measurements to validate the algorithms for HES/ABI data processing.
- Continue non-sounding product retrieval (surface emissivity, land surface temperature, cloud emissivity, cloud-top pressure) from combination of HES/ABI.
- Continue to evaluate the ABI performance with comparison of current imaging systems such as current GOES imager, AVHRR, MODIS and FY-1C. MODIS and AVIRIS data would be used for this. The range of events may include severe storms, blowing snow, volcanoes, etc. Information analysis will be carried out to evaluate ABI performance on those events with comparison of current GOES imager, AVHRR, MODIS and FY-1C.

2. Accomplishments and Findings from April 1 to September 30, 2003

2.1 ABI study without a green band (0.55um)The objective is to study the impact of without green band on ABI true color image. A look-up table for ABI green band from other ABI visible and near IR bands was created to predict ABI green band. The natural color image of true red-green-blue was compared with that created from red-"green"-blue, where the ABI "green" band was created from the look-up table. MODIS data were used for the comparison. Results show that the difference between the two natural color images is generally small, indicating that to the first approximation ABI without green band should be able to generate natural color image with good quality

2.2 ABI Band studies and ABI band simulation with AIRS and MODIS data

The objective is to continue the ABI band study use MODIS and AIRS data; continue a number of ABI band trade-off studies. Some accomplishments include:
(a) Of the 16 ABI bands, the relative merits of the various bands were outlined.
(b) Trade-off study on shifting the spectral response function for certain ABI bands.

The reason to shift these bands would be to get a better signature of SO_2, while still maintaining the water vapor applications. The effects of shifting were studied; Figure 47 shows ABI 7.4 μm brightness temperature (BT) (left panel) and the BT difference (right panel) between the 7.4 μm and 7.34 μm simulated from AIRS measurements. BT difference is larger in warm scene than in cold scene.

2.3 ABI ozone band study

It was first suggested by Dr. Chesters (NASA) to consider spectrally broadening the ABI "ozone-sensitive" band. Adopting this wider band would mitigate several risk factors (including signal-to-noise). This has been investigated. The over-all similarity of the current and proposed ozone band on the ABI is found. The wide band is, in general, warmer (by 1-2 K in non-cloudy regions from the case study) than the narrow band. Simulations were done at the CIMSS to assess the ozone retrieval quality of either imager band. The retrieval performance is similar, for the nadir-viewing case. The noise of the spectrally wider band was decreased, but only slightly improved the overall performance. In general, the narrow and wide bands give similar estimated BTs. The differences are due to the range of local zenith angle and the total amount of ozone. Given the similarity of the ozone product between either the "narrow" or "wide" ABI band, and the small surface signal (at large angles), and the fact that the more precise ozone product will be derived from high-spectral HES data, it is demonstrated to consider the spectrally wider band for the ABI.

2.4 HES trade-off studies (spectral coverage, spectral resolution, spatial resolution and signal-to-noise)

The objective is to find optimal balance among spectral coverage, spectral resolution, spatial resolution and signal-to-noise based on the users' requirement and technical requirement.

(a) Water vapor information from LMW versus SMW

One important issue for HES instrument design is to select water vapor spectral coverage. Usually longwave coverage (LW, approximately 650 – 1200cm^{-1}) is selected for temperature, ozone and surface property retrievals. For the water vapor region, one can use either longer middlewave (LMW, approximately 1200 – 1650cm^{-1}) or shorter middlewave (SMW, approximately 1650 – 2250cm^{-1}). AIRS, for example, uses LMW while Geosynchronous Imaging Fourier Transform Spectrometer (GIFTS) uses SMW. Selection of both water vapor sides might be a better option in terms of information. For example, having both sides of the water vapor continuum would allow better trace gas measurements, and improved ABI back-up mode, better continuity for climate applications and improved retrievals. However, data volume will be increased. In order to compare the water vapor information from LMW versus SMW, a simulation study was carried out to simulate the retrieval performance for HES LW + LMW versus LW + SMW.

Figure 48 shows temperature retrieval rmse at 1km vertical resolution for LW + LMW, LW + SMW, and LW + SMW with SMW noise reduced by half (NF=0.5) (left panel), and the water vapor RH retrieval rmse at 2km vertical resolution (right panel). The spectral resolution is 0.625 cm^{-1} and the 14bit noise from HES Technical Requirement Document (TRD) is used in the simulation. In general, the temperature retrieval difference between LW+LMW and LW+SMW is about 0.1K, while the water vapor retrieval difference is about 1%. With SMW noise reduced by half, both temperature and water vapor retrieval differences between LW+LMW and LW+SMW are reduced.

Considering other factors for LMW (for example, lower spectral resolution than SMW, more trace gas other than water vapor, etc.), the temperature and moisture retrieval differences between LW + LMW and LW + SMW are very small.

(b) ABI/HES spatial resolution study using MODIS 1km data.

The spatial resolution for HES is very important because "hole hunting" will be the effective method to find clear pixels for atmospheric sounding without microwave sounding capability on the geostationary satellite. Fine spatial resolution allows a higher possibility of finding clear pixels and maintains the spatial gradients. This is very important because (a) fine spatial resolution HES measurements will meet the mesoscale forecast requirement, and (b) fine spatial resolution enable to find more homogeneous 2 by 2 or 3 by 3 fields-of-view (FOV) scenes for the possible cloud-clearing process with ABI/HES synergism,

Figure 49 shows the 1km MODIS TPW at 1900UTC on July 20, 2002 from EOS AQUA satellite, and a number of reduced spatial resolutions for IR sounders. It can be seen that coarser spatial resolution results in smoothed TPW gradients and less clear coverage. The spatial resolution of 2km or better for ABI and 5 ~ 10km for HES-DS should be considered.

(c) Spectral resolution study for non-sounding

In order to help define the requirement for HES spectral coverage and spectral resolution, trade-off studies are necessary to investigate the impact of long-wave IR window spectral resolution on non-sounding products. A study has been conducted to demonstrate that in the IR longwave window region, a spectral resolution of $1 cm^{-1}$ or better is necessary for accurately retrieving the non-sounding products such as IR surface emissivity and surface skin temperature by using the minimum local emissivity variance (MLEV) algorithm. Figure 50 shows from upper to lower panels the BT spectrum with rock emissivity, true emissivity spectrum (black line), retrieved emissivity spectra with true surface skin temperature (green line) and surface skin temperature deviated by 1K (green and red lines). The noise factor indicates the noise added in the simulation (e.g., 0.5 means half noise). The mean local emissivity variance is also indicated in each panel. Both half noise and nominal noise will create emissivity variance contrasts between true skin temperature and wrong skin temperature, indicating that both surface skin temperature and IR emissivity spectrum can be retrieved. However, the emissivity variance contrasts are very small with doubled noise, indicating that the skin temperature and surface emissivity retrieval will be difficult with doubled noise. The spectral resolution in the figure is $0.625 cm^{-1}$.

Figure 51 shows the emissivity variance differences between the wrong skin temperature and the true skin temperature as a function of skin temperature error, different lines correspond to various spectral resolutions and noise factors. It clearly indicates that a spectral resolution of $0.625 cm^{-1}$ with half noise and nominal noise will create an accurate emissivity and skin temperature retrievals, while only half noise will create good surface property retrieval with lower spectral resolution (e.g., $1.25 cm^{-1}$). Note that this effect is not the only error source in estimating surface emissivity and skin temperature.

2.5 ABI/HES SYNERGISM

ABI products such as atmospheric temperature/moisture profiles and cloud properties can serve as background information, the atmospheric and cloud parameters can be retrieved from sounder radiances with much better accuracy; this is demonstrated by cloud property retrieval from synergistically MODIS/AIRS data.

Figure 52 shows an AIRS BT image at a window region at 19:17UTC on 6 September 2003 (granule 193) (left panel) and the MODIS classification mask at 1km spatial resolution superposed to the AIRS footprints for the study area indicated in the left panel. The AIRS footprint indicated by an arrow in right panel of Figure 52 is used to demonstrate the MODIS/AIRS synergistic cloud retrieval. This pixel is identified by MODIS classification mask as middle level clouds and the clouds belong to ice clouds according to the MODIS cloud phase mask at 1km resolution. The upper panel of Figure 53 shows the AIRS longwave clear BT calculation from the ECMWF forecast model analysis (yellow line), the cloudy BT calculation with the MODIS CTP and ECA (green line), the BT calculation from the AIRS retrieved CTP and ECA, and the BT calculation with AIRS retrieved CTP as well as cloud particle size (CPS) and cloud optical thickness (COT) (redline), along with the cloudy BT observation (black line) spectra for footprint indicated by an arrow in Figure 52; the lower panel of Figure 53 shows the corresponding BT difference between observation and calculation. As described, the MODIS cloud products serves as the background information in the AIRS retrieval; a variational (1DVAR) approach is used for MODIS/AIRS synergistic retrieval of CTP, ECA, CPS and COT products. It shows that there is a large difference between calculation with the MODIS cloud products and observation in the CO_2 region, the difference in the CO_2 region is almost removed by the calculation with the AIRS retrieved CTP and ECA; AIRS adjusted the MODIS CTP by 68 hPa. However, the slope of the BT in the spectral window region for the AIRS footprint is still significantly large because of CPS effects. With AIRS retrieved CPS and COT for this footprint, the calculation (red line in this figure) fits the slope very well, indicating that the cloud microphysical properties can be retrieved effectively by the AIRS radiance measurements.

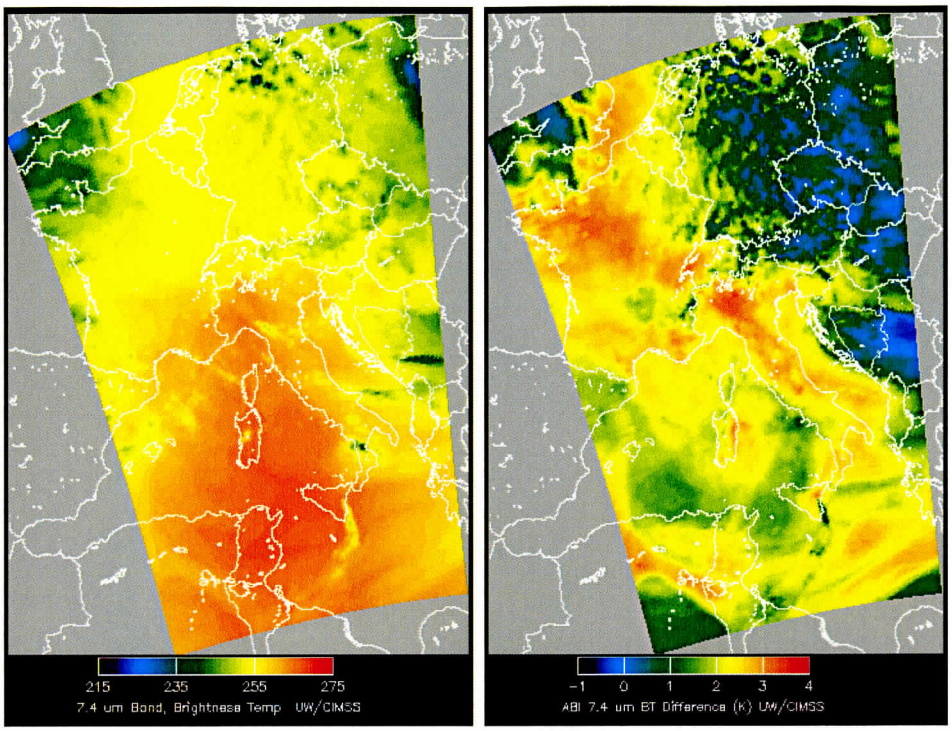

Figure 47. ABI 7.4 μm (left panel) BT and the BT difference (right panel) ABI 7.4 μm and 7.34 μm simulated from AIRS measurements.

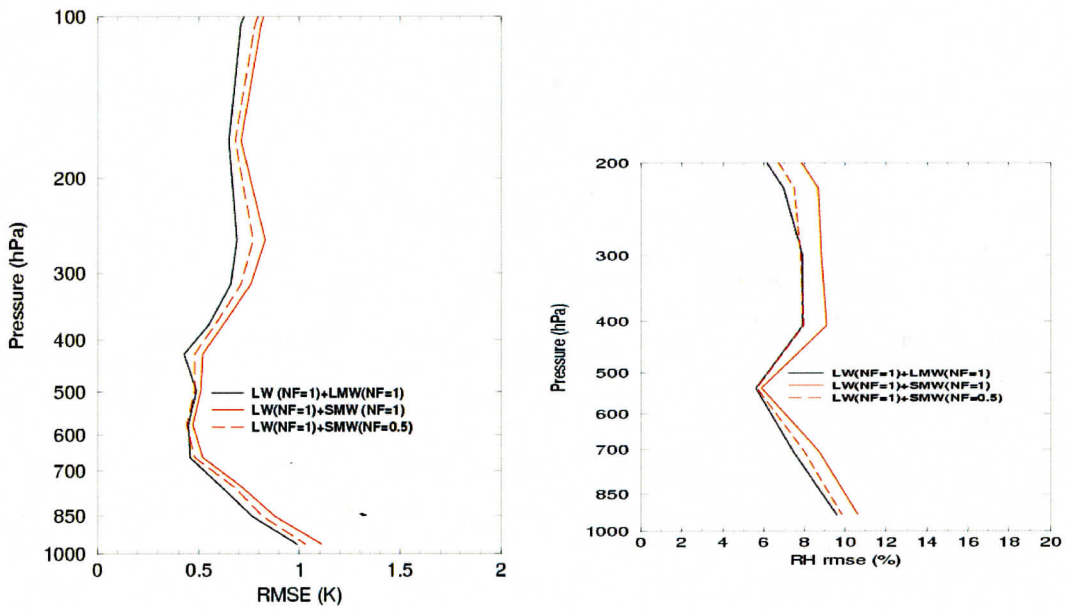

Figure 48. The temperature retrieval rmse at 1km vertical resolution and water vapor RH retrieval rmse at 2km vertical resolution from LW + LMW, LW + SMW, and LW + SMW with the SMW noise reduced by half.

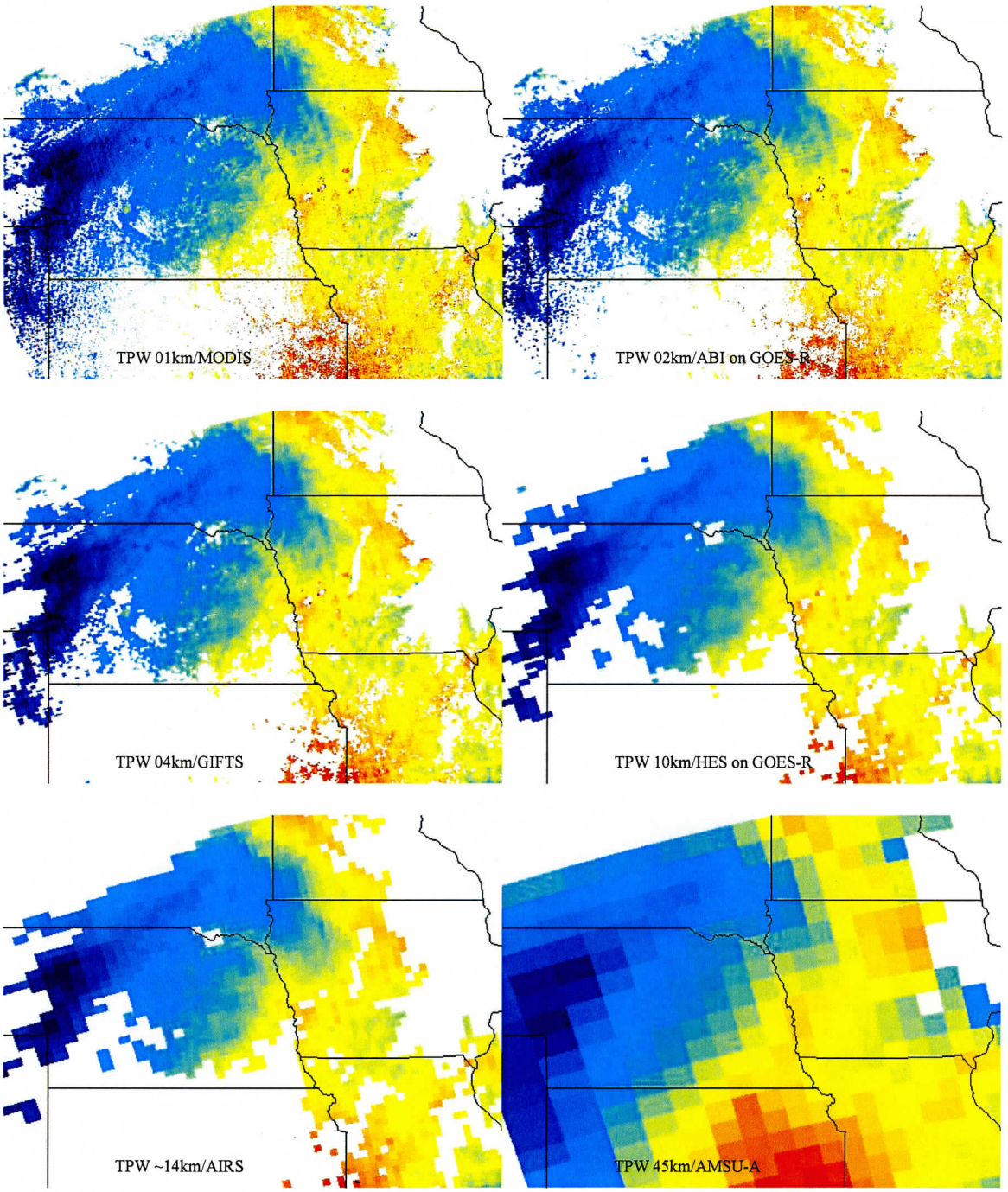

Figure 49. The 1km MODIS TPW (upper left panel) at 1900UTC on July 20, 2002 from the AQUA satellite, simulated ABI TPW at 2km (upper right panel), GIFTS or HES severe weather/mesoscale (SW/M) TPW at 4km (middle left panel), HES disk sounding (DS) TPW at 10km (middle right panel), AIRS TPW at 14km from MODIS 1km TPW (lower left panel), and AMSU TPW at 45km spatial resolution, respectively, from the MODIS 1km TPW.

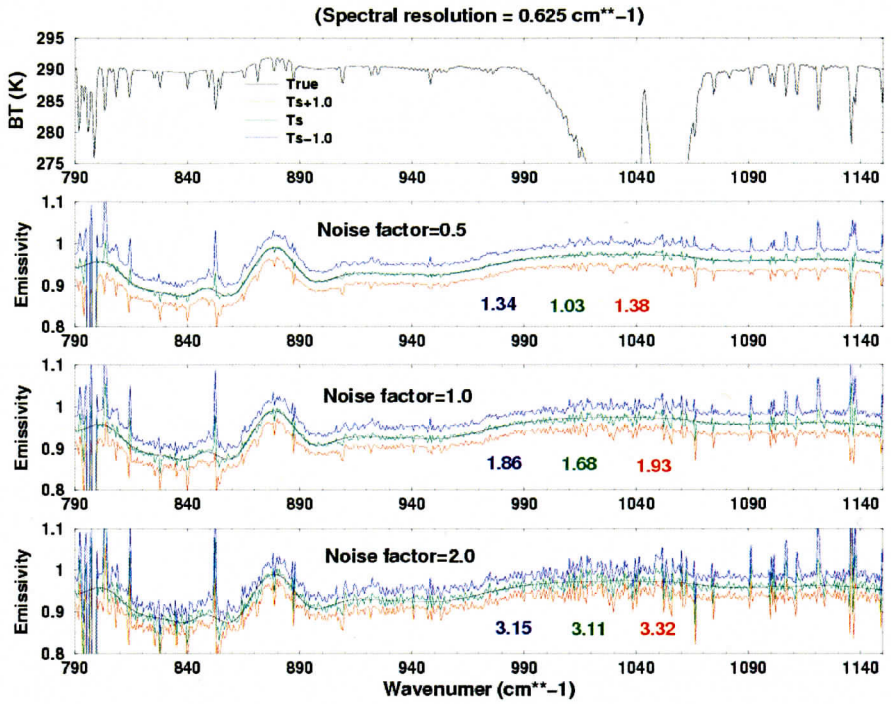

Figure 50. The BT spectrum with an observed rock emissivity spectrum, true emissivity (black line), retrieved emissivity spectra with true surface skin temperature (green line) and surface skin temperature deviated by 1K (green and red lines). The noise factor indicates the noise added in the simulation (e.g., 0.5 means half noise). The mean retrieved local emissivity variance is also indicated in each panel.

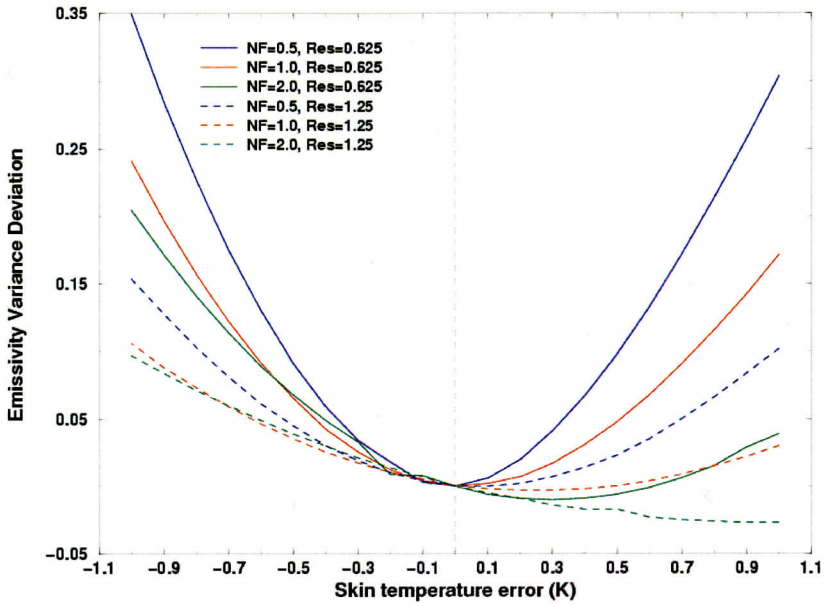

Figure 51. The emissivity variance difference between wrong skin temperature and true skin temperature as a function of skin temperature error, different lines correspond to various spectral resolutions and noise factors.

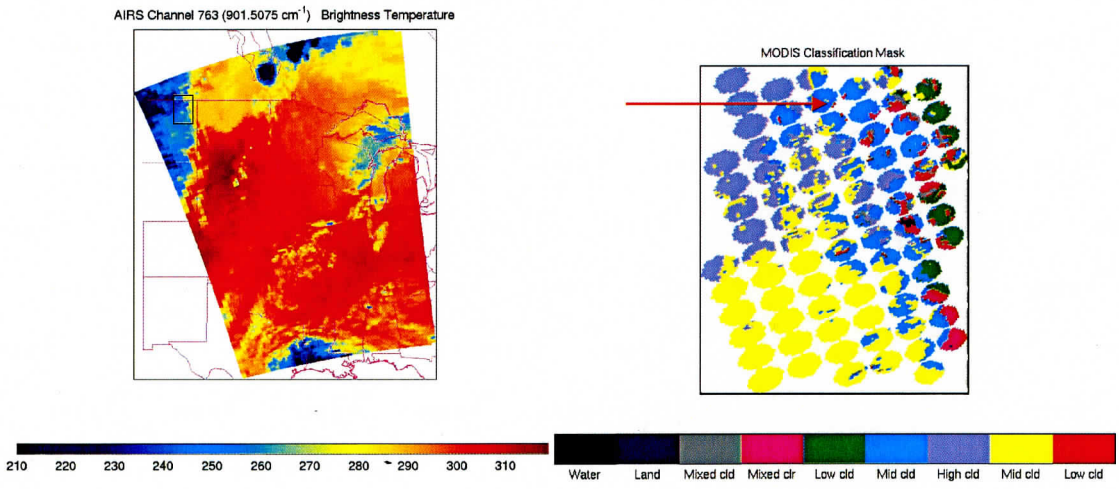

Figure 52. An AIRS BT image at a window region at 19:17UTC on 6 September 2003 (granule 193) (left panel) and the MODIS classification mask at 1km spatial resolution superimposed to the AIRS footprints for the study area indicated in the left panel.

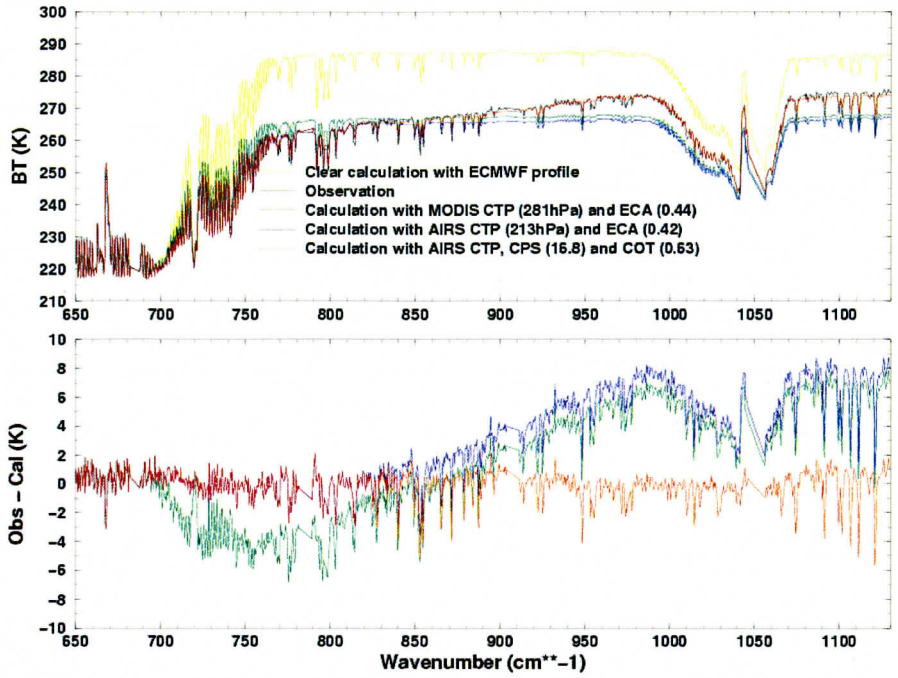

Figure 53. The AIRS longwave clear BT calculation from the ECMWF forecast analysis (yellow line), the cloudy BT calculation with the MODIS CTP and ECA (green line), the BT calculation from the AIRS retrieved CTP and ECA, and the BT calculation with AIRS retrieved CTP as well as CPS and COT (redline), along with the cloudy BT observation (black line) spectra for footprint indicated by Figure 52; the lower panel shows the corresponding BT difference between observation and calculation.

VII. VISIT

During the March-September 2003 period we continued to prepare educational material and explore new techniques to demonstrate the application of integrated meteorological datasets to the operational weather forecasting community. Improvements were made to the VISITview tele-training and collaboration software, and new VISITview lessons were developed and demonstrated.

The following significant changes were made to the VISITview application software.

- allow for larger image loops to be used without running out of memory
- enhance the web-based playback and viewing of lessons for better
- synchronization, nicknamed "VISITview TV"
- more formal support for Linux and MacOS-X
- detect when lesson creator attempts to use an invalid image file format
- updated the on-line tutorial to include examples on creating quizzes
- cosmetic changes to improve the centering of the images in the window
- added menu items to the lesson builder to help out with testing
- re-factored the code for animation to significantly enhance the performance

- when zooming images
- allow overlays to be zoomed in conjunction with "base" images
- a few minor bug and feature fixes in the Lesson Builder
- updated on-line documentation to reflect software changes

In addition, we have applied for a U.S. Trademark on the name "VISITview" to avoid having the name usurped by a company in California that also applied to trademark the name.

The "Introducing GOES-12" VISITview lesson module was developed and completed, and was demonstrated to 72 National Weather Service forecast offices during March-September 2003. This lesson highlights changes made to the GOES-12 imager, with an emphasis on the 6.5 micrometer "water vapor" channel. Several water vapor channel comparisons of GOES-12 with GOES-8 demonstrate the significant improvements in detection of mesoscale features such as jet streaks. The new 13.3 micrometer CO_2 absorption channel is also discussed, with examples of the new cloud top height products that are now available for the first time using the GOES imager. Figure 54 is a screen capture from the GOES-12 lesson, showing that the improved water vapor channel on GOES-12 allows better detection of a clear air turbulence signature over the eastern US.

The "Trough of Warm Air Aloft (TROWAL) Identification" VISITview lesson (using a winter storm case over the central US) was demonstrated to 6 NWS forecast offices during this period. This lesson features a winter storm case over the central US, and was the first VISITview lesson to employ Display 3-Dimensions (D3D) graphics (a new experimental component of AWIPS). Figure 55 is a screen capture from the TROWAL lesson, showing how the trajectory display capability in D3D AWIPS can aid in visualizing the flow associated with the TROWAL airstream.

We continue to utilize the AWIPS Weather Event Simulator (WES) for building new lesson content using archived events. Ten full case study data sets are now available, including a variety of severe convection events and winter weather events. Using these archived WES cases, work was begun on new VISITview lesson modules "Water Vapor Channel Satellite Imagery" and "Mesoscale Convective Vorticities".

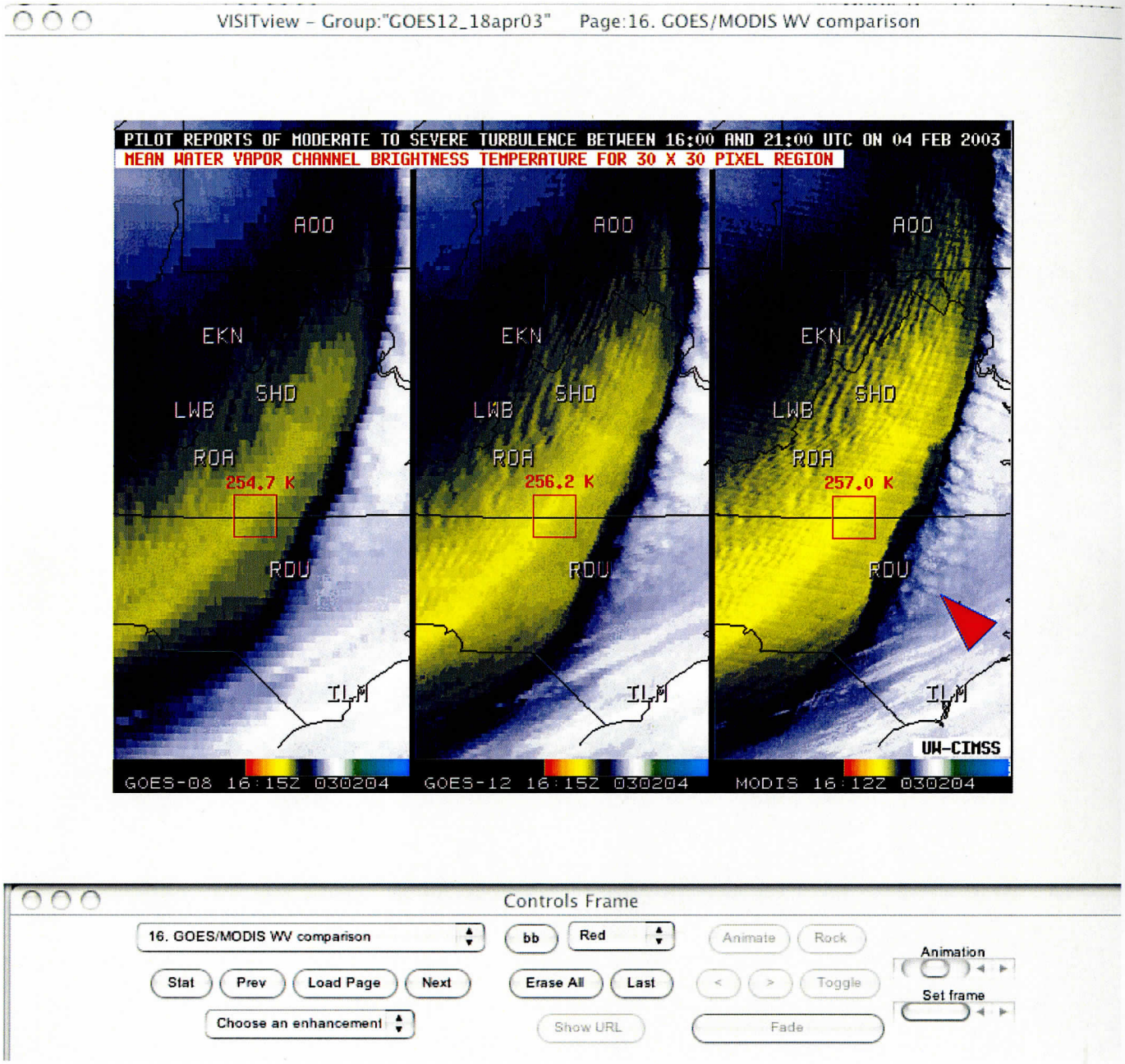

Figure 54: VISITview screenshot showing the improved water vapor channel on GOES-12.

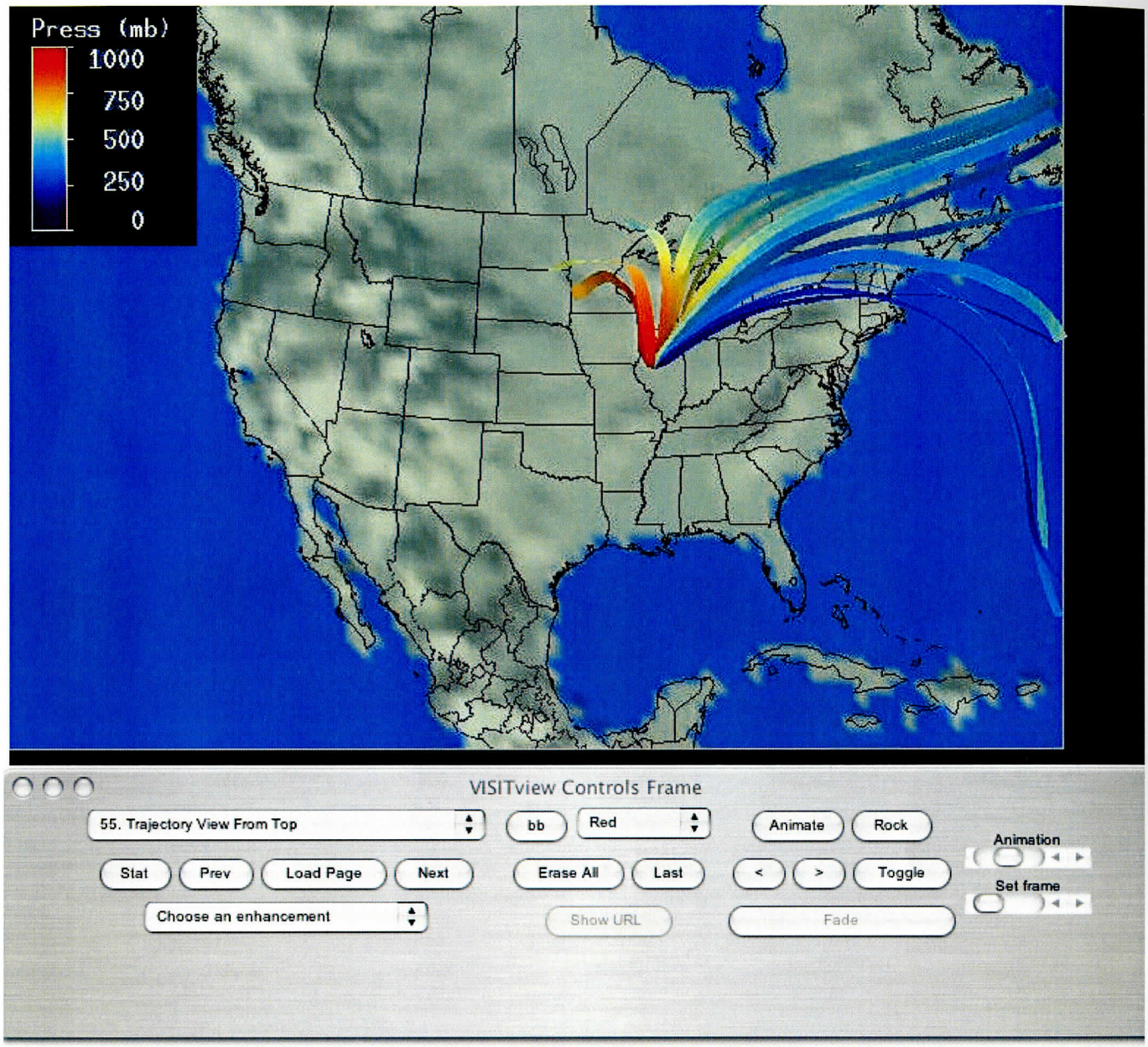

Figure 55: VISITview example of trajectory display capability in D3D AWIPS

VIII. Radiance Calibration/Validation, Cloud Property Determination, and Combined Geometric plus Radiometric Soundings for the NPOESS

Brief Description of Work

This project deals with scientific studies aimed at improving the cloud products from the VIIRS sensor during the NPOESS era.

During this period we finished the development of a cloud type algorithm for VIIRS. The cloud type algorithm's basis was that used in the NOAA AVHRR processing. Given the spectral information contained in VIIRS, several improvements were possible. One of the strengths of this algorithm is the detection of multilayer or overlapped cirrus. In this context, overlapped cirrus clouds are cirrus clouds that occur above a layer of lower cloud. Figure 56 shows an RGB image created from MODIS data using channels available on VIIRS. Figure 57 shows the corresponding cloud type image using the new VIIRS algorithm. The results have been validated through comparison with radar observations. This work has positively impacted the development of the VIIRS algorithms. One paper has been accepted for publication and two are being drafted in association with this effort.

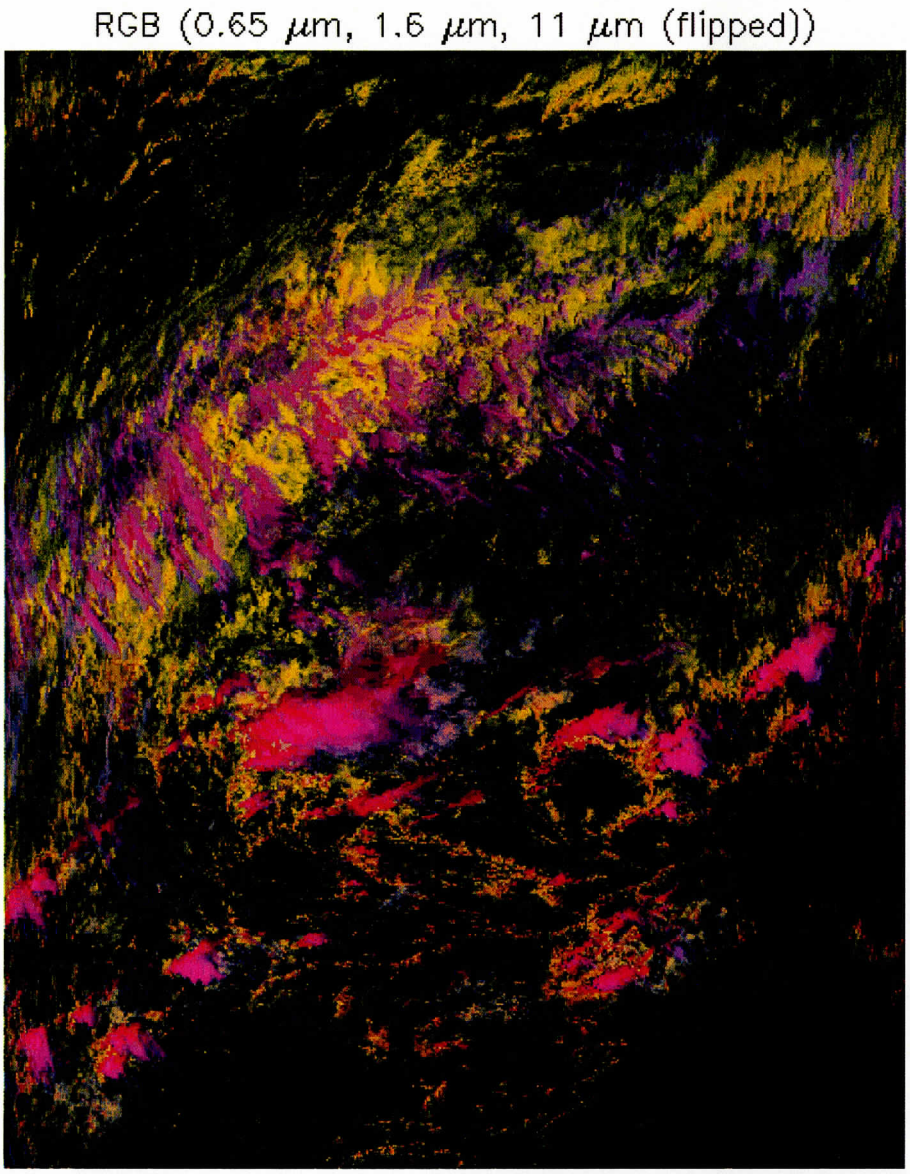

Figure 56. RGB image from MODIS (using VIIRS channels) of a complex tropical cloud system.

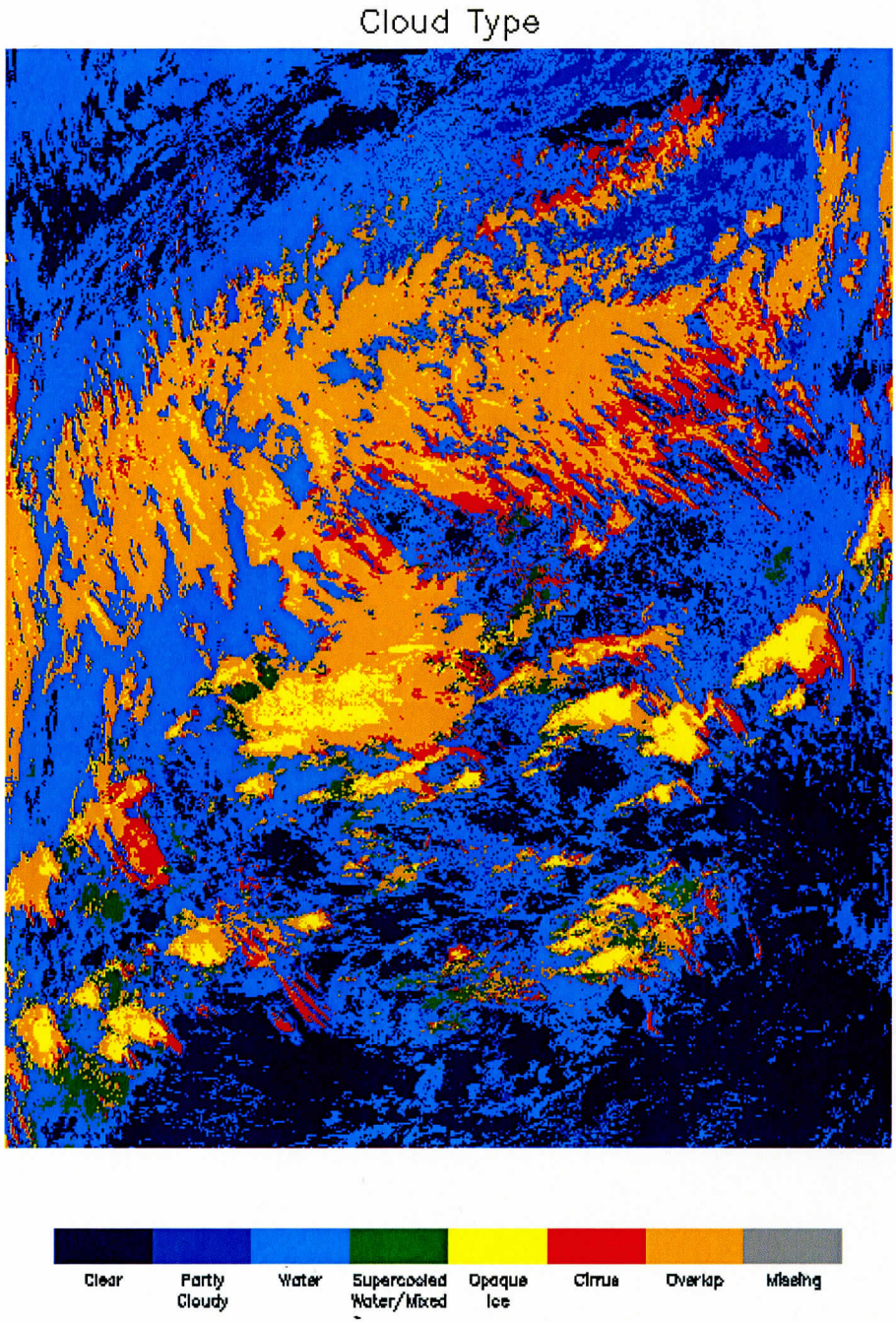

Figure 57. Cloud type results using the VIIRS algorithm.

IX. CIMSS Outreach Activities

1. Satellite Meteorology for Grades 7-12

After developing an interactive on-line and CD-ROM course in Satellite Meteorology for grades 7-12 (http://cimss.ssec.wisc.edu/satmet/), CIMSS has made great strides to inform educators and researchers of this valuable resource, as well as improve course content and structure as we obtain reiterative rounds of feedback from teachers and students. In March 2003 at the Wisconsin Society for Science Teachers (WSST) Meeting, we presented an initial version of the course and announced an upcoming satellite meteorology teacher workshop with an emphasis on classroom implementation. Fifty CD-ROMS were distributed at WSST. Later that month, CIMSS staff presented at the Satellites & Education Conference XVI in California where additional CD-ROMs were distributed. In June CIMSS conducted a half-day hands-on workshop with middle school students at the UW Space Place, a science outreach venue in Madison. In July 2003 we hosted a two-day teacher workshop to formally launch our satellite meteorology course for middle and high school students. Sixteen teachers from 4 different states came to CIMSS and worked through each module of the course, providing valuable feedback and recommendations for improvement. A few recommendations and requests were incorporated in time for distribution at the 13th Annual Wisconsin Space Grant Conference in August 2003; we also made a presentation on our efforts and progress. Since then we have been implementing more recommendations, as well as further developing and adding to the course content. We also communicate electronically with our growing network of teachers to inform them of updates and solicit feedback. Starting with the Seattle AMS conference in January, CIMSS plans to participate broadly in educational conferences in 2004 to continue expanding our outreach efforts in satellite meteorology.

2. Summer Workshop in Atmospheric, Earth and Space Science

In July 2003 CIMSS hosted its 11th Summer Workshop in Atmospheric, Earth, and Space Sciences. We decided to offer a students only Summer Workshop in order to better focus on the needs of students (previous workshops had been for students and teachers).

Following a May deadline, we evaluated the applications from prospective attendees, based on grades, personal essay, and teacher recommendation letter. Letters were sent informing applicants as to whether they had been accepted. Additional information was sent to participants in June. In the meantime, planning the logistics for the workshop continued (agenda and workshop content, housing, meals, field trips, transportation, chaperones, etc.).

The Summer Workshop was attended by about twenty high school students and was hosted by SSEC/CIMSS on the UW campus. The week long Workshop offered

numerous hands-on experiences for the participants working with measurement systems, weather data, and data manipulation and display computer systems. CIMSS scientists played the major role in the Summer Workshop, working with the students to understand GOES weather satellite instrumentation, data and its applications.

Following the workshop, organizers met to discuss the week's events, what went well and what might need improvement. Organizers also discussed the daily evaluations that students had filled out with their own impressions of the workshop. Preliminary arrangements for the 2004 Summer Workshop were begun.

3. Suomi Scholarship program

Established in 1998, the Verner E. Suomi Scholarship for Outstanding Achievement in the Physical Sciences was offered for the sixth consecutive year in 2003. The Suomi Scholarship is awarded to high school seniors who will be attending a University of Wisconsin campus and will major in the physical sciences (meteorology, earth science, oceanography, physics, astronomy, science or math education, environmental science and engineering). A flyer and application form were prepared and mailed to all Wisconsin high school science teachers; this information was also posted to the CIMSS web site. Twenty-one applications were collected and prepared for evaluation following an April postmark deadline. Applications were evaluated based on a one-page essay, grades, and letter of recommendation. We typically award five scholarships each year; four scholarships were awarded in 2003. The Scholarship funds come from a UW Fund created from Suomi's monetary awards.